Technische Universität München

Fakultät für Chemie
Lehrstuhl für Biotechnologie

Institut für Klinische Chemie und Pathobiochemie
Klinikum rechts der Isar

Markierungsfreier Protein-Microarray zur Detektion von Autoantikörpern beim Antiphospholipid-Syndrom

Aline Ramona Schindler

Vollständiger Abdruck der von der Fakultät für Chemie der Technischen Universität München zur Erlangung des akademischen Grads eines

Doktors der Naturwissenschaften

genehmigten Dissertation.

Vorsitzender:	Univ.-Prof. Dr. Franz Hagn
Prüfer der Dissertation:	1. Univ.-Prof. Dr. Johannes Buchner
	2. apl. Prof. Dr. Peter B. Luppa

Die Dissertation wurde am 30.10.2015 bei der Technischen Universität München eingereicht und durch die Fakultät für Chemie am 18.01.2016 angenommen.

Danksagung

Diese Doktorarbeit ist entstanden mit der Unterstützung von Kollegen und Freunde. Sie ist auch ihr Werk, weshalb ich an dieser Stelle "Danke" sagen möchte.

Als erstes möchte ich Prof. Dr. Peter B. Luppa danken, für das spannende und vielseitige Thema, für all seine Unterstützung und für das Vertrauen, das er in mich und meine Arbeit gesetzt hat.

Herrn Prof. Dr. Johannes Buchner danke ich für die Übernahme der Betreuung und dem entgegengebrachten Interesse an meiner Arbeit.

Ein lieber Dank geht an meine Kollegen, Dr. Heike Bittersohl, Dr. Alice Schlichtiger, Anita Schreiegg, Dr. Alexander Le Blanc, Dr. Markus Thaler, Dr. Andreas Bietenbeck, Michael Schmalenberg und Ludwig Bulst, die mich mit anregenden Gesprächen und stetigem Gedankenaustausch weiter gebracht haben. Ganz besonders möchte ich meine Kollegin und Freundin Carmen Kocot hervorheben. Danke für deine Unterstützung, deinen Rat, deine Hilfe, dafür dass du immer wieder den Ehrgeiz in mir geweckt hast und dass ich mich immer auf dich verlassen kann.

An dieser Stelle danke ich auch Herrn PD Dr. Dr. Hans Günter Wahl, der mir mit seinen Korrekturen viel geholfen und mich stets motiviert hat während des Prozesses des Schreibens.

Ein Dankeschön geht auch an meinen Kooperationspartner in Tübingen. In erster Linie an Herrn Dr. Günther Proll und Herrn Prof. Dr. Günter Gauglitz, die diese Arbeit mit ermöglicht haben, sowie an Dr. Oliver Bleher, der mit mir gemeinsam an diesem Projekt gearbeitet hat. Außerdem danke ich allen Mitarbeitern des Instituts für Physikalische und Theoretische Chemie sowie der Firma Biametrics, die mich bei meinen unzähligen Besuchen in Tübingen immer herzlich empfangen haben.

Ein großer Dank geht an die Deutsche Forschungsgemeinschaft für die Bereitstellung der Mittel und für ihr Interesse an diesem Forschungsgebiet.

Ich danke der Arbeitsgruppe um Prof. Holmes, die mir das amino-derivatisierte Cardiolipin zur Verfügung gestellt haben, sowie dem Zentrallabor des Universitätsklinikums Würzburg (Dr. med. Udo Steigerwald) für die Bereitstellung der.

Mein Studium und die daraus entstandene Doktorarbeit wären so nicht möglich gewesen ohne die Unterstützung meiner Liebsten. Ich danke meiner Schwester Hanna Schindler, meinen Eltern, Regula Schindler und Reinhard Tegtmeier-Schindler, und meinem Freund, Tobias Schürtz von ganzem Herzen. Danke für euren Zuspruch und eure Unterstützung, eure offenen Ohren und Arme.

Teile der vorliegenden Arbeit wurden bereits veröffentlicht in:

1. Bleher, O., Schindler, A.,Yin, V., Holmes, A. B., Luppa, P. B., Gauglitz, G., Proll, G., Development of a new parallelized, optical biosensor platform for label -free detection of autoimmunity-relatedantibodies. *Analytical and Bioanalytical Chemistry,* 406: 3305-3314 (2014)

2. Schindler, A. R.,Bleher, O.,Thaler, M. A.,Kocot, C. J.,Steigerwald, U.,Proll, G., Gauglitz, G., Luppa, P. B., Diagnostic Performance Study of a Microarray Biosensor for the detection of Antiphospholipid Antibodies . *Clinical Chemistry and Laboratory Medicine, 53: 801-808* (2015).

„Der höchste Lohn für unsere Bemühungen ist nicht das, was wir dafür bekommen, sondern das, was wir dadurch werden.“ - John Ruskin

Meiner Familie, Hanna, Regula und Reinhard Schindler und meinem Freund Tobias Schürtz.
Danke für eure Unterstützung und eure Liebe.

table of contents

figure index

table index

1 abstract

The antiphospholipid syndrome (APS) is an autoimmune disease with a prevalence of 1-6 % in the European population. Deep vein thrombosis, repeated miscarriages and myocardial infarction are just some symptoms that can occur during the course of APS. But patients also suffer from a history of premature births and hematologic complications like thrombocytopenia or haemolytic anaemia. Migraine headaches, livedo reticularis, unexplained adrenal insufficiency and lung embolism have been described. Due to this heterogeneity in terms of clinical manifestations but also antibody spectrum a definite diagnose of APS is often not straight forward. The revised Sydney classification criteria try to give guidelines for the diagnosis of APS. They define one clinical criteria (either vascular thrombosis or pregnancy morbidity) as well as one laboratory criteria (anti-cardiolipin, anti-β_2-glycoprotein I or lupus anticoagulants) to be present for a distinct diagnosis. Cardiolipin and β_2-glycoprotein I (β_2-GPI) are the main antibody targets. In routine, anti-cardiolipin and anti-β_2-GPI are detected by standardized ELISA systems. Less important, because of low specificity for APS diagnostics are antibodies against prothrombin and phosphatidylserine. Still, they seem to be important as anti-pothrombin are a more reliable marker for possible thrombotic events than anti-cardiolipin and anti-β_2-GPI. Other antibody targets include annexins A5 and A2, protein C and S and tissue plasminogen activator.

The heterogeneity of APS relevant antigens creates a variety of different antibodies, which requires a simultaneous detection mode. For this reason a parallelized, label-free, optical biosensor was developed to monitor multiple antigen-antibody interactions within a single measurement. The parallelization of multiple analytes is of growing importance in numerous fields of biomolecular interaction analysis. Applications are given in pharmaceutical screenings, epitope mapping of antigens, and medical diagnostics. In these areas the combination of a short analysis time and low sample consumption is particularly important and means a step forward compared to classical analytics.

This work describes the establishment of a suitable surface chemistry as well as assay conditions for the detection of anti-β_2-GPI, anti-cardiolipin, and anti-prothrombin in parallel. To this end, a simplified 1-λ-reflectometry format was initially used that allowed the assay evaluation for every antigen in a single-spot biosensor format. Transducers were modified with di-amino-poly(ethylene)glycol, amino dextran and 11-aminoundecyltrimethoxysilane. Latter was found to be the most suitable surface modification for the covalent coupling of proteins as well as an amino-functionalized cardiolipin. Covalent immobilization via this silane resulted in a sensitive biosensor with attenuated unspecific binding and a clear differentiation of patient and control sera.

This simplified biosensor was then extended to a multiplexed format by using “polarized imaging reflectometric interference spectroscopy” (pi-RIfS). It uses a camera with charge coupled device (CCD)-detector that takes one picture per second of the transducer and monitors the changes

in refractive index upon binding of the antibody to the respective antigen. Data is received as pixel values and further processed resulting in a binding curve with relative signal intensities plotted as a function of time. Thereby, several hundreds of interactions can be recorded in parallel.

Simultaneous detection of multiple anti-phospholipid antibodies can provide helpful information for individualized treatment by identification and characterization of subpopulations of patients. With this microarray based assay format the detection of four different antibodies, namely anti-β_2-GPI, anti-cardiolipin, anti-prothrombin, and antibodies to a complex between β_2-GPI and cardiolipin could be achieved within one single measurement. Thereby, the biosensor showed a performance in terms of sensitivity and specificity comparable to the existing ELISA systems. Especially for β_2-GPI, the ROC curve gave an area under the curve (AUC) of 0.946 with an confidence interval (CI) of 0.860 - 0.987. But also the detection of anti-prothrombin with an AUC of 0.926 and CI of 0.833 - 0.976 was convincing.

2 zusammenfassung

Das Antiphospholipid-Syndrom (APS) ist eine Autoimmunerkrankung mit einer Prävalenz von 1-6 % innerhalb der europäischen Population. Tiefe Beinvenenthrombosen, Fehlgeburten und Herzinfarkte sind nur einige der Symptome, die im Laufe des APS auftreten. Die Patienten leiden außerdem unter rezidivierenden Frühgeburten und hämatologischen Komplikationen wie Thrombozytopenie oder hämolytische Anämie. Migräne-Kopfschmerzen, Livedo reticularis, ungeklärte Nebennierenrindeninsuffizienz sowie Lungenembolie sind ebenfalls beschrieben worden. Aufgrund dieser Heterogenität in Bezug auf die klinischen Symptome, wie auch das Antikörperspektrum, ist eine definitive Diagnose oft nicht einfach. Die im Jahr 1999 in Sapporo ursprünglich beschlossenen Klassifizierungskriterien sollten dazu beitragen, die Diagnose eines Antiphospholipid-Syndroms zu vereinheitlichen. In 2006, beim elften internationalen Kongress für Antiphospholipid-Antikörper in Sydney, sind diese Leitlinien noch einmal überarbeitet worden aufgrund neuer klinischer, laborchemischer und experimenteller Erkenntnisse. Diese legen fest, dass sowohl ein klinisches Kriterium (entweder Gefäßthrombose oder Schwangerschaftsmortalität), sowie ein Laborkriterium (der Nachweis von anti-Cardiolipin, anti-β_2-Glykoprotein I oder Lupus-Antikoagulans) vorhanden sein muss, um eine zweifelsfreie Diagnose zu stellen. Dabei sind Cardiolipin und β_2-Glykoprotein I (β_2-GPI) die Zielstrukturen der Autoantikörper. Weniger wichtig, aufgrund einer geringeren Spezifität für die APS-Diagnostik sind Prothrombin und Phosphatidylserin. Dennoch scheint auch deren Nachweis eine Berechtigung zu besitzen, da anti-Prothrombin zuverlässigere Marker darstellen für das mögliche Auftreten thrombotischer Komplikationen im Vergleich zu anti-Cardiolipin und anti-β_2-GPI. Zu den weiteren Antigenen gehören Annexine A5 und A2, Protein C, Protein S, sowie Gewebsplasminogenaktivator. Routinemäßig werden anti-Cardiolipin und anti-β_2-GPI bestimmt, und zwar mit Hilfe von standardisierten ELISA-Systemen.

Die Heterogenität der APS-relevanten Antigene erzeugt eine Vielzahl von verschiedenen Antikörpern, für die ein simultaner Nachweis einen Vorteil bieten würde gegenüber den gängigen Einzelbestimmungsmethoden. Aus diesem Grund wurde ein parallelisierter, markierungsfreier, optischer Biosensor entwickelt, der es ermöglicht mehrere Antigen-Antikörper-Wechselwirkungen in einer einzigen Messung zu detektieren. Parallelisierte Screeningmethoden, sogenannte Microarrays, haben ihren Ursprung in der Entwicklung des Southern Blots durch Ed Southern in 1975. Seit der Miniaturisierung dieser Methode in den 90er Jahren, sind sie von wachsender Bedeutung und spielen eine Rolle in vielen Bereichen der biomolekularen Interaktionsanalyse. Anwendungen finden sich im pharmazeutischen Screening, im Epitop-Mapping von Antigenen und in der medizinischen Diagnostik. In diesen Bereichen ist eine kurze Analysezeit in Kombination mit einem geringen Probenverbrauch besonders wünschenswert und bedeutet einen signifikanten Fortschritt.

Diese Arbeit beschreibt die Etablierung einer geeigneten Oberflächenchemie sowie optimaler Assay-Bedingungen für die simultane Detektion von anti-β_2-GPI, anti-Cardiolipin und anti-

Prothrombin. Zu diesem Zweck wurde zunächst die einfachere 1-λ-Reflektometrie verwendet, die die Evaluierung der Testbedingungen für jedes Antigen in einem Einzelanalyten-Biosensor ermöglicht.

Glas-Chips wurden mit unterschiedlichen Polymeren beschichtet, nämlich di-Amino-Polyethylenglycol, Aminodextran und 11-Aminoundecyltrimethoxysilan. Dabei zeigte sich, dass für eine kovalente Immobilisierung von Proteinen sowie eines Amino-funktionalisierten Cardiolipins, letzteres die am besten geeignete Oberflächenmodifizierung ist. Die Beschichtung mit diesem Silan führte zu einem sensitiven Biosensor mit gleichzeitig reduzierten unspezifischen Bindungssignalen, sowie einer klaren Differenzierung zwischen Patienten und Kontrollseren.

Dieser Biosensor wurde dann auf ein Micorarray-Format erweitert, der mit Hilfe von "polarisierter, bildgebender reflektometrischer Interferenzspektroskopie" (pi-RIfS) ausgelesen werden konnte. Eine Kamera mit CCD-Detektor nimmt dabei ein Bild pro Sekunde von dem Array-Glaschip in der Flusszelle auf und detektiert die Veränderung des Brechungsindex bedingt durch die Anbindung der Antikörper an die jeweils präsentierten Antigene. Die Daten werden als Pixelwerte ausgegeben, mathematisch bearbeitet und als Bindungskurve dargestellt, mit den relativen Signalstärken auf der Ordinaten- und der Zeit auf der Abszissenachse. Dadurch können mehrere hundert Wechselwirkungen parallel aufgezeichnet werden.

Der gleichzeitige Nachweis mehrerer Antiphospholipid-Antikörper kann hilfreiche Informationen für eine individualisierte Therapie zur Verfügung stellen, indem er die Identifizierung und Charakterisierung von Subpopulationen von Patienten ermöglicht. Mit diesem Mikroarray-basierten Assay-Format war es möglich, vier verschiedene Antikörper, nämlich anti-β_2-GPI, anti-Cardiolipin, anti-Prothrombin, und Antikörper gegen einen Komplex aus β_2-GPI und Cardiolipin in einer einzigen Messung zu erfassen. Dabei zeigte der Biosensor eine Effizienz in Bezug auf Sensitivität und Spezifität, die vergleichbar mit den bestehenden ELISA-Systemen ist. Insbesondere für β_2-GPI, ergab die ROC-Analyse eine Fläche unter der Kurve (AUC) von 0.946 mit einem Konfidenzintervall (CI) von 0.860 - 0.987. Aber auch der Nachweis von anti-Prothrombin mit einer AUC von 0.926 und einem CI von 0.833 - 0.976 war überzeugend.

3 introduction

3.1. Antiphospholipid syndrome

3.1.1. Clinical manifestations and historical background

The antiphospholipid syndrome (APS) is a systemic autoimmunopathy associated with peculiar clinical manifestations like vascular thrombosis and recurrent fetal loss or prematurity. The prevalence in a normal population is between 1.0 and 5.6 % (BMJ 2014). Thereby elderly people are more often affected than younger ones and females more often than males (BMJ 2014; Gezer 2003). During a 10-year follow-up study in a European APS cohort, the survival probability after 5 years was 94.7 % and after 10 years 90.7 % compared to a normal population (Cervera et al. 2015). Major causes of death were thrombotic complications like myocardial infarction, stroke and pulmonary embolism and infection. During this study, a total of 188 pregnancies occurred, of which 72.9 % were successful (obstetric morbidity of 27.1 %). Main antigenic targets are phospholipids like cardiolipin or phosphatidylserine and phospholipid binding plasma proteins, such as β_2-glycoprotein I (β_2-GPI) or prothrombin. Other antibody targets include annexin A5, annexin A2, protein C, protein S and tissue plasminogen activator (Hanly 2003; Mehdi et al. 2010).

Formerly a differentiation was made between primary and secondary APS based on whether the syndrome occurs in isolation or with an underlying connective tissue diseases, such as systemic lupus erythematosus (SLE) or rheumatoid arthritis (Hanly 2003). In a publication of Miyakis et al., the authors suggest not to use this nomenclature anymore, because it is unknown if SLE promotes the development of APS or if they are two elements of the same process (Miyakis et al. 2006). They recommend describing patients with primary APS as simply having APS and in the case of secondary APS to name the second autoimmune disorder associated with the APS (Wong & Favaloro 2008).

Of all reported cases of APS, less than 1 % of the patients develop a catastrophic APS (CAPS). The term was first used by Asherson in 1992 to describe an accelerated form of APS. Therefore it is also known as Asherson's syndrome. It displays a life threatening situation characterized by an acute thrombotic microangiopathy in multiple small vascular beds. It usually evolves within less than one week and often results in multiorgan failure (Nayer & Ortega 2014; Cervera et al. 2014). Due to its severe progression during the acute event, patients have a higher mortality rate (Espinosa & Cervera 2010). In the European APS cohort study by Cervera et al (Cervera et al. 2015) 0.9 % of the patients developed a CAPS and 55.6 % of them died. Formerly, it was believed, that patients who develop a CAPS, have had a history of APS and/or antiphospholipid antibodies. Recent studies show, that almost half of all reported cases have been developed *de novo* (Bucciarelli et al. 2009).

History of APS

Historically, antiphospholipid antibodies (aPL) were first described by Wassermann et al. in 1906 although the antigen was unknown then (McIntyre et al. 2003). They developed a serological test for syphilis in which they used an extract of bovine hearts (Levine et al. 2002). Some years later

in 1941, this antigen was identified by Pangborn (Pangborn 1941) and named cardiolipin, based on its origin (cardio = heart). This became the basis for a new serological test for syphilis named after the institute that invented it: VDRL (Veneral Disease Research Laboratory). A mixture of cardiolipin, lecithin and cholesterol was applied as antigenic substance for antibody detection and large numbers of patients were screened. As a result, groups of individuals tested positive for syphilis with this test were found to be without any symptoms of infection and it became evident that these reactions were biologic false positive serological tests for syphilis (BFP-STS) (Vlachoyiannopoulos et al. 2007; Hanly 2003). Soon, a correlation was drawn between these BFP-STS and underlying other infectious diseases. Many of the patients with a BFP-reaction for syphilis were diagnosed with an systemic lupus erythematosus (SLE) and vice versa. SLE is an autoimmune disease, affecting many organs in the body. Many of the developed autoantibodies are directed against proteins in the cell nucleus (Sherer et al. 2004). But also high titers of anti-cardiolipin are detected in patients with SLE giving a positive reaction in the VDRL test. Furthermore, one third of persons tested positive for syphilis had lupus anticoagulants (LA), antibodies, that cause a prolonged clotting time (de Laat et al. 2004). Such anticoagulants were not detected in syphilis patients. In 1990, several independent groups found that some antibodies associated with SLE or APS are directed against plasma proteins, such as β_2-GPI, bound to cardiolipin or other negatively charged phospholipids (McIntyre et al. 2003). In contrast, antibodies from patients with syphilis or other infectious disease directly bind to cardiolipin and the presence of β_2-GPI can even be disruptive for the interaction because the protein covers the phospholipid and shields the epitope from the antibodies. The term “antiphospholipid antibodies” can be misleading. The most relevant antibodies in APS are either directed against a complex of β_2-GPI and phospholipids (e. g. cardiolipin) or just against β_2-GPI alone without the presence of any phospholipids (Levine et al. 2002).

Sapporo and revised Sydney classification criteria

Due to this heterogeneity of the antibody spectrum, the need for consensus criteria was given (Wilson et al. 1999). In October 1998, after the Eighth International Symposium on Antiphospholipid Antibodies in Sapporo (Japan), a workshop was held to define the first, preliminary classification criteria for the diagnosis of a definite APS. They should provide clinicians with uniformly guidelines for the classification of APS. In 2006, at the Eleventh International Symposium on Antiphospholipid Antibodies in Sydney (Australia), these criteria have been revised due to novel clinical, laboratory, and experimental insights (Miyakis et al. 2006). The revised Sydney classification define one clinical as well as one laboratory criteria to be relevant for a definite diagnosis of APS (Table 1). Clinical symptoms are vascular thrombosis and pregnancy morbidity. Most frequently, patients suffer from deep vein thrombosis (31.7 % of APS patients), thrombocytopenia (21.9 %), livedo reticularis (20.4 %), and stroke (13.1 %). Serological parameters are determined by two different kinds of tests,

a solid-phase test for anti-cardiolipin and anti-β_2-GPI as well as a coagulation-based for lupus anticoagulants. Laboratory criteria have to be tested positive two or more times with at least 12 weeks apart to exclude false positive anti-cardiolipin titers due to acute infection for example.

Table 1: International consensus statement on the clinical and laboratory criteria essential for a definite diagnosis of antiphospholipid syndrome. From Miyakis et al. 2006.

Clinical criteria

1. Vascular thrombosis:
   At least one clinical episode of arterial, venous, or small vessel thrombosis in any tissue or organ. Thereby it should be discriminated between patients with presence or absence of additional risk factors for thrombosis, like cardiovascular disease, age, inherited thrombophilias, and others.
2. Pregnancy complications:
   One or more unexplained deaths of a morphologically normal fetus at or beyond the 10th week of gestation.

   One or more premature births of a morphologically normal neonate before the 34th week of gestation due to eclampsia or severe pre-eclampsia or placental insufficiency.

   At least three unexplained consecutive spontaneous abortions before the 10th week of gestation, thereby excluding any maternal anatomic or hormonal abnormalities as well as paternal and maternal chromosomal causes.

Laboratory criteria

1. Lupus anticoagulant (LA)
   Detected in plasma with activated partial thromboplastin time (aPTT) or dilute Russell's viper venom time (dRVVT).
2. Anti-cardiolipin autoantibodies of the IgG and/or IgM isotype
   Measured in serum or plasma with medium or high titer (> 40 GPL or MPL, or > 99th percentile of the reference range obtained within a collective of healthy subjects) by use of standardized ELISA.
3. Anti-β_2-GPI autoantibodies of IgG and/or IgM isotype
   Measured in serum or plasma (in titer > the 99th percentile) by use of a standardized ELISA.

The former Sapporo classification criteria (1998) have been evaluated in terms of sensitivity and specificity, which were found to be 0.71 and 0.98, respectively (Lockshin et al. 2000). For the revised Sydney classification (2006) there have been no studies performed to address these attributes. In the following, the three laboratory criteria and the respective tests shall be explained.

3.1.2. Detection of APS relevant antibodies

3.1.2.1. Lupus anticoagulant

The detection of LA is based on the ability of these antibodies to cause a prolonged clotting time *in vitro*. This can be tested by activated partial thromboplastin time (aPTT), dilute Russell's viper venom time (dRVVT), the kaolin clotting time (KCT), or the prothrombin time (Bermas et al. 2014). In 2009, Pengo et al. defined the most important aspects for the pre-analytical and analytical phase of lupus anticoagulant detection (Pengo et al. 2009). Briefly, fresh venous blood should be collected (with citrate that stops coagulation by binding Ca^{2+}) before or sufficient time after anticoagulant therapy and double centrifuged to obtain platelet poor plasma (platelet count $< 10 \times 10^9$/L). Two tests should be performed, based on different principles. Thereby the aPTT as well as the dRVVT are the most common in a routine laboratory.

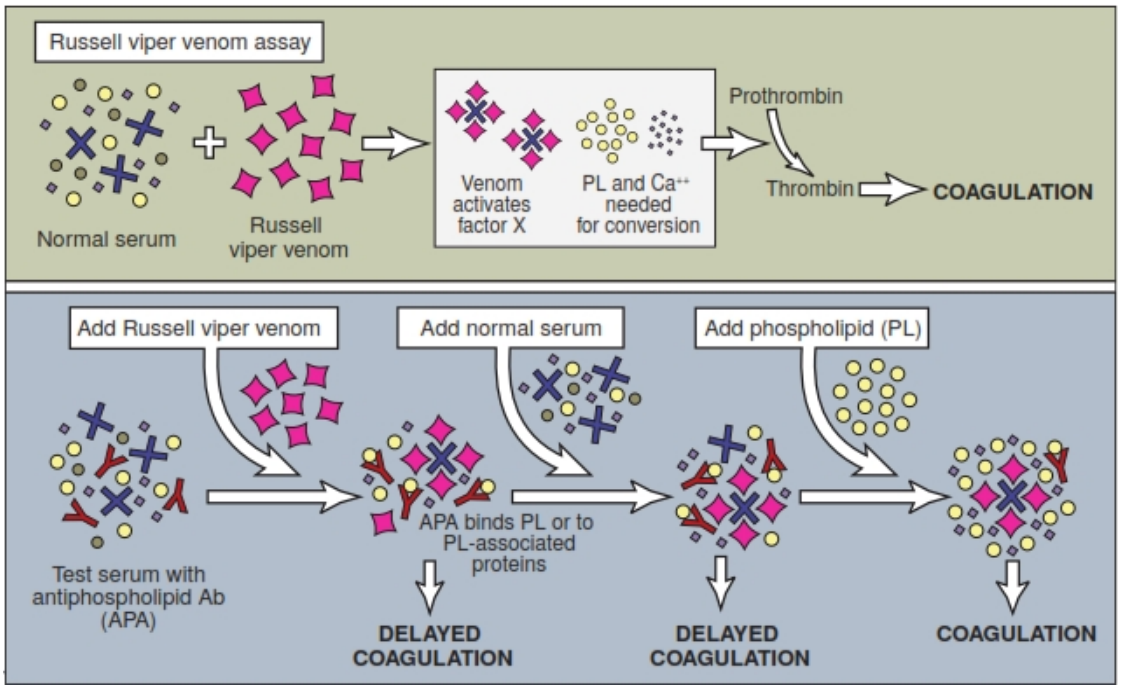

Figure 1: Basic principle of the dRVVT, from Hanly 2003, reprinted with permission of the Canadian Medical Association © «2003».

The aPTT is an *in vitro* screening test for the intrinsic coagulation pathway. After addition of a surface activator, such as silica or kaolin, and Ca^{2+}, coagulation is activated and the time (seconds) is measured until a fibrin clot is formed. But preferentially, the dRVVT should be used for the detection of lupus anticoagulant. The reason is its robustness and higher specificity compared to the aPTT because latter also depends on several coagulation factors (Pengo et al. 2009). The dRVVT is a diagnostic test in which the venom of the Russel's viper is added to the plasma sample. It activates coagulation factor X and together with factor V, phospholipids and Ca^{2+}, the so called prothrombinase complex, prothrombin is converted into thrombin and a stable clot is formed (Figure 1, a detailed description of the coagulation cascade is given in Figure 3). In the presence of LA,

clotting time is prolonged, because the antibodies bind the phospholipids essential for coagulation. They provide a surface (e. g. on blood platelets) where certain coagulation factor complexes, such as the prothrombinase complex, can assemble (Rumbaut & Thiagarajan 2010). A mixing test is part of the dRVVT. Thereby, patient plasma is mixed with pooled normal plasma in a 1:1 ratio to rule out a deficiency of coagulation factors. If a disorder of the coagulation cascade would be the reason for a prolonged clotting time, mixing with pooled normal plasma would restore the clotting time to normal ranges. Finally, a confirmatory study of the dRVVT is required in case of prolonged clotting time in the initial test. In the confirmatory test, phospholipids are added with increasing concentrations, to document the phospholipid dependence of the inhibitory effect of LA (Hanly 2003; Pengo et al. 2009; Bermas et al. 2014).

3.1.2.2. β_2-Glycoprotein I and the β_2-glycoprotein I-ELISA

Besides lupus anticoagulants, the confirmation of anti-β_2-GPI is one of the main laboratory criteria in routine diagnostics of APS.

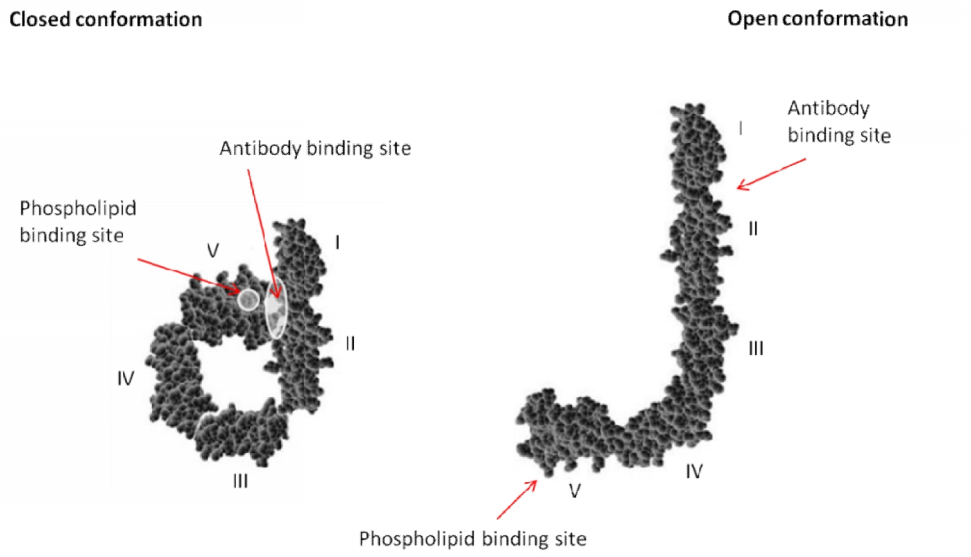

Figure 2: Closed and open conformation of β_2-GPI. Upon binding to negatively charged surfaces, the protein opens up into a J-shaped structure. Adapted from Pelkmans et al. 2013; de Groot & Meijers 2011.

β_2-GPI is a globular protein of 326 amino acids and a molecular weight of about 54 kDa, depending on the degree of glycosylation (Wang & Chiang 2004). It circulates with a concentration of about 0.2 mg/mL in human plasma and is primarily synthesized in the liver (Gamsjaeger et al. 2005), but also in intestinal epithelial and placenta cells (Miyakis et al. 2004). As a member of the so-called complement control protein (CCP) superfamily, it comprises 5 short consensus repeat domains of approximately 60 amino acids each (de Groot & Urbanus 2012). The 5th domain exhibits an additional 6-residue insertion forming a hydrophobic loop as well as a 19 amino acid long C-terminal extension. These extra amino acids include several positively charged lysine residues (positions 282, 284, 286

and 287) responsible for the interaction of β_2-GPI with anionic phospholipids like cardiolipin (Schwarzenbacher et al. 1999). The plasma protein also binds to endothelial or apoptotic cells, nitric oxide and superoxide radicals as well as oxidized LDL (low density lipoprotein) and other micro-particles. This could implicate a neutralizing and cleaning function for β_2-GPI (Sheng et al. 1998; de Groot et al. 2012), but its physiological role is not yet completely elucidated (de Groot & Meijers 2011). Individuals without detectable β_2-GPI levels appear to be clinically well (Miyakis et al. 2004).

It has been shown, that plasma-derived β_2-GPI is in a circular conformation caused by interaction of domains I and V (Figure 2). As a result, the epitope in domain I (Gly40-Arg43), essential for antibody binding is hidden and circulating β_2-GPI is not recognized by anti-β_2-GPI (de Groot et al. 2012; Agar et al. 2010; Iverson et al. 2002). Upon binding to a negatively charged surface, it changes into a J-shaped conformation, thereby exposing the epitope in domain I (Iverson et al. 1998). In 2014, Agostinis et al. used animal models to study the domain specificities of different monoclonal antibodies (Agostinis et al. 2014). The domain I anti-β_2-GPI, similar to the patient autoantibodies, was capable of inducing clot formation as well as pregnancy failure. This proved, that domain I antibodies are the main pathogenic antibodies which are more often related to clinical manifestations than antibodies to other domains.

The interaction of β_2-GPI with negatively charged surfaces is also the basis for the development of commercially available anti-β_2-GPI IgG/IgM ELISA kits. They utilize gamma irradiated microplates with a hydrophilic surface. β_2-GPI can directly bind via electrostatic interactions resulting in a conformational change and the exposition of the epitope. Recommendations to the test include the application of a whole-molecule β_2-GPI of human origin since human anti-bovine antibodies are not uncommon (de Groot & Urbanus 2012). Furthermore, the use of serum specimen should be preferred (Lakos et al. 2012). After binding of the patient's anti-β_2-GPI autoantibodies they are detected with a labelled secondary anti-human IgG or IgM. This secondary antibody has not only the advantage of signal enhancement, but is also necessary for the discrimination between autoantibodies of the IgG and IgM species. Their levels are reported in "GPL" and "MPL", arbitrary units of IgG/IgM antibodies ("G"/"M") with specificity for phospholipid antigens ("PL") (Lakos et al. 2012; Bermas et al. 2014). Thereby, 1 GPL or MPL unit refers to 1 µg of IgG or IgM antibody.

3.1.2.3. Cardiolipin and the cardiolipin-ELISA

Although it has been shown, that clinical manifestations in APS patients are stronger associated with anti-β_2-GPI than with anti-cardiolipin (Božič et al. 2005), they constitute an important tool in APS diagnostics.

Cardiolipin is an anionic phospholipid with a symmetric structure. It is composed of two phosphatidyl groups connected with a glycerol backbone (Nowicki et al. 2005). Therefore, cardiolipin

has, in contrast to other phospholipids, four hydrophobic alkyl groups instead of two and also two negative charges within the hydrophilic head group. In mammalian and plant cells, cardiolipin is the major component of the inner mitochondrial membrane. There it interacts with a number of inner mitochondrial membrane proteins and is required for their optimal functionality. These include the members of the electron transport chain, as well as several anion carriers, such as the adenine nucleotide translocator or the phosphate and pyruvate carriers (Paradies et al. 2009). Evidence rises that structural characteristics of cardiolipin play a key role in mitochondrial dynamics as well as apoptosis (Ortiz et al. 1999; Paradies et al. 2009). As mentioned above, cardiolipin is primarily located in the inner mitochondrial membrane. When cells undergo apoptosis, the interior will be exposed and cardiolipin might become the target of β_2-GPI and subsequently of anti-cardiolipin that recognize this complex (Schwarzenbacher et al. 1999).

The test for anti-cardiolipin was established in 1983 (Harris & Pierangeli 2002). Thereby, APS associated anti-cardiolipin are always detected with a complex of cardiolipin and β_2-GPI (Miyakis et al. 2004). They are coated together on most ELISA plates or β_2-GPI is included in the dilution or blocking solution (Keeling et al. 1993). In this context, it is recommended to use β_2-GPI of bovine or human origin (Lakos et al. 2012). As in the case of β_2-GPI the principle of the assay is based on an indirect ELISA. Specific antibodies in the sample bind to the antigenic surface and are then detected with an enzyme-labeled secondary antibody. After addition of the substrate a colored product is formed which is detected by a certain wavelength.

3.1.2.4. Standardization

For all these test, described above, one problem remains: the poor standardization of the ELISA systems and the concordance between assays of different distributors (Andreoli et al. 2008). Traditionally, calibrators produced by Louisville APL (Antiphosphlipid Standardization Laboratory) Diagnostics are used for the determination of anti-cardiolipin IgG and IgM (Harris & Pierangeli 2002). These are based on pooled positive sera from APS patients as well as negative sera from healthy donors with varying proportions to cover a wide range of different concentrations (Louisville APL Diagnostics 2013). Medium or moderate levels have been reported with values ≥ 20 and ≤ 80 GPL/MPL, ≥ 80 GPL/MPL is referred to as high-positive. Values > cut off but ≤ 20 represents low positive results (Lakos et al. 2012). For anti-β_2-GPI assays, there are still no universally accepted calibrators although there exist standardized calibrators, such as the humanized monoclonal antibodies HCAL (IgG) and EY2C9 (IgM) (Giannakopoulos et al. 2009).

Differences in the classification of patients are largely due to different cut off values chosen by the manufacturers (Reber et al. 2005). These depend on the distribution of the investigated normal individuals but also on the performance of previously approved kits that are used as reference to

determine sensitivity and specificity of the evaluated assay. Other factors that contribute to the discrepancies include differences in microplate brand and therefore a possible difference in antigen immobilization, the way to prepare the antigen and what kind of β_2-GPI isoform is used.

When combining IgG and IgM detection, commercial available assays exhibit a good diagnostic performance in terms of sensitivity and specificity (Andreoli et al. 2008). Although the determination of aPL of the IgA type is not recommended, it should be considered in cases in which IgG and IgM cannot be detected, but APS is still suspected (Lakos et al. 2012).

3.1.3. Prothrombin and prothrombin antibodies

Although not included in the Sapporo criteria, antibodies against prothrombin shall be briefly discussed at this point, since they are part of the established microarray.

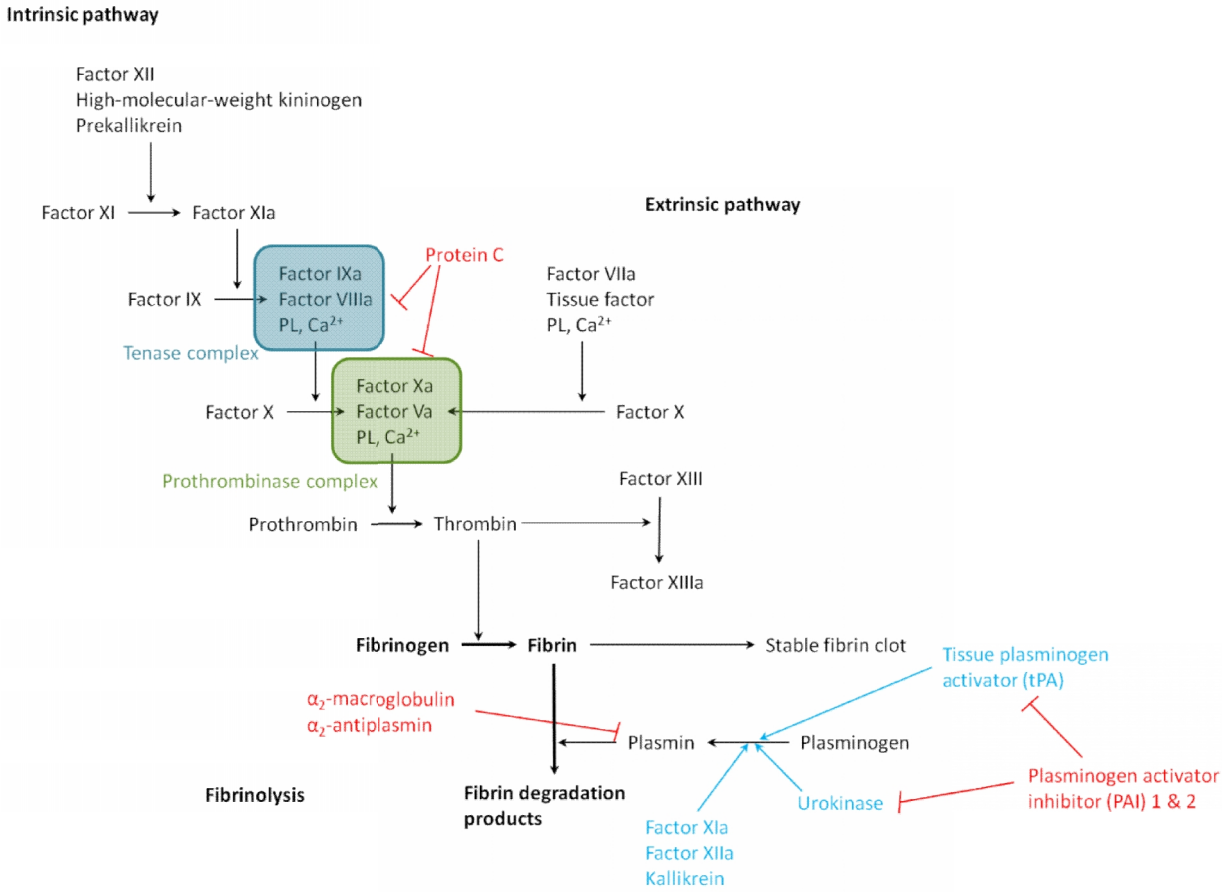

Figure 3: Summary of the classical coagulation cascade. Adapted from Hoffman & Monroe III 2001. PL stands for phospholipids.

Prothrombin, or coagulation factor II, is synthesized by the liver and posttranslationally modified. This results in a 72 kDa large glycoprotein that binds to negatively charged phospholipid surfaces, usually membranes of activated platelets (Donohoe et al. 2001; Sciascia et al. 2014). In the presence of Ca^{2+}, prothrombin is there converted into the active α-thrombin by factors Va and Xa, the so-called prothrombinase complex (Wood et al. 2011). This is the critical step in the response to

vascular injury. Thrombin itself acts as serine protease to cleave fibrinogen into fibrin that is essential for blood coagulation.

During the 1980s, several groups investigated the occurrence of hypoprothrombinemia in patients with lupus anticoagulants (LA) and provided the first evidence of antibodies that bind to human prothrombin (Galli & Barbui 1999). In 1991, Bevers et al. were able to show with their experiments that LAs of the IgG type are not directed to phospholipids alone (Bevers et al. 1991). They found that these antibodies recognize an epitope, which is exposed after the binding of human prothrombin to phospholipids mediated by Ca^{2+} ions.

Prothrombin autoantibodies are the most frequent antibodies in APS that are not routinely measured. Their prevalence in APS was shown to be around 30 % for the IgG subtype and about 60 % in the case of IgM (Donohoe et al. 2001). But they are a heterogeneous group of antibodies and their detection is largely dependent on the assay conditions. Donohoe et al. found that γ-irradiated ELISA plates are essential for the immobilization of prothrombin (Donohoe et al. 2001). When coated together with anionic phospholipids, e. g. phosphatidylserine, the detection of different populations of anti-prothrombin as well as low avidity antibodies is facilitated (Žigon et al. 2011).

Less specificity and sensitivity for APS compared to anti-β_2-GPI, anti-cardiolipin, or LA is probably the reason why they are not incorporated in the Sapporo classification. However, Žigon et al. confirmed in their study that an additional anti-prothrombin/phosphatidylserine assay improves the diagnosis of APS and should therefore be included in the laboratory criteria (Žigon et al. 2011).

3.1.4. Differential diagnosis for APS

Many genetic predispositions as well as acquired disorders can result in symptoms that are similar as in APS, such as thromboembolic disease or pregnancy loss. The differential diagnosis for APS includes various diseases, dependent on the vascular bed involved. Examples are cancer and myeloproliferative disorders, nephrotic syndrome, atherosclerosis, HIT (heparin-induced thrombocytopenia) or systemic vasculititis (a detailed list of the differential diagnosis is given in the appendix, Table 9). Furthermore, anti-cardiolipin have been reported in rheumatic diseases and autoimmunopathies other than APS. Infectious diseases, such as syphilis, hepatitis C, human immunodeficiency virus (HIV), and bacterial sepsis can also cause the occurrence of anti-cardiolipin as well as the intake of certain drugs (Vlachoyiannopoulos et al. 2007). But medications do not trigger anti-β_2-GPI formation and are also not associated with clinical symptoms (Bermas et al. 2014). In all of the above mentioned cases, a second positive test for antiphospholipid antibodies after 12 weeks can clarify the situation.

The differential diagnosis for CAPS includes HELLP syndrome (Haemolysis, Elevated Liver enzyme levels, Low Platelet count) as well as sepsis with multiorgan failure and disseminated

intravascular coagulation. These are difficult to distinguish from CAPS, because thrombotic microangiopathies occur in multiple organs simultaneously.

In summary, the most important antibodies are anti-β_2-GPI and anti-cardiolipin with the best specificity for anti-β_2-GPI. In commercially available anti-cardiolipin ELISA systems, β_2-GPI is always included in the test. Therefore these antibodies should be designated as “complex-specific” antibodies. Anti-prothrombin is not included in the Sapporo or revised Sydney classification due to test variance, but can provide additional information that might be helpful in some cases, where a definite diagnosis of APS is not straight forward.

3.1.5. Pathogenic mechanisms in APS

As diverse the antibody repertoire, as diverse the pathogenic mechanisms they induce. Antiphospholipid antibodies activate cellular components, such as platelets, endothelial cells and monocytes as well as responses on the molecular level, including the coagulation cascade and complement (Mehdi et al. 2010) (an overview is depicted in Figure 5).

For the role of β_2-GPI itself, many possible modes of action have been proposed on how it might interfere with different steps of the coagulation cascade. These include procoagulant as well as anticoagulant properties (Miyakis et al. 2004). Anticoagulatory effects are thought to be due to inhibition of prothrombinase as well as tenase activity and factor XII autoactivation (Nimpf et al. 1986; Schousboe & Rasmussen 1995). Thereby, the role of β_2-GPI is rather indirect. By binding to negatively charged phospholipid surfaces it reduces the binding sites essential for the assembly of the prothrombinase and tenase complex, respectively. Also for the autoactivation of factor XII, phospholipids are essential. In this context, binding of anti-β_2-GPI to β_2-GPI further enhances this inhibitory and therefore anticoagulant effect. On the other side, binding of β_2-GPI to phospholipid surfaces in a competitively manner is also the reason for reduced activated protein C levels leading to a procoagulant state (Yasuda et al. 2004). Additionally, anti-β_2-GPI can interact with enzymatic domains of serine proteases such as protein C, protein S, thrombin, and tissue plasminogen, thereby also hampering fibrinolysis (Mehdi et al. 2010). Interestingly, β_2-GPI deficiency itself does not lead to altered hemostatic and fibrinolytic markers, indicating that affected persons are not at a higher risk of thrombosis than individuals with normal plasma levels of β_2-GPI (Miyakis et al. 2004). This all leads to the assumption, that the impact of β_2-GPI and anti-β_2-GPI on the coagulation cascade is rather indirect and other factors seem to play a more critical role in the development of thrombotic events.

Activation of the complement system

Agostinis et al. investigated a "non-complement-fixing" human antibody, which means it binds to domain I of β_2-GPI but its F_c part was not recognized by complement component C1. This neither lead to a procoagulant state nor to proabortion activity (Agostinis et al. 2014). Thereby, they could

link complement-mediated thrombosis and pregnancy complications to one type of antibody, being responsible for the onset of two completely different symptoms. The role of complement activation by antiphospholipid antibodies (aPL) has been studied intensively. As mentioned above, there are three pathways of complement activation, the classical, lectine and alternative pathway.

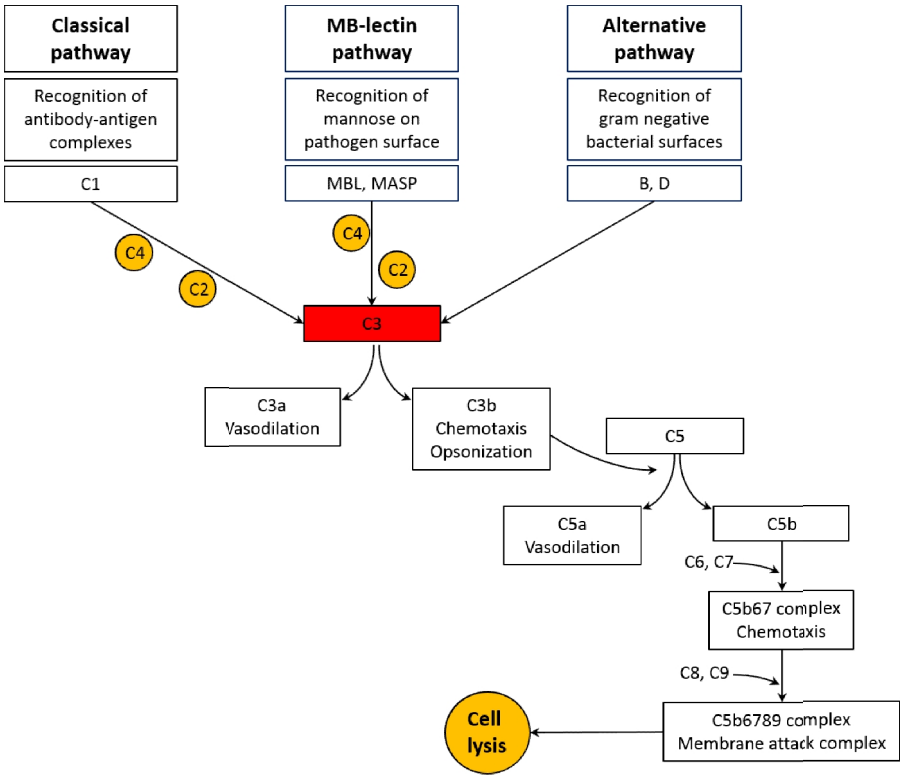

Figure 4: Schematic presentation of the three pathways of complement activation, namely classical, MB-lectine, and alternative pathway. All lead to activation of complement component C3. Adapted from Janeway et al. 2001a; Noris & Remuzzi 2013.

The first has been associated predominantly with the APS (Agostinis et al. 2014; Oku et al. 2009). IgG and IgM antibodies bound to antigen are recognized by C1. This starts a cascade via complement components C2 and C4, which leads to the cleavage of C3 into its subunits C3a and C3b (Figure 4) (Janeway et al. 2001). These subunits have different functions: they label invaders for their destruction by cells of the immune system (opsonization), trigger inflammation (e. g. vasodilation) and act as proteases, cleaving further components of the complement system. Binding of C3a to a C3a-receptor on platelet surfaces causes their activation, adhesion and aggregation. C3b promotes phagocytosis and is itself responsible for the cleavage of C5 into its subunits C5a and C5b. C5a binds to C5a-receptor and stimulates tissue factor (TF) expression (on monocytes, neutrophils, and endothelial cells) as well as plasminogen activator inhibitor 1 (PAI-1) upregulation (on mast cells and basophils). Both mechanisms promote a procoagulant state. C5b participates in formation of the membrane attack complex (MAC) (Nayer & Ortega 2014; Mehdi et al. 2010). The MAC, composed of C5b, C6, C7, C8, and C9, causes cell lysis but also triggers coagulation. Shedding of vesicles is stimulated, that support the formation of the prothrombinase complex by activating the extrinsic

pathway of the coagulation cascade (Fischetti et al. 2005). Therefore, aPL, namely anti-cardiolipin, anti-β_2-GPI and LA, but also anti-prothrombin/phosphatidylserine, facilitate a hypercoagulable state by increased complement activation (Oku et al. 2009).

Besides C5a-mediated TF release, Redecha et al. have shown that the interaction of C5a with its receptor also recruits and activates neutrophils (Redecha et al. 2007). The transmigration of neutrophils was experimentally linked to fetal tissue injury (Girardi et al. 2003). By infiltration into decidual tissue neutrophils can initiate placental thrombosis causing fetal death (Pierangeli et al. 2005). This also implies a critical role for complement activation in this context.

Activation of cells of the immune system

More than 10 different cell receptors have been suggested, where complexes of anti-β_2-GPI and β_2-GPI can bind to (de Groot et al. 2012) (Figure 5). These include apolipoprotein E receptor 2 (apoER2) on platelets and annexin A2 as well as A5 and toll-like receptors TLR-8 and TLR-4 on endothelial cells and monocytes (Mehdi et al. 2010). A signal transduction cascade is started, mainly based on p38 mitogen-activated protein kinase (p38 MAPK) and nuclear factor-κB (NF-κB) (Nayer & Ortega 2014). NF-κB is translocated into the cells' nucleolus and the expression of several proteins is upregulated. These include tissue factor (TF) and adhesion molecules like intercellular cell adhesion molecule-1 (ICAM-1), vascular cell adhesion molecule-1 (VCAM-1), and E-selectin. Latter are exposed on the cell surface of endothelial cells (Espinola et al. 2003) leading to an enhanced adherence of monocytes and leukocytes to endothelium and a hypercoagulable state (Horstman et al. 2009; Hanly 2003). Prostaglandines as well as proinflammatory cytokines (IL-2, IL-6, IL-8, TNF-α) are secreted. Also the expression of glycoprotein IIb/IIIa (GPIIb/IIIa), a fibrinogen receptor, located on platelet surfaces is stimulated. It plays an important role in platelet aggregation (Espinola et al. 2002).

Ames et al. detected an upregulation of PAI-1 in patients with aPL, while tissue plasminogen activator (tPA) was reduced in these individuals (Ames et al. 1996). The enhanced expression of PAI-1 results in a PAI-1/tPA imbalance which might be responsible for a hypofibrinolytic state in APS patients. Furthermore, annexin A2 is a receptor for tPA and plaminogen and facilitates plasmin generation through tPA-mediated plasminogen preoteolysis (Nayer & Ortega 2014). Also β_2-GPI is important as it is a cofactor for tPA. Therefore, aPL can inhibit tPA dependent fibrinolysis by blocking β_2-GPI and interfering with annexin A2.

However, activation of platelets, endothelial cells and monocytes, as illustrated above, seems not to be sufficient alone for thrombosis, as stated by several groups (Horstman et al. 2009; Bermas & Schur 2014; de Groot & Urbanus 2012; Cervera et al. 2014). Initial weak or subclinical aPL activation of target cells induces a prothrombotic state, but a so called "second hit" is required to develop the full-blown syndrome. Involvement of complement by F_c interaction might be a key step. Other potentially candidates for the "second hit" include vascular injury, an increased inflammatory

state, pregnancy and the postpartum period, oral contraceptives, hypertension or something completely different. In most of the described CAPS cases, the triggering "second hit" was an acute viral or bacterial infection (Cervera et al. 2014).

Taken together, antiphospholipid antibodies might have some effects on the coagulation cascade, but their main pathogenic mechanisms are focussed on cells and proteins of the immune system like endothelial cell and monocytes or complement. Therefore, forward-looking therapies should focus on the suppression of misguided response mechanisms of the immune system.

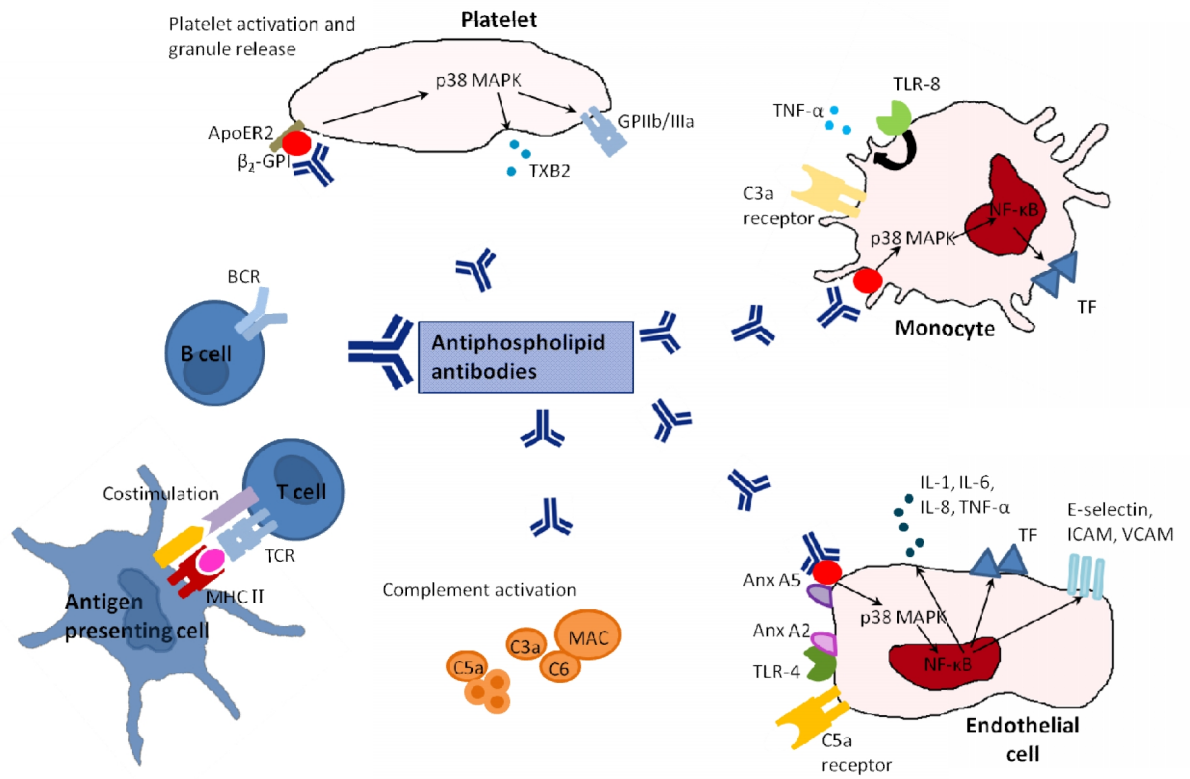

Figure 5: Schematic picture of the patho-physiological processes induced by aPL. C3a and C5a refer to the activated complement proteins 3 and 5, respectively. Activation of complement results in formation of MAC. Binding of aPL to apoER2 leads to activation of p38 MAPK pathway, TXB2 (thromboxane B2) generation, upregulation of GPIIb/IIIa and to further activation of platelets. Endothelial cells and monocytes are activated trough TLRs and annexin A2 (Anx A2) which leads to expression of adhesion molecules like ICAM and VCAM, upregulation of tissue factor (TF), and release of proinflammatory cytokines, such as IL-1, IL-6, IL-8, and TNF-α. BCR and TCR refer to B-cell and T-cell receptor, respectively, MHC to major histocompatibility complex. Modified from Mehdi et al. 2010.

3.1.6. Treatment of APS patients

The optimal management of different APS patients is still a challenge. Venous thrombosis is the most reported clinical manifestation (about 32 %). Up to now the initial treatment is still based on intravenous unfractionated or subcutaneous low-molecular-weight heparin (UFH and LMWH) rather than immunosuppressives (Wong & Favaloro 2008; Jayakody Arachchillage & Greaves 2014). The anticoagulant properties of heparin are based on its promotion of the *in vivo* inactivation of coagulation factors. But it also binds to the lysine-rich domain V of β_2-GPI, inhibiting its adsorption to

phospholipid surfaces (Miyakis et al. 2004). Recommended is a target international normalized ratio (INR) of 2.0 to 3.0. It reduces the risk of recrudescence to 80-90 %. After 7-10 days the treatment with UFH or LMWH is followed by oral anticoagulants.

Girardi et al. investigated the protective effects of heparin during pregnancy due to preventing complement activation (Girardi et al. 2004). They found, that complement activation via the classical pathway is inhibited by UFH and LMWH, thereby preventing obstetrical complications. Meanwhile, a combination of LMWH and low dose aspirin is recommended during pregnancy. Postpartum LMWH should be given for another 6 weeks unless a deep vein thrombosis has occurred. In this case a lifelong medication with oral anticoagulants is necessary (INR 2.0-3.0).

It has been shown, that thromboprophylaxis based on long-term anticoagulation therapy leads to significantly reduced recurrence of thrombotic complications in APS (Espinosa & Cervera 2010). However, antiphospholipid antibodies lead to multifactorial symptoms and up to 30 % of APS patients suffer from recurrent thrombotic events (Comarmond & Cacoub 2013). Furthermore, in 2-3 % bleeding complications can arise from conventional anticoagulation therapy. Therefore, the "ideal" treatment of APS is different for every patient. Current therapies are mainly restricted to anticoagulation and therefore only address the symptoms associated with APS. This might not be sufficient for all APS patients.

As outlined above, aPL have many pathogenic effects, like the activation of platelets, endothelial cells and monocytes. New therapeutic strategies should be designed to target these reactions (Figure 6). There are several possibilities that have been speculated to constitute a benefit for managing APS. These include inhibitors for the aPL receptors TLR-4, TLR-8, and annexin A2, but also for components of the signaling cascade like p38 MAPK and NF-κB. Targeting proinflammatory and prothrombotic cytokines, namely IL-1, IL-6, and TNF are further alternatives. Hydroxychloroquine (HCQ) for example has several immunological effects, like inhibition of proinflammatory cytokines or TLR activation (Erkan et al. 2014; Comarmond & Cacoub 2013). Humanized monoclonal antibodies like eculizumab or rituximab inhibit cleavage of complement component C5 and are responsible for B cell depletion, respectively. Agents, that downregulate TF expression on activated endothelial cells and monocytes, are potential therapeutic options. These include defibrotide (an adenosine receptor agonist) and dilazep (an adenosine uptake inhibitor and anti-platelet agent). Similarly, increased levels of GPIIb/IIIa on platelet membrane surfaces due to their activation could be managed with specific GPIIb/IIIa inhibitors, such as abciximab (Mehdi et al. 2010). Finally, statins that are usually administered to lower cholesterol levels also have anti-inflammatory properties. They lower the amount of expressed adhesion molecules probably due to p38 MAPK and NF-κB signal transduction inhibition. However, all of these agents discussed above have not been studied adequately for

treatment of APS and more cohort studies have to be performed to address the risks and side effects of these therapies.

Treatment of catastrophic APS (CAPS) is even more difficult due to the low frequency of its occurrence. Anticoagulation, corticosteroids and plasma-exchange are recommended as combination during a first-line therapy. Corticosteroids inhibit cytokine release and plasma-exchange removes pathogenic aPL as well as cytokines and complement proteins. This treatment led to a recovery rate of 77.8 % (Bucciarelli et al. 2009). On the course of CAPS management, plasma-exchange can partly be substituted by intravenous immunoglobulins.

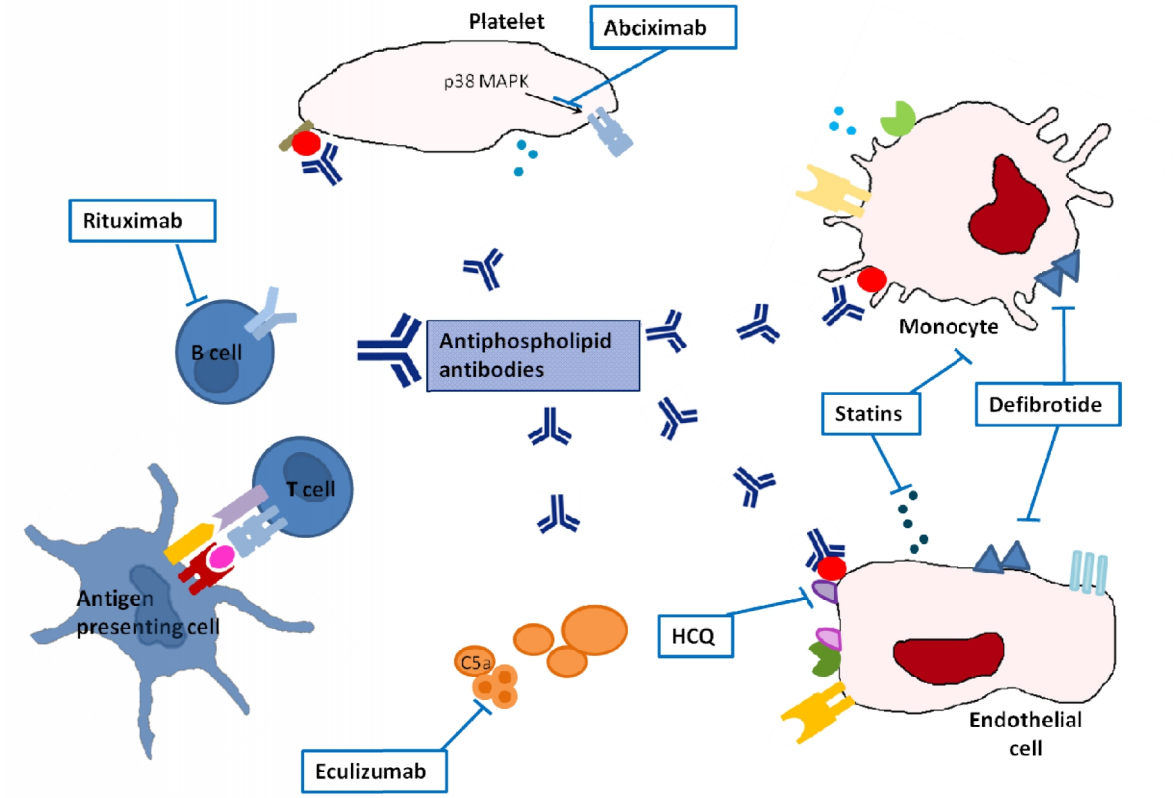

Figure 6: Possible action of new treatment opportunities include the use of therapeutic, humanized monoclonal antibodies (abciximab, rituximab, eculizumab), adenosine receptor agonist (defibrotide), statins and hydroxychloroquine (HCQ) (Mehdi et al. 2010).

In summary, the development of targeted treatments is still in progression. Current therapies focus on the management of APS-associated thrombosis, while immunosuppressive strategies are not recommended up to now. But they might be an option worth investigating. To this end, more cohort studies are required with higher patient numbers. Furthermore, the heterogeneity of APS-relevant antibodies needs to be considered. A more detailed analysis of the antibody spectrum can provide a first step towards targeted therapy.

3.2. Biosensors

3.2.1. Definition

The development of a biosensor, capable of detecting multiple APS-associated autoantibodies in parallel was the central aspect of this thesis. The goal was to find optimal immobilization and buffer as well as regeneration conditions for multiplexed, repeated detection of APS antibodies in serum. First of all, in this thesis, as is conventional in the field of biosensors, the biochemical recognition element, immobilized on the sensor surface, is referred to as ligand, and the biomolecular interaction partner, detected in a sample, is termed analyte.

According to the International Union of Pure and Applied Chemistry (IUPAC), a biosensor is defined as "a device that uses specific biochemical reactions mediated by isolated enzymes, immunosystems, tissues, organelles or whole cells to detect chemical compounds usually by electrical, thermal or optical signals" (Nagel et al. 1992). It is a self-contained device, which can provide quantitative or semi-quantitative analytical information. A biochemical receptor, i. e. a biological recognition element, is combined with an transduction element (detector) (Thévenot et al. 2001). A biosensor should be capable to monitor the analyte concentration continuously or reproducible after a regeneration step. If this is not the case it should be designated as single-use biosensor, like the pregnancy or glucose tests for example.

3.2.2. Challenges in biosensor development

Challenges in biosensor development are various especially for label-free detection. An appropriate immobilization of the ligand is essential. This is complicated by many factors, such as the type of immobilized protein and its functionality, protein stability and surface topography (Tan et al. 2011). Denaturation and orientation are just two aspects that have to be considered. A protein might lose its natural conformation due to different solvent, pH change, or simply by covalent attachment to a solid surface. The disruption of the antigen tertiary structure might cause a loss in binding ability and antigeneity. Also, orientation of the immobilized antigen is of importance. Random orientation results from unspecific immobilization for example via amine coupling reaction. Uniform orientation can be achieve by so called capture assays, a technique that applies monoclonal antibodies for antigen immobilization or by use of antigens with a certain tag. Both methods have their preferences and draw backs. A random orientation might detect polyclonal antibodies, whereas a site-specific immobilization might lead to a more sensitive surface concerning one type of antibody to be detected. Furthermore, immobilization of antigen on a three-dimensional matrix does not necessarily require an oriented ligand (Johnsson et al. 1995). This leads to the question what surface matrix to use? A three-dimensional sensor surface as achieved with dextranes for example creates a high ligand content but often causes increased unspecific binding. This is especially the case when

analyzing complex biological fluids such as serum or plasma, which contain many sticky proteins like fibrinogen (Ericsson 2013). Nonspecific protein adsorption occurs when the adsorbed state is more energetically favored than the solubilized form. Electrostatic or hydrophobic interactions are the main causes of unspecific binding to the sensor surface. On a two-dimensional surface like self-assembled monolayers (SAMs) this is reduced as is also the content of immobilized ligand. Next, the optimal buffer conditions have to be chosen. Salt concentrations and pH adjustment can minimize electrostatic interactions (Johnsson et al. 1991). Additives like bovine serum albumin (BSA) or fetal calf serum (FCS) can block unspecific binding to the sensor surface. Some interactions require the presence of ions for binding activity. Finally, a classical biosensor requires the regeneration of the antigenic surface. Antibody regeneration is achieved using alkaline or acidic solutions, or with high ionic strength as for example 6 M guanidine hydrochloride. All of them are potentially harmful to the immobilized ligand and its antigeneity. Its stability after regeneration as well as its lifetime in terms of regeneration cycles has to be tested properly (Luppa et al. 2001).

Taken together, many variables need to be carefully assessed during biosensor development. These mainly include the surface chemistry, ligand orientation and buffer as well as regeneration conditions.

3.2.3. Protein microarrays

Microarray techniques have become a versatile tool for fast and high-throughput screenings. The first parallelized screenings have their origin in the Southern blot. A technique invented by Ed Southern in 1975 that uses fixed single-stranded DNA and labeled complementary strands to monitor their hybridization (Maskos & Southern 1992). The miniaturization for complex gene expression profiling was first reported in 1995 (Schena et al. 1995) and was a big step forward in microarray technology. Since then arrays are of growing importance and applied also in other fields of biomolecular interactions. There are many reviews dealing with this topic (Zhu & Snyder 2003; Hartmann et al. 2009; Kattah et al. 2008; Seidel & Niessner 2008; Balboni et al. 2006; Ekins 1998; Kricka et al. 2006; Yeste & Quintana 2013). Microarrays are applicable in a wide field of interaction studies, including antigen-antibody, protein-lipid, protein-drug, enzyme-substrate, receptor-ligand, protein-nucleic acid, nucleic acid-nucleic acid, and many more (Zhu & Snyder 2003). Fully automated printing robots further promoted their implementation. They simplified the application of hundreds of spots each with a diameter of less than 1 nm to the sensor surface (Bleher et al. 2014).

3.2.4. Biosensor surface generation

Due to relevance, this section will focus predominantly on protein immobilization and roughly touch lipid immobilization on glass transducers.

SiO_2 surfaces can be coated with polymers like amino dextran (AMD) or amino functionalized polyethylene glycol (PEG). With the former, a three-dimensional surface matrix is created with high ligand capacity. Latter can form a three- or two-dimensional coating, depending on whether PEGs of one length or varying lengths is used. Another approach is based on short silanes that form two-dimensional surfaces likewise an SAM (Senaratne et al. 2005). SAMs are made of small organic molecules that assemble spontaneously on a surface by adsorption, forming a two-dimensional brush-shaped surface coating. Among others, the most common compounds are thiols, silanes and phosphonates. They are often used for the modification of gold chips. The initial fast step of chemisorption can occur from either vapour or liquid phase and is followed by a slow organization step of the alkyl chains (Häkkinen 2012; Ulman 1996). Latter can take several hours. Due to van der Waals interactions, the alkyl chains pack tightly. The functional group at the end of the alkyl chain can be further modified. Density of the exposed antigen on a two-dimensional surface is less compared to three-dimensional coatings but it has been shown that unspecific binding of serum matrix was diminished on a two-dimensional sensing surface (Bleher et al. 2014). Whether the antigen density is efficient enough in terms of sensitivity and whether unspecific binding is a problem or not has to be evaluated for every biosensor surface independently.

As mentioned above, a critical aspect in biosensor development is the appropriate presentation of the antigenic structure on the surface. There are many immobilization strategies to address this issue, which have been focused on proteinogenic ligands. But also for peptides, DNA or RNA, carbohydrates and other organic molecules like lipids there are several methods that are well established (Homola et al. 2006). The different strategies can be classified into three main categories: physical, covalent, and bioaffinity immobilization (Tan et al. 2011).

Physical immobilization

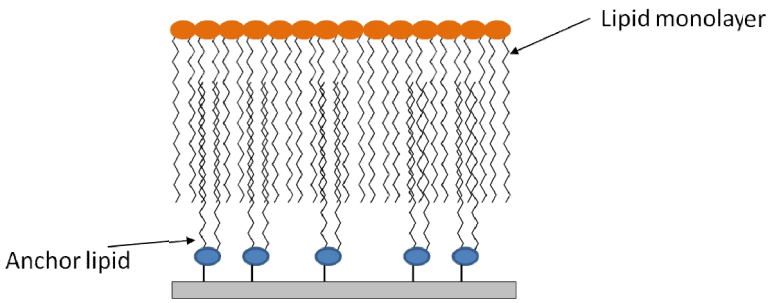

Figure 7: Adsorption of a lipid monolayer to a planar surface modified with lipid anchors.

The spontaneous adsorption of proteins to a sensor surface was an early procedure in surface plasmon resonance (SPR) technology due to its' simplicity (Liedberg et al. 1983). It is driven by intermolecular forces, mainly electrostatic, hydrophobic, and polar interactions and results in a non-covalent attachment of the ligand with random orientation (Rusmini et al. 2007). A major drawback

is a possible loss of activity due to a reorganization of the adsorbed protein. For example, hydrophobic segments of the ligand rearrange to be able to interact with a hydrophobic surface. Thereby the thermodynamic state is optimized, which in turn can interfere with functional properties that are altered during this process (Homola et al. 2006).

Immobilization techniques based on physical adsorption have also been developed for lipids (Hilbig et al. 2012). They can be injected as vesicles and upon contact with a planar surface the spherical shaped complexes open up. The lipids align in a monolayer with the hydrophilic head groups facing the aqueous solution (Homola et al. 2006). This can be facilitated by so-called lipid anchors like DSPE-PEG (1,2-distearoyl-sn-glycerol-3 phosphoethanolamine-N-carboxypoly(ethylene glycol)). With this modification, lipid membranes can easily be tethered to a surface (Figure 7).

Physical immobilization of proteins as well as lipids often results in high background signals caused by nonspecific interactions. This drastically lowers sensitivity and selectivity (Rusmini et al. 2007). Furthermore, a regeneration of the sensor surface leads to removal of the ligand, which has to be immobilized again after every regeneration step. Therefore, the surface slightly varies for every measurement and a good reproducibility is not guaranteed.

Covalent immobilization

In contrast to physical immobilization, a more controlled antigen presentation can be achieved by chemical reaction of a functionalized surface with another functional group of the ligand.

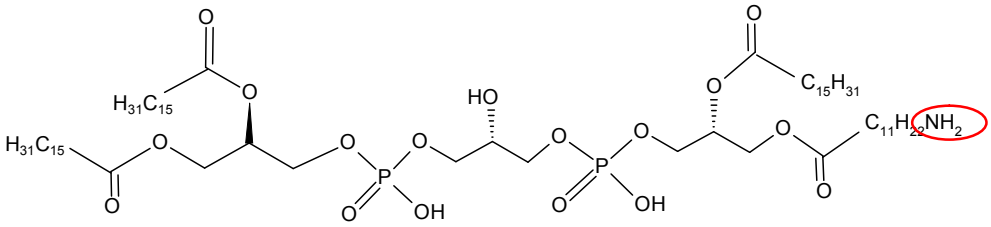

Figure 8: Structure of a ω-amine cardiolipin synthesized by the group of Andrew B. Holmes (Johns et al. 2009).

Lipids usually do not contain functional groups at their hydrocarbon chains. A covalent immobilization can be accomplished via their head groups, unless the head group is not required for recognition. As mentioned in chapter 3.1.2.2 in this section, the exposition of the β_2-GPI epitope is dependent on its interaction with the negatively charged head groups of cardiolipin. Therefore, an immobilization of the cardiolipin via its head group would prevent this interaction. The ω-amine cardiolipin utilized, was synthesized by the group of Prof. Dr. Andrew B. Holmes (Johns et al. 2009). It exhibits an amino group at the end of one carboxylic chain, as depicted in Figure 8.

Nucleophiles, like primary amines, are prone for the most widely used immobilization technique, the amino coupling. In the case of proteins, primary amines are found in lysine residues. They can react with carboxyl groups to form peptide bonds. First, the carboxyl groups on the sensor platform are activated by carbodiimides like N,N'-diisopropycarbodiimide (DIC) or

1-ethyl-3-(3-dimethylaminopropyl)carbodiimide hydrochloride (EDC). Thereby, an ester is formed, so reactive, it would rapidly hydrolyse in aqueous solution. Derivatisation with N-hydroxysuccinimide (NHS) results in an ester that is more reactive than the original carboxyl group, but still stable for several hours (half-life is about 4-5 h at pH 7.0; a reaction scheme is depicted in Figure 9) (Hermanson 2008). Amine coupling reaction is irreversible, most often random, and generally not limited to a single bond between surface and ligand. This is due to the fact that any protein typically exhibits several functional side chains of one amino acid leading to multipoint attachment.

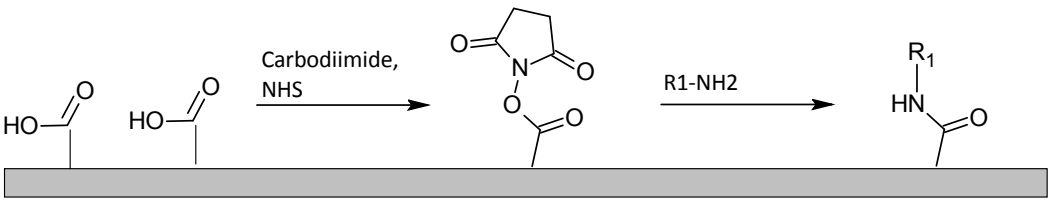

Figure 9: Amine coupling reaction. After activation of carboxyl groups, primary amines as found in lysines can be attached to the surface by formation of peptide bonds (Homola et al. 2006).

The second important surface chemistry is based on thiol coupling. It utilizes cysteine thiol groups that form stable thioether bonds with maleimide-, disulfide-, or vinyl sulfone-derivatized surfaces (Rusmini et al. 2007). Figure 10 shows the reaction procedure. One advantage is a more directed immobilization than with amine coupling, since cysteines are not as abundant as lysine residues. A drawback might be a limited stability under certain conditions. Buffers containing thiols like mercaptoethanol can induce a cleavage of the disulfide bonds and therefore a dissociation of the ligand (Homola et al. 2006).

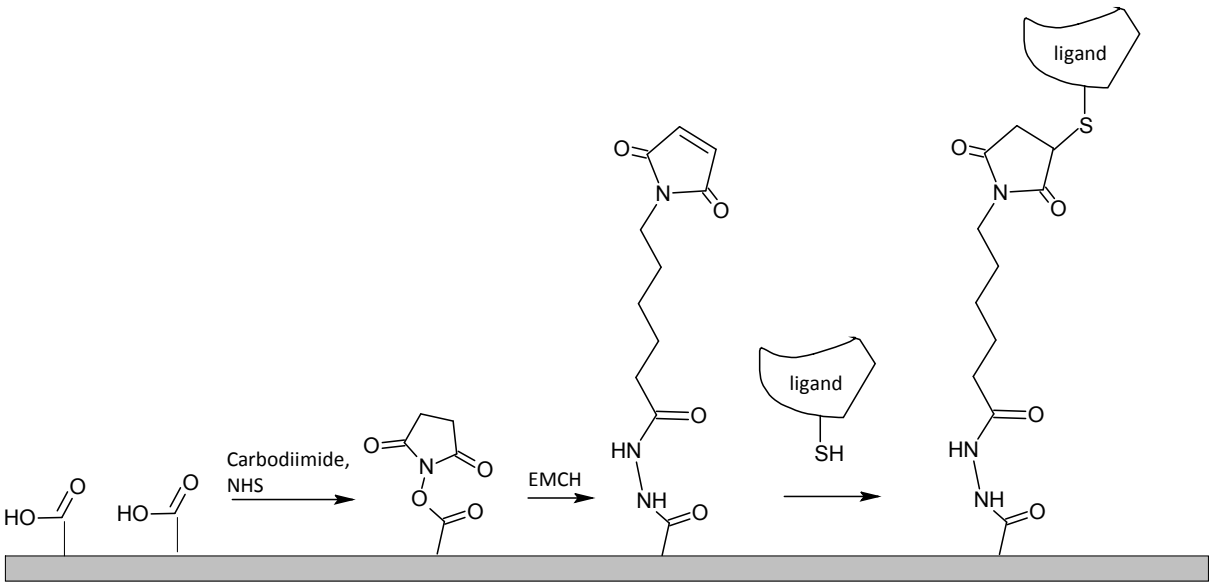

Figure 10: Thiol coupling chemistry. After activation of the surface and modification with 3,3´-N-[ε-Maleimidocaproic acid] hydrazide (EMCH), cysteine side chains can be coupled to the surface (Homola et al. 2006).

Besides amino and thiol coupling, carboxyl and hydroxyl groups are possible options. Table 2 summarizes commonly used amino acid side chains for immobilization together with the respective surface modification required. Other covalent immobilization strategies include click and photoactive chemistry. The former is based on the reaction between small modular units that are coupled to different substances, like the Huisgen cycloaddition of an azide and an alkyne (Huisgen 1961). In photochemical reactions, the sensor surface is modified with a photolabile agent. These can be activated by irradiation of ultraviolet light with a wavelength ≥ 350 nm that is not harmful for proteins or cells (Ericsson 2013).

Table 2: Overview of possible immobilization techniques for different amino acid side chains (Rusmini et al. 2007).

Amino acid side chain	Amino acid	Functional groups on surface
-NH2	Lysine Hydroxyl-Lysine	Carboxylic acid Active ester (NHS) Epoxy Aldehyde
-SH	Cysteine	Maleimide Pyridyil disulfide Vinyl sulfone
-COOH	Aspartic acid Glutamic acid	Amine
-OH	Serine Theronine	Epoxy

Bioaffinity immobilization

Bioaffinity reactions provide a gentle immobilization procedure with oriented ligand presentation. Especially in cases in which covalent binding of the ligand would cause a denaturation or loss of functionality this is a preferred technique. But also for the immobilization of small amounts of a specific protein within a complex solution (Homola et al. 2006). The most common approaches use F_c receptors, like recombinant protein A/G for antibody immobilization. Fusion tags like glutathione S-transferase (GST) or poly(His) can be applied for coupling to glutathione- or nickel-nitrilotriacetic acid (Ni-NTA)-modified sensor surfaces (Ericsson 2013; Rusmini et al. 2007). Another possibility is the streptavidine-biotine reaction and with an affinity constant of 10^{12} to 10^{14} it is almost as strong as covalent attachment (Borisov & Wolfbeis 2008). A ligand immobilized via bioaffinity reaction can be removed by regeneration solutions and then a renewed capture can be performed for the next cycle. Thereby a steady quality is achieved but the sample consumption is

increased (Homola et al. 2006). Also the interaction has to exhibit a minimum stability to avoid dissociation during the whole measuring cycle.

3.2.5. RIfS – reflectometric interference spectroscopy

Optical detectors are the most diverse class of biosensors in bioanalysis (Fan et al. 2008). They monitor changes in absorption, fluorescence, Raman, refractive index, evanescence, luminescence or scatter and can be applied in either label-free or labeled techniques. Reflectometric interference spectroscopy (RIfS) is a label-free technique that uses basic optical principles.

Basic principles

In 1678, the dutch physicist Huygen developed what we today call the Huygens' principle:

Every point on a wave-front may be considered as a source of a new spherical wavelet that spreads out with the same speed and frequency as the primary wave-front. The tangential surface of all secondary wavelets results in the new wave-front (Tipler & Mosca 2003a).

It describes the propagation of every wave-front. For example, a wave-front at time t and radius r has at the time $t + \Delta t$ a radius of $r + c\,\Delta t$, with c being the speed of propagation (speed of light). If the wave-front hits a hindrance or a different medium, the position of the new wave-front is altered. This was the basis for the derivation of the refraction as well as the reflection law. The speed of light, c, is different for every medium and can be used to calculate the index of refraction, n, a characteristic of all transparent media:

$$n = \frac{c}{v}$$

Thereby, v refers to the velocity of light in the particular medium.

When a light beam hits an interface of two different media, for example air and glass, part of the light is reflected and part enters the second medium. If the angle of incidence is not perpendicular to the surface, the direction of the transmitted is not the same as for the incident light. This effect is known as refraction. The angle of refraction depends on the angle of incidence and the difference in the speed of light between the two media. This correlation was found in 1621 by Willebrord Snellius and is therefore termed Snell's law (Tipler & Mosca 2003a). For the reflected ray, the emergent angle is equal to the angle of incidence. This is called the law of reflection. When the angle of incidence exceeds a critical degree, all of the light is reflected and no light is transmitted into the second medium. This is called total internal reflection.

Huygens' principle was later modified by Augustin Fresnel in a way that the new wave-front can be calculated from the old wave-front by the superposition of the single wavelets. Thereby taking into account their relative amplitude and phase. The superposition of two or more propagating waves is called interference. It can take place, if the interacting waves are from the same source or

exhibit the same or almost the same frequency. The resulting wave displays higher amplitude in the case of constructive or lower amplitude in the case of destructive interference.

When a light beam with the intensity of 1 hits a surface, it splits up in a reflected (*R*), a transmitted (*T*) and an absorbed part (*A*), whereat the latter is negligible for a dielectric:

$$1 = R + T + (A)$$

The amplitudes of the transmitted and the reflected components can be quantified using Fresnel's equations, thereby superimposing the emerging wavelets to a new wave-front. To this end, it has to be differentiated between perpendicular and parallel polarized light regarding the plane of incidence. This results in the reflectance and transmittance at an interface between two media with different refraction indices depending on the angle of incidence.

Reflectometric interference spectroscopy

RIfS is an optical phenomenon occurring when light hits a transparent film and is partially reflected at parallel interfaces which are 0.5 to some 10 µm apart (Leopold et al. 2009). In principle, a light beam hits a sensor glass chip from the bottom where part is reflected, while the other part is transmitted. The transmitted ray hits the next interface and is again partially reflected and partially transmitted and so on. Therefore, the reflected parts, travel different optical paths and a phase difference is introduced. On condition that the optical path length through these layers is smaller than the coherence wavelength, an interference of the reflected light beams can occur. The coherence length is deduced from the coherence time and is defined as the maximum shift between two reflected waves where a stable interference pattern can be produced (Proll et al. 2007; Tipler & Mosca 2003b).

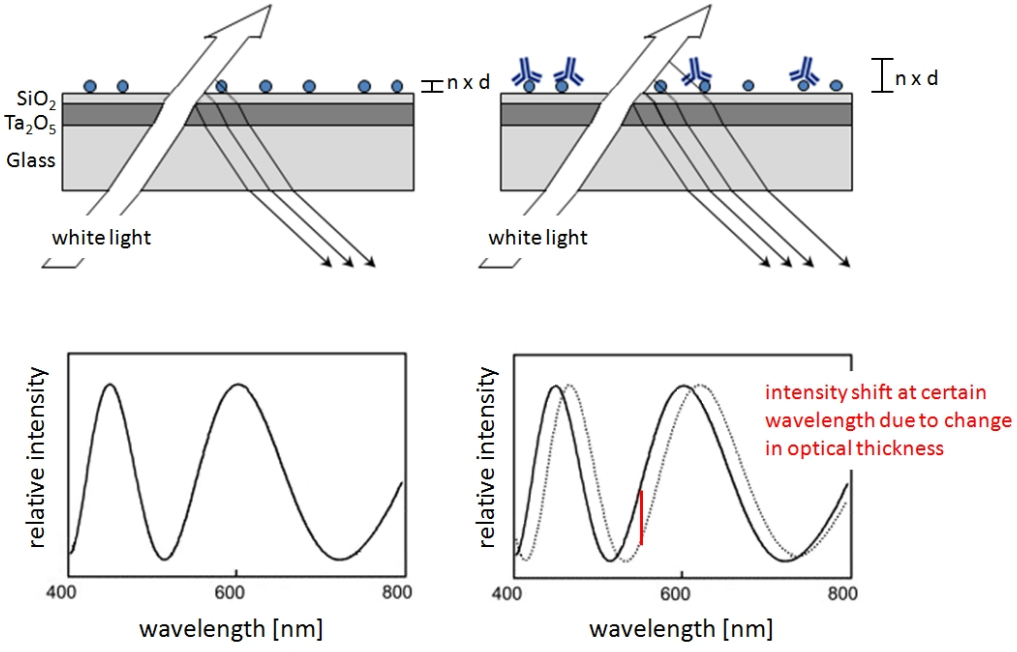

Figure 11: Schematic drawing of the underlying principle of RIfS; from Ewald et al. 2013.

In summary, the superposition of the reflected light beams and the resulting interference pattern is a characteristic for a certain chip-ligand-analyte layer system (Figure 11) (Gauglitz 2010). It depends on the wavelength of the incident light as well as the angle of incidence and the optical thickness (*od*) of the film, which is a product of physical thickness (*d*) and refractive index (*n*) (Schmitt et al. 1997).

$$od = n \times d$$

Interfaces of a biosensor include glass-matrix, matrix-ligand, ligand-buffer system or ligand-analyte. During a biomolecular interaction between a ligand, immobilized on the sensor surface, and an analyte, passing the surface in a buffer system, the optical properties in or at the top layer of the biosensor are altered. This results in a change of the interference spectrum, which is plotted as function of time and gives the binding curve of the analyte to the sensor surface.

1-λ-reflectometry

As a form of reflectometric interference spectroscopy, the 1-λ-reflectometry in particular uses monochromatic light and detects an intensity shift in the reflection spectrum at a certain wavelength and not over the whole spectrum of the visible light (see also materials & methods, chapter 5.11.1) (Ewald et al. 2013). With the 1-λ-reflectometry set-up, only one antigen-antibody interaction at a time could be detected. Therefore it was used for assay development.

Polarized imaging reflectometric interference spectroscopy (pi-RIfS)

With pi-RIfS, a parallel detection of multiple biomolecular interactions at the same time can be accomplished. A two-dimensional picture of the biosensor platform is generated by including a CCD-camera in the instrumental set-up (details of the instrumental set-up are depicted in Figure 12). Thereby, the intensity of the reflected light is monitored time-resolved and independently for every spot on the transducer (see also chapter 5.11.2) (Fechner et al. 2011).

Advantages of RIfS

As mentioned above, RIfS is a label-free technique and provides real-time measurements without any chemical modification of the analyte or usage of secondary antibodies. On-line monitoring of biomolecular interactions allows a separate evaluation of association and dissociation phases and by using serial dilutions of the analyte, a determination of kinetic rate constants (Gesellchen et al. 2003). Furthermore, the incident light has a depth of penetration into the solution of up to 40 µm, depending on the wavelength. Compared to SPR with 300 nm, RIfS thus enables the detection of cell-cell interactions (Möhrle et al. 2006).

RIfS, 1-λ-reflectometry as well as pi-RIfS, utilizes glass carrier chips, but also transducers made of plastic can be applied. A coating with gold as for SPR is not necessary, which makes them cheap consumables. (Ewald et al. 2013). The transducers are coated with a thin layer of tantalum pentoxide (Ta_2O_5), an optically transparent metal oxide. It comprises a high refractive index and coated as thin

film on substances with lower refractive index, such as glass, Ta_2O_5 displays an ideal waveguiding material (Schmitt et al. 2008). The SiO_2 coating on top is compatible with a series of bioconjugate chemistries.

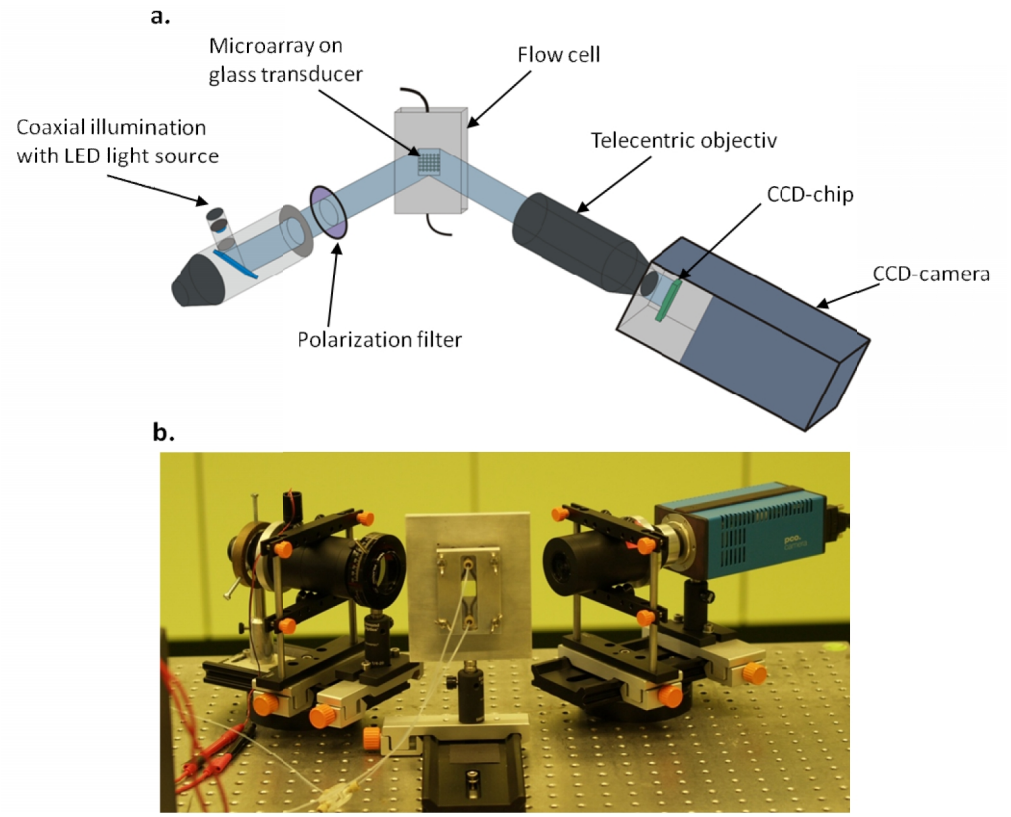

Figure 12: Scheme (a.) and picture (b.) of the technical pi-RIfS set-up. On the left of the flow cell there is a telecentric objective with LED for illumination and a polarization filter. On the right is aligned a CCD camera with a second telecentric objective for detection purposes. Adapted from Bleher et al. 2014, reprinted with permission of Springer © «2003».

Another major advantage of RIfS is that it is nearly temperature independent because physical thickness and refractive index change with opposing trends upon temperature fluctuations. Refractive index is dependent on the density which changes upon thermal expansion. This leads to a decrease in refractive index with increasing temperature. But thermal expansion also leads to an increase in physical thickness (Proll et al. 2007). Therefore, these two effects compensate and no temperature control device is necessary.

3.2.6. Receiver Operating Characteristic - ROC

Any classification model that is employed to differentiate between two groups can be evaluated in terms of sensitivity and selectivity. The performance is visualized with a Receiver Operating Characteristic (ROC)-analysis. Formerly it has been used in signal detection to discriminate between hit rates and false alarms (Fawcett 2003). In the late 1980s it has been extended to diagnostic systems. For a diagnosis, clinical tests are applied to distinguish between a pathological

indication (= positive) and a non-pathological finding (= negative). For every measured sample there are four possible outcomes: If the predicted result matches the experimental, the instance is true positive respectively true negative. If the predicted does not match the experimental finding, it is classified as false positive or false negative. This can be depicted in a confusion matrix:

	Positive (predicted)	**Negative (predicted)**
Positive (actual)	True positive (tp)	False negative (fn)
Negative (actual)	False positive (fp)	True negative (tn)

The amount of true positive patients detected within the group of all positives is termed senstitivity:

$$Sensitivity = \frac{tp}{tp + fn} \; ; sensitivity \; \in [0,1]$$

The part of true negative within all negatives is described by the specificity:

$$Specificity = \frac{tn}{tn + fp} \; specificity \; \in [0,1]$$

A ROC curve is generated as follows: every data point of a collective of positive and negative samples is set as cut off. For each situation sensitivity and specificity are calculated. The determined sensitivities are represented on the abscissas and 1-specificity on the ordinate. A diagonal is drawn from point (0/0) to (1/1). For a valid selectivity the ROC curve is in the left triangular. Finally the AUC (area under the curve) is calculated, which further describes the performance. It can adopt values between 0.5 and 1.0. The greater, the better the selectivity of the test.

4 results & discussion

4.1. Basic principles of reflectometric interference spectroscopy

The development of the immobilization strategy as well as buffer and regeneration conditions were mainly accomplished on the 1-λ-reflectometry system. Its simplified set-up included a sample inlet, a flow cell and a tubing pump (for details see materials & methods, chapter 5.11.1 and Figure 36). The sample inlet was made of a single tubing through which running buffer, analyte solution and regeneration was guided over the flow cell. It has to be mentioned, that the analyte solution could not be separated from the running buffer prior and after the injection phase. This leads to decreased analyte concentration at the beginning of the injection as well as in the end. A separation, for example by introduction of an air bubble between running buffer and analyte solution was not reasonable, because the air would have run over the flow cell as well, disturbing the measurement. A typical binding curve is depicted in Figure 13. In this case binding of the cofactor β_2-GPI to a cardiolipin-modified sensor surface was monitored. In general, a positive interaction of ligand and analyte is always characterized by a negative curve progression due to chip properties.

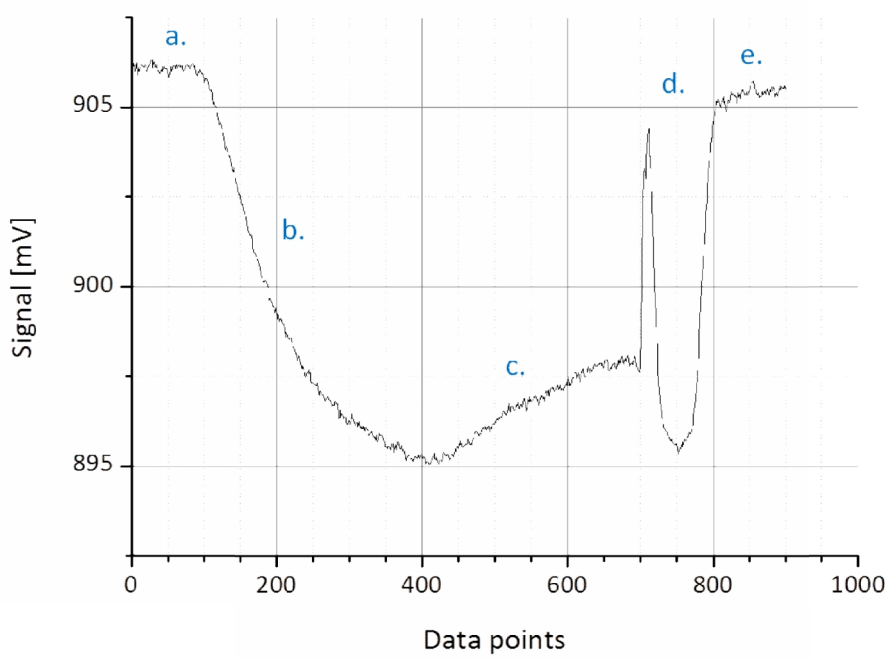

Figure 13: Typical binding curve detected with 1-λ-reflectometry. Specific interaction is indicated by negative curve progression. Association of analyte is followed by dissociation phase and regeneration of the biosensor surface.

Every measurement starts with a base line detected with running buffer (Figure 13, a.), followed by injection of the analyte solution. Although the analyte solution could not be separated from the running buffer, the onset of the binding event can be clearly located (Figure 13, b.). In the beginning, the curve progression is defined by strong association due to free ligand capacities. As more and more analyte is bound to ligand, association decreases and dissociation increases until an equilibrium is reached (here at around data point 400). Injection of the analyte was followed again by

running buffer (Figure 13, c.). Now, dissociation is the predominant process, in which unbound analyte that was adsorbed to the surface in an unspecific manner is washed away, as well as bound analyte, whose interaction with the ligand is broken up. The degree to which latter happens is defined by the dissociation constant. At around data point 650, a steady state is reached. Remaining analyte-ligand complexes do not dissolve by simply letting running buffer flow over the sensor surface. A regeneration is necessary to actively break up these interactions and to restore the sensor surface. Injection of the regeneration solution is indicated by the jump in refractive index (Figure 13, d.) caused by high salt concentration. Afterwards, running buffer is applied again until the base line is monitored (Figure 13, e.). When a single injection of regeneration solution is not sufficient, this step is repeated and, if necessary, followed by injection of an alternative regeneration solution. In a very few cases, the biosensor surface could not be restored adequately or the three-dimensional structure of the antigenic protein was altered in a way, recognition with a specific antibody was significantly reduced. Then, a new chip was placed into the flow cell and measurements repeated with a fresh biosensor surface.

Although all different phases of the interaction process can be assigned, i. e. association and dissociation, determination of kinetic parameters should not be performed with this experimental set-up due to uncertainty of the exact sample concentration. The amount of every applied solution (analyte solution, running buffer, regeneration solution) was constant between all measurements of one experiment. Still, slight differences in the length of every injection phase might occur, since every measurement was performed manually. Furthermore, the signal value (in mV) of the baseline varied for every sensor chip, due to small inconstancies in glass thickness between the chips. To overcome this problem, all values of one measurement (in mV) were divided by the first value, which resulted in a normalized signal and a better comparability between the transducers.

4.2. Biosensor development for anti-β_2-GPI detection using 1-λ-reflectometry

Immobilization strategy

A functional immobilization of the antigen is one of the first and crucial aspects in biosensor development. Different strategies and their advantages as well as disadvantages have been discussed in the introduction, chapter 3.2.4. Major differences concern the surface matrix, i. e. whether a two- or three-dimensional coating is used and if the ligand is immobilized covalently or non-covalently. Since there was a lot of experience with amino dextran (AMD) and polyethylene glycol (PEG) matrices on glass transducers for RIfS applications from our collaboration partner, these were the first choice.

Technical know-how for our 1-λ-RIfS set-up was accomplished by monitoring the interaction between cardiolipin and its cofactor β_2-GPI. We started with a nearly covalent immobilization

technique by using streptavidin-biotin interaction. To this end, chips were coated with PEG and AMD, respectively, and further modified with streptavidin (for details see materials & methods, chapter 5.7.3). Subsequently, a biotinylated cardiolipin analog was attached and remaining binding sites blocked with biotin. This approach allowed repeated analyte injection on the same surface and a direct comparison between the different measurements.

Testing of different flow rates and sample volume

Different conditions were tested that not only included the variation of the flow rate (20-40 µL/min), but also the sample volume (0.3-1.0 mL). Thereby, the total amount of analyte was the same for every measurement (15 µg), resulting in concentrations between 15 and 50 µg/mL, depending on the dilution factor. As negative control, transferrin was applied, which gave no positive binding signal (Figure 14).

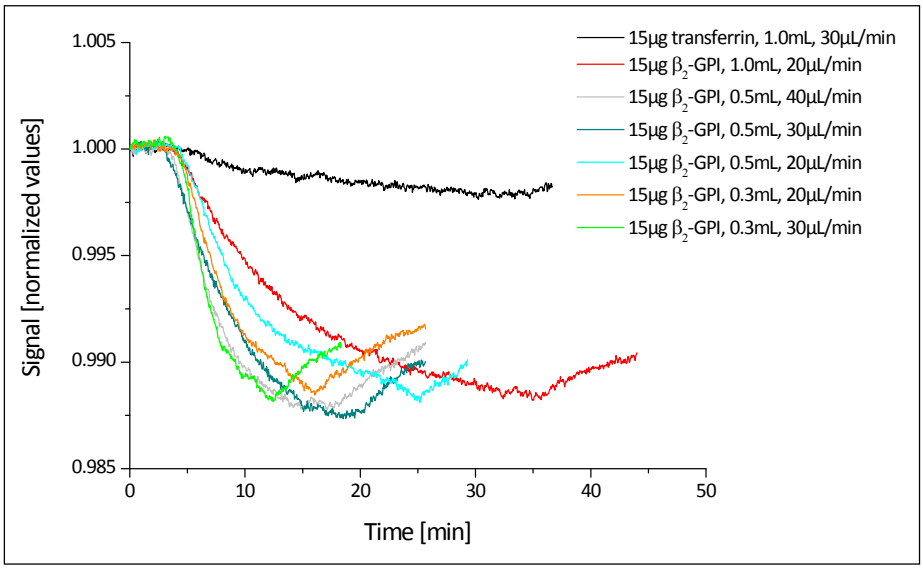

Figure 14: Different sample volume and flow rates for interaction analysis with the 1-λ-reflectometry.

Surprisingly, for the binding of β_2-GPI to the cardiolipin modified surface, neither the flow rate nor the sample volume did show a strong impact on total binding intensity (some of the curves are exemplarily shown in Figure 14). The maximum signal detected was comparable for all the measurements. For example, the light blue curve (0.5 mL, 20 µL/min) and the orange curve (0.3 mL, 20 µL/min) show the same binding intensity, although different concentrations are applied with the same flow rate and over a different time interval due to different sample volume. This means, if the total amount of injected analyte is the same, the sample volume (and therefore the dilution of the analyte) had no consequence, at least within the tested range. But curve shape and measurement feasibility were important limiting factors. For example a medium sample volume (0.5 mL) combined with a high flow rate (40 µL/min; grey curve) gave a smooth transition between association and dissociation (compare to **Figure 13:** Typical binding curve detected with 1-λ-reflectometry. Specific

interaction is indicated by negative curve progression. Association of analyte is followed by dissociation phase and regeneration of the biosensor surface.Figure 13, data point 400). A lot of analyte is flushed over the surface without interaction with the ligand. This might lead to lower signal intensities. Also, for a small sample volume (0.3 mL; high concentration), the medium flow rate (30 µL/min) was too fast and the shape of the curve is unsteady (light green). Finally, a high sample volume (1 mL) is not practicable on one hand, because measurements simply take too long. On the other hand, a high sample volume together with a low flow rate leads to a flattening of the binding curve and at some point to a reduced signal intensity, due to increased dissociation already during the association phase.

Taken together, the total amount of injected analyte is more important than its concentration, at least within certain boundaries. Below and above, concentration seems to have an impact on the curve shape and even further also on the binding intensity. This usually is a decrease in detected signal either because flow rate is too fast and most of the analyte just passes the sensor surface, or because dissociation is already strong during association phase caused by low concentration.

Binding of β_2-GPI to a cardiolipin-surface could be shown and was reproducible after regeneration (Figure 15). For these measurements, a flow rate of 30 µL/min and a medium sample volume of 0.5 mL were chosen. However, the injection of a specific polyclonal anti-cardiolipin did not give any binding signal (data not shown), which was tested several times on different glass transducers. Unspecific interaction of the β_2-GPI with the plain PEG surface could be excluded, since injection of 15 µg of β_2-GPI as well as BSA and transferrin without prior immobilization of cardiolipin in none of the cases led to observable signals, respectively (Figure 15).

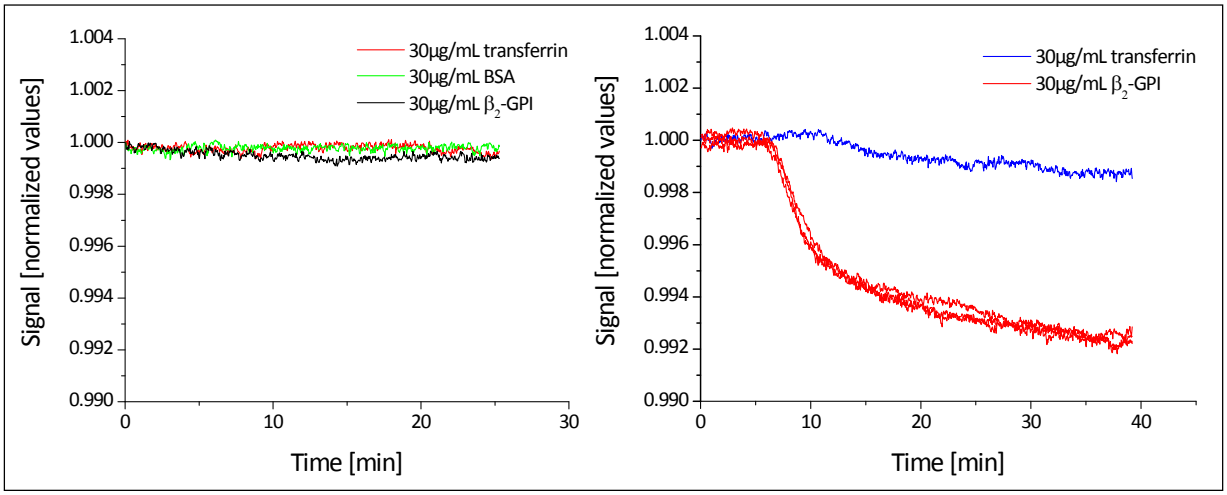

Figure 15: Unspecific binding to plain PEG surface could be excluded as shown by measurements with different protein solutions (left). Binding of cofactor β_2-GPI to immobilized cardiolipin gave positive binding signal in contrast to injections of transferrin over the same surface (right).

The next step was the injection of a polyclonal anti-β_2-GPI after the binding of β_2-GPI to the cardiolipin surface. The expected interaction between the protein (β_2-GPI) and the specific antibody,

also, was not detectable. The same was found by using an amino dextran modified surface. Again, binding of the cofactor β_2-GPI to cardiolipin was positive, but the β_2-GPI was not recognized by specific anti-β_2-GPI in the next step. Neither was the cardiolipin itself recognized by anti-cardiolipin. Former could be due to a strong dissociation of the β_2-GPI from the cardiolipin surface, since their interaction is not covalent. As a consequence, no anti-β_2-GPI binding would occur. An explanation for the latter might be sterical hindrance between the surface matrix and the large immunoglobulins, preventing their binding. This is especially the case for the amino dextran coating that exhibits a "sponge-like" structure where the antigen can diffuse into that is supported by the small size of the cardiolipin.

To solve these problems, different approaches were tested. First, a shorter, brush-like surface modification was chosen to have a better exposition of the antigenic structure, and second, a direct (without cardiolipin) immobilization of the β_2-GPI was considered to overcome dissociation. Covalent immobilization of the β_2-GPI also had the advantage of simplifying the detection method without loss of relevant information, because anti-β_2-GPI are the major, pathogenic autoantibodies related with APS as discussed in the introduction, chapter 3.1.2.2.

4.2.1. Immobilization via 11-aminoundecyltrimethoxysilane

For the generation of a two-dimensional surface, a silane was chosen with a short carbohydrate chain. Short, SAM-like coatings lead to low antigen density but also reduced unspecific binding of the serum matrix (for details see introduction, chapter 3.2.4). The efficiency of applying SAMs or SAM-like structures for the immobilization of antigens has been shown in previous studies of our group using surface plasmon resonance (SPR) (Metzger et al. 2007; Müller et al. 2010; Schlichtiger et al. 2013). They were found to be suitable for sensitive detection of specific antibodies in complex matrices like human samples.

The biotinylated cardiolipin was immobilized on an 11-aminoundecyltrimethoxysilane (11-AUTMS)-streptavidin surface followed by injection of β_2-GPI and an anti-β_2-GPI (Figure 16). On the short 11-AUTMS surface, the cardiolipin was recognized by a polyclonal anti-cardiolipin (black curve). The two blue curves represent binding of the cofactor β_2-GPI to the immobilized phospholipid. Finally, a β_2-GPI solution with physiological concentration and subsequently a β_2-GPI antibody solution was injected (with running buffer in between). This is represented by the two red curves in Figure 16. From about minutes 3 to 18, association of the protein takes place, followed by a slight dissociation phase (minutes 20 to 28), where running buffer was guided over the flow cell. When the curve progression was nearly constant, antibody solution was injected and the interaction monitored (minutes 30 to 40).

Compared to the PEG and AMD coated transducers, the antigenic structures cannot diffuse into the short silane like into the larger polymers. Therefore, more ligand is exposed at the interface between biosensor surface and analyte containing buffer solution. This could explain the stronger binding of the β_2-GPI to the cardiolipin on one hand and the interaction between β_2-GPI and a specific antibody, which is now observable, on the other hand.

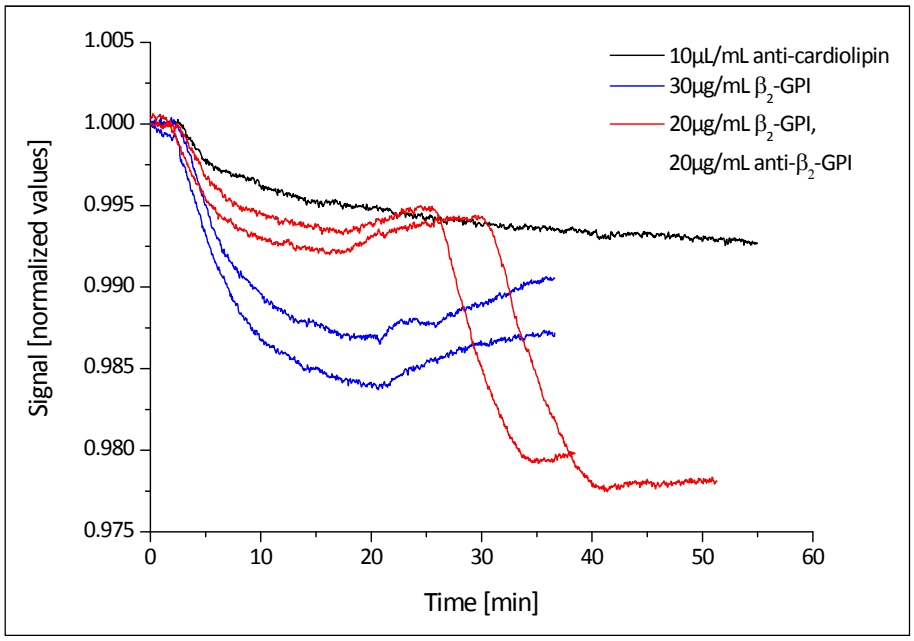

Figure 16: Specific interaction of polyclonal antibody with cardiolipin surface (black curve), binding of cofactor β_2-GPI can be shown (blue curves) and injection of β_2-GPI followed by a β_2-GPI antibody gave strong binding signal (red curves).

4.2.2. Titration experiment with β_2-GPI covalently immobilized on 11-AUTMS

Next, β_2-GPI was directly immobilized on the 11-AUTMS modified surface via amine coupling reaction. Antigeneity of the covalently bound protein was confirmed by binding of a polyclonal anti-β_2-GPI. A titration experiment was performed with 5.0 - 40.0 µg/mL of a specific antibody. Measurements with a monoclonal anti-prothrombin under the same conditions gave almost no signal and therefore verified the specificity of the system (Figure 17, black curve). Binding of 5 µg/mL of anti-β_2-GPI (light blue) was the same as with the monoclonal anti-prothrombin (black curve) whose concentration was five times higher (25 µg/mL). The low signal observed for the latter is due to unspecific interactions. Therefore, it can be deduced, that a concentration of 5 µg/mL of anti-β_2-GPI is below the limit of detection. Measurements with 10 µg/mL of anti-β_2-GPI led to binding signals that can be clearly differentiated from the unspecific interaction obtained with anti-prothrombin. Injection of 20 µg/mL gave a signal a little bit more than twice as high as with 10 µg/mL and injecting 25 µg/mL anti-β_2-GPI also resulted in a proportional increase of binding intensity (mean signals in mV are given in Table 3). This correlation indicates that the detected signal arises from

specific antigen-antibody interaction. Application of 40 µg/mL did not double the signal intensity compared to 20 µg/mL. This is probably due to a saturation of the antigenic surface.

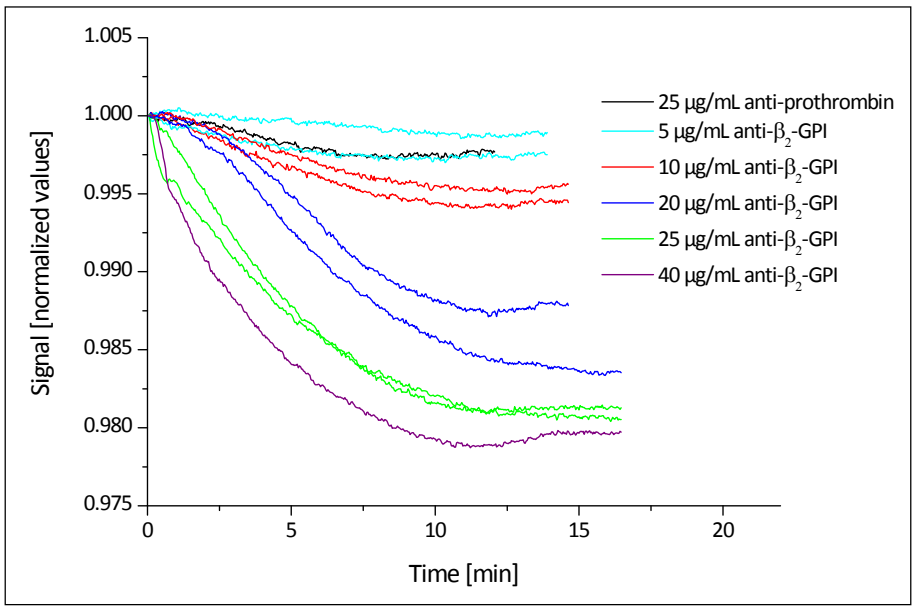

Figure 17: Titration series with polyclonal anti-β_2-GPI on 11-AUTMS-β_2-GPI surface. monoclonal anti-prothrombin (anti-PT) was injected to test for unspecific binding (black curve).

Table 3: Summary of the measured signal intensities for different antibody concentrations.

anti-PT	**anti-β_2-GPI**				
25 µg/mL	5 µg/mL	10 µg/mL	20 µg/mL	25 µg/mL	40 µg/mL
1,7 mV	1,5 mV	4,4 mV	10,6 mV	12,7 mV	16,0 mV

4.2.3. Comparison of six different surface modifications

After the specific detection of anti-β_2-GPI and the low signal observed for anti-prothrombin injection, the first patient and control serum samples were investigated on the 11-AUTMS-β_2-GPI surface. Since human samples were limited concerning the total amount per individual, sample volume was reduced to 100 µL. Therefore, also flow rate was downregulated to 10 µL/min. A dilution factor of 1:10 was chosen. Initially, a PBS buffer was used as running and dilution buffer without any additives to block background signals. This already led to a discrimination between healthy controls (n=2) and APS patients (n=2) (results not shown). Further evaluation was carried out with different buffer salts and various additives like human serum albumin (HSA), BSA, FCS, and polysorbat 20 (Tween 20). Albumin, BSA or HSA, is a common blocking agent that binds unspecifically to charged groups of the biosensor surface. By covering them, the antibodies in the sample solution cannot interact with the charged sites in an unspecific manner. Thereby, it is important to apply proteinogenic blocking agents, that are not potentially recognized by the antibody themself (Burry 2009). FCS exhibits a broader spectrum of different proteins. Although the major component is albumin, this complex blocking agent might be more suitable for some antigen-antibody interactions.

A draw back are the low concentrations of immunoglobulins that can cross-react with the injected antibodies. Tween 20 is a surfactant that is often used in immunoassays, because it prevents non-specific antibody binding by reducing non-ionic interactions such as hydrophobic and H-bonding (Burry 2009).

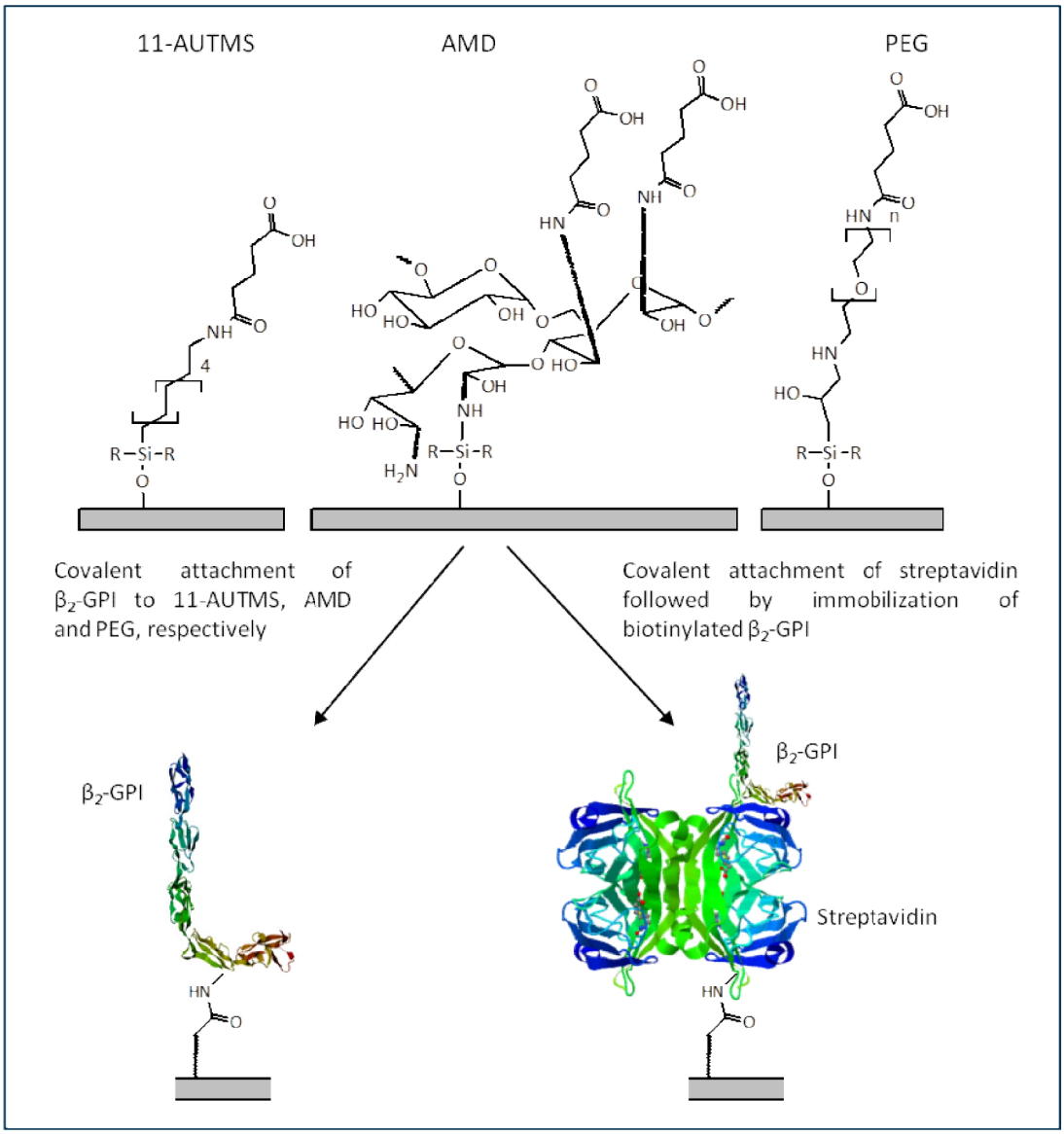

Figure 18: Immobilization of β_2-GPI using six different approaches. Onto a surface modified with 11-AUTMS, PEG and AMD, respectively, β_2-GPI was coupled using either peptide chemistry (left) or streptavidine-biotin interaction (right).

Buffer optimization finally resulted in a HBS buffer with 0.2 % Tween 20 and 0.05 % HSA. With this running and dilution buffer and using guanidine hydrochloride as regeneration solution, more APS patients (n=5) as well as negative controls (n=5) were measured on one chip (curves are depicted in Figure 19). Afterwards, also the PEG and AMD surfaces should be tested under the same conditons and a total of six different surface modifications was evaluated. These were based on the two polymers PEG and AMD as well as the short silane 11-AUTMS that were coupled to the glass

transducer in a first step. Next, β_2-GPI was either covalently immobilized, directly onto the modified surface or non-covalently as biotinylated derivative via streptavidin-biotin interaction (Figure 18). To this end, streptavidin was coupled prior to the PEG-, AMD-, and 11-AUTMS-modiefied surface, respectively.

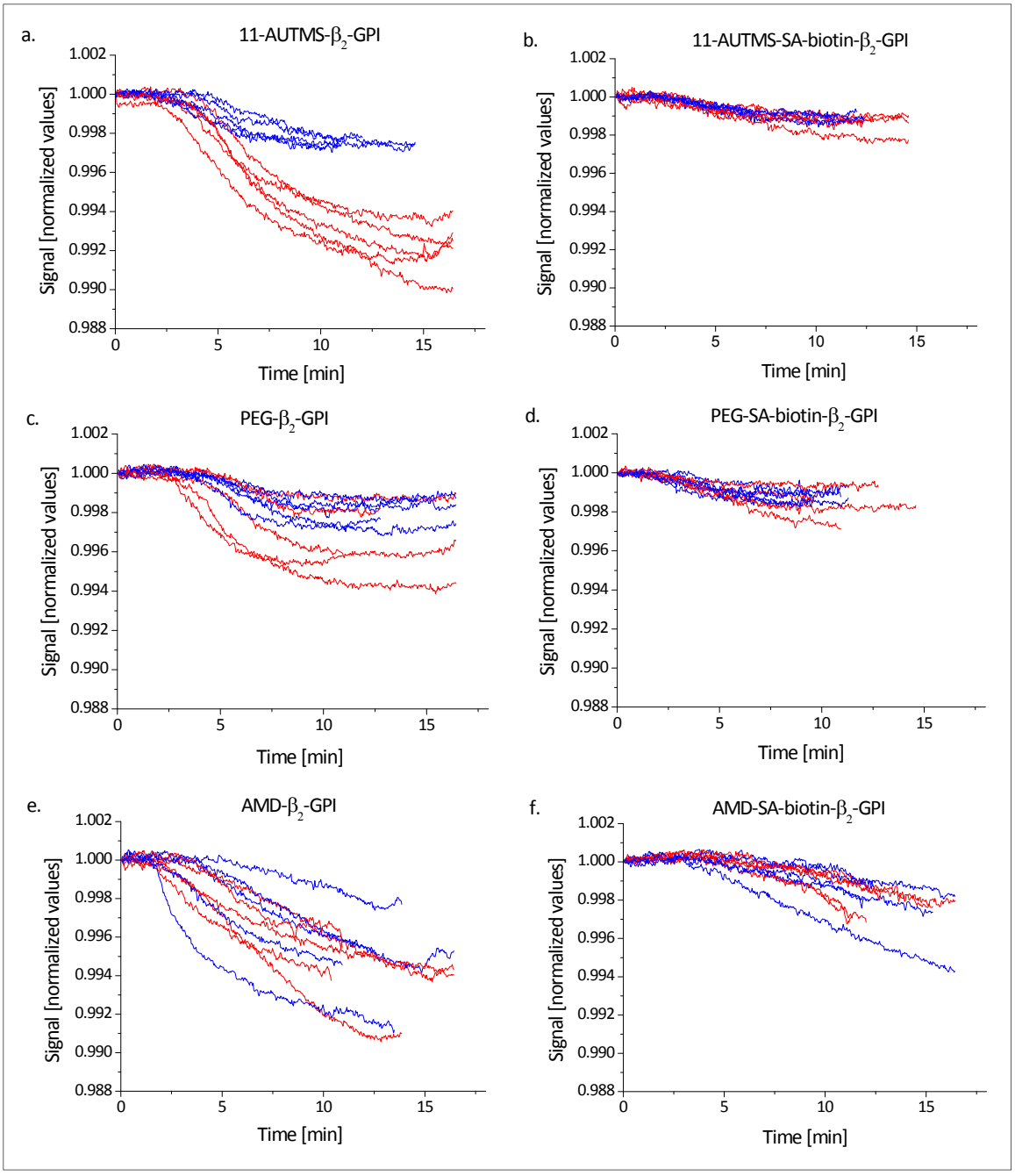

Figure 19: Measurements of five APS patient (red curves) and five control sera (blue curves) on six different surface modifications. β_2-GPI was immobilized either directly (left panel) or as biotinylated form to a streptavidin molecule (right panel).

On each surface, the same five APS patient and healthy control sera were investigated, with alternating injection of positive and negative samples. In the beginnig, middle and at the end, measurements of a healthy control serum spiked with 25 µg/mL of a polyclonal anti-β_2-GPI

guaranteed for a stable antigenic surface throughout the whole experiment. The binding curves of the human samples are depicted in Figure 19.

As already asserted with a smaller number of samples, the 11-AUTMS-β_2-GPI surface provides for a good discrimination between patients' sera (Figure 19a, depicted in red) and healthy controls (blue curves). The curves of the two groups are clearly separated from each other. Negative controls show small binding due to unspecific interaction of the serum components with the biosensor surface. Samples of APS patients all give positive binding curves, that exhibit the typical binding curve shape with a strong association in the beginning, decreasing over time until an equilibrium is reached. Differences in binding intensity can be observed but are just small. Reason was the choice to measure samples first, that all have a high antibody titer. For further evaluation of this system, also patients with low antibody titer need to be investigated to assure, that these would also be detected as positive. In contrast, the 11-AUTMS-streptavidine(SA)-biotin-β_2-GPI surface (Figure 19b) gives only small unspecific binding signals. Signal intensities for APS patient samples are the same as for the healthy controls. Therefore, no specific antibodies are detected. A possible explanation could be, that the β_2-GPI immobilized with this technique did not obtain its antigenic structure or that the epitope was blocked and thus not recognized by the antibodies. Also the PEG- and AMD-streptavidine(SA)-biotin-β_2-GPI surface modifications were both inadequate (Figure 19d and f).

PEG-β_2-GPI shows a promising tendency as can be seen in Figure 19c, yet the overall performance was not convincing. The negative controls exhibit about the same binding behavior as on 11-AUTMS, but not all patients would have been detected as positive due to flatter curves. Overall, binding of specific anti-β_2-GPI to the PEG-β_2-GPI does not have the same intensity as on 11-AUTMS-β_2-GPI.

The AMD surface turned out to be completely inappropriate for this biosensor (Figure 19e). Both, positive patients and negative controls bind very strong to the dextrane modified surface making a differentiation impossible. Also, the curve shape itself varies for every measurement, indicating that the signal is probably not due to specific recognition of the antigen. Some exhibit a typical shape, others show an almost straight, descending binding behaviour. Latter could implicate a continuous interaction with the AMD polymer itself throughout the whole injection phase of the serum sample.

4.2.4. Intra-chip stability

When evaluating the different surface modifications, all measurements were performed on one chip. Therefore, the bound antibodies had to be removed for the next cycle. This was realized by injections of 6 M guanidine hydrochloride (pH 2). Stability of the β_2-GPI surface under these harsh conditions was tested with repeated injections of one serum sample over three days. After 10

consecutive measurements on one chip a loss of 8.5 % of binding signal was detected. Remaining signal intensity was 91.5 % (Figure 20) and variation coefficient (CV) for these 10 measurements was calculated as 6.7 %. After 20 measurements the signal intensity still was 83.1 % of the initial binding signal (CV = 8.8 %). Further injections of the sample revealed a strong decrease in signal intensity with 73.1 % of initial binding signal detected after 30 injections (CV = 11.8 %). Therefore, with this biosensor surface and using guanidine hydrochloride as regeneration solution, not more than 20 consecutive measurements on one chip should be performed. This is also the amount of measurements feasable for one day because about 30 minutes are required for each cycle (including regeneration).

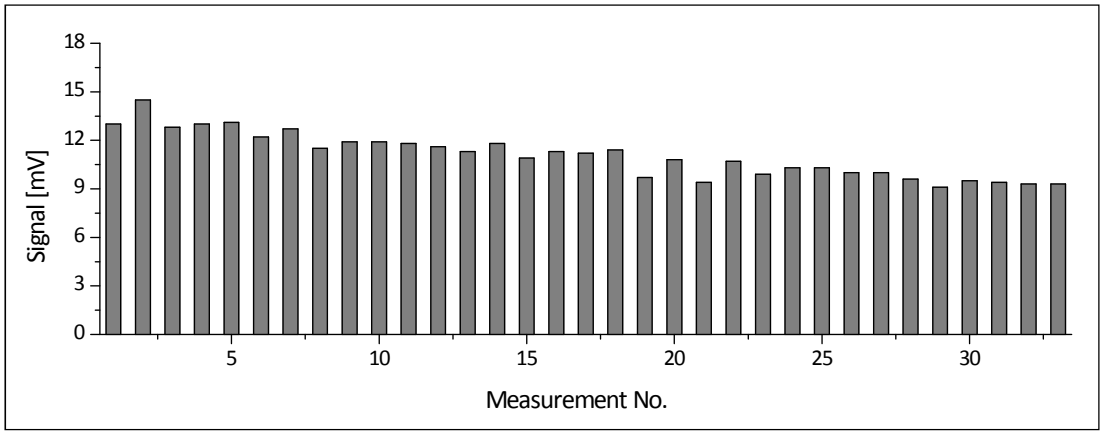

Figure 20: Stability of the antigenic surface was tested with repeated injections of one serum sample. After 20 measurements and regeneration cycles of the biosensor surface a decrease in signal intensity of 16.9 % was detected, which is still acceptable.

4.2.5. Inter-chip variability

As mentioned above, each transducer is unique. Glass thickness and manuel surface coating are major factors that contribute to chip variability. Therefore, it is necessary to test for inter-chip variances. To this end, the same APS patient and control samples, measured on the six different surface modifications, were investigated on three different 11-AUTMS-β_2-GPI biosensors (Figure 21). Furthermore, three more APS serum samples were applied all exhibiting a lower antibody titer. The initial five positive sera had antibody titers above 100 GPL of anti-β_2-GPI (for details to the classification, see introduction, chapter 3.1.2.4). With 23, 41, and 65 GPL, respectively, the three additional samples are in the low medium to medium range of β_2-GPI antibodies. Again, 25 µg/mL of polyclonal anti-β_2-GPI spiked into a negative control was injected every 6th cycle to verify the stable antigeneity of the biosensor surface throughout the whole experiment. Figure 21 summarizes all measurements with the green bars being the antibody-spiked negative samples, APS positive individuals with high antibody titer are depicted in red and with low antibody titer in orange. Negative controls are represented in blue.

In general, measurements of β_2-GPI antibody spiked in serum matrix gives lower binding intensity compared to antibody measurements in buffer (see also Figure 17). This can be explained

with a possible interaction of the anti-β_2-GPI with serum components, especially the β_2-GPI present in a concentration of about 0.2 µg/mL. Furthermore, signal of the first antibody injection is slightly stronger than of the following two measurements. Usually, the first measurement on a new chip gave a larger signal than the others due to drift effects. Therefore, no patient sample was injected first. APS patients with high antibody titer all exhibit a stronger binding than patient samples with lower antibody titer. Signal intensities for the latter partly correlate with GPL units determined with a standardized ELISA. Still, a direct comparison is not recommendable, since they are two distinct different test systems with completely different working procedures.

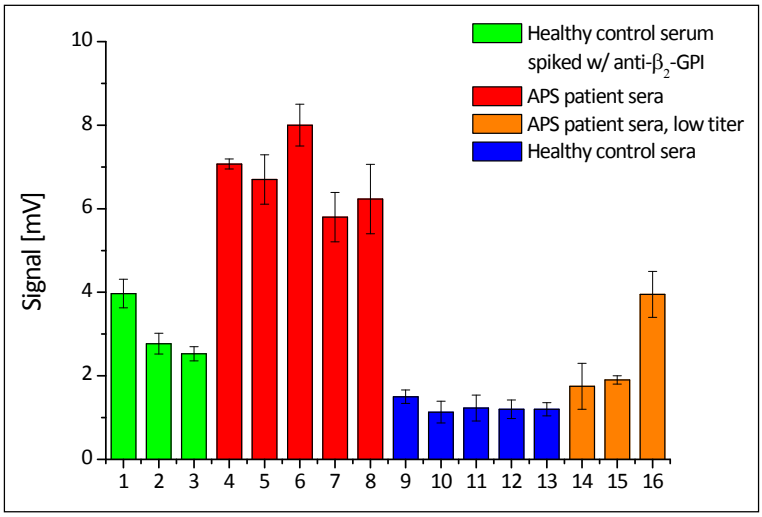

Figure 21: Measurements of the same samples on three different chips. Polyclonal antibody spiked in serum (depicted in green) guaranteed for antigen stability, APS patient samples with high (red) and low antibody titer (orange) roughly correlate to GPL units determined with standardized ELISA. Negative controls (blue) just show slight unspecific binding.

Table 4: Mean and calculated standard deviation (SD) for every sample investigated on three different chips. Results are listed in groups referring to the respective colour code used in Figure 21.

	No.	Polyclonal antibody	APS,high titer	Negative controls	APS, low titer
Signal [mV] (SD [mV])	1	4.0 (0.34)	7.1 (0.12)	1.5 (0.16)	1.8 (0.55)
	2	2.8 (0.25)	6.7 (0.59)	1.1 (0.26)	1.9 (0.10)
	3	2.5 (0.17)	8.0 (0.50)	1.2 (0.31)	4.0 (0.55)
	4		5.8 (0.59)	1.2 (0.22)	
	5		6.2 (0.83)	1.2 (0.16)	

Overall, positive samples, high titer as well as low titer, can be clearly separated from negative controls, which just show slight unspecific binding. Only the sample with the lowest amount of antibodies (referring to ELISA measurements) gives a marginal positive binding signal that is not significant. Error bars overlap with the data from the healthy control sera. Reason could be the missing separation between sample and running buffer which leads to sample dilution, and a sensitivity of our experimental set-up that is not sufficient enough. Both aspects will be considered

with the more advanced pi-RIfS set-up. Measurements on the three different chips are in good agreement. Table 4 summarizes the mean value and the corresponding standard deviation for every sample investigated. The inter-chip variability is low (SD ranges from 0.1 to 0.83, mean CV = 13 %) and results obtained with different transducers are comparable.

Taken together, first, different surface modifications were tested and the optimum was found with the short silane 11-AUTMS. Covalent immobilization of the β_2-GPI via amine coupling reaction was successful and led to an antigenic surface that could discriminate between APS patient samples and negative contols. Buffer and regeneration conditions were tested and stability of the β_2-GPI was investigated. Our biosensor chips are stable for about 20 consecutive measurement and we could shown, that inter-chip variability is small.

4.2.6. First patient screening on the 1-λ-biosensor

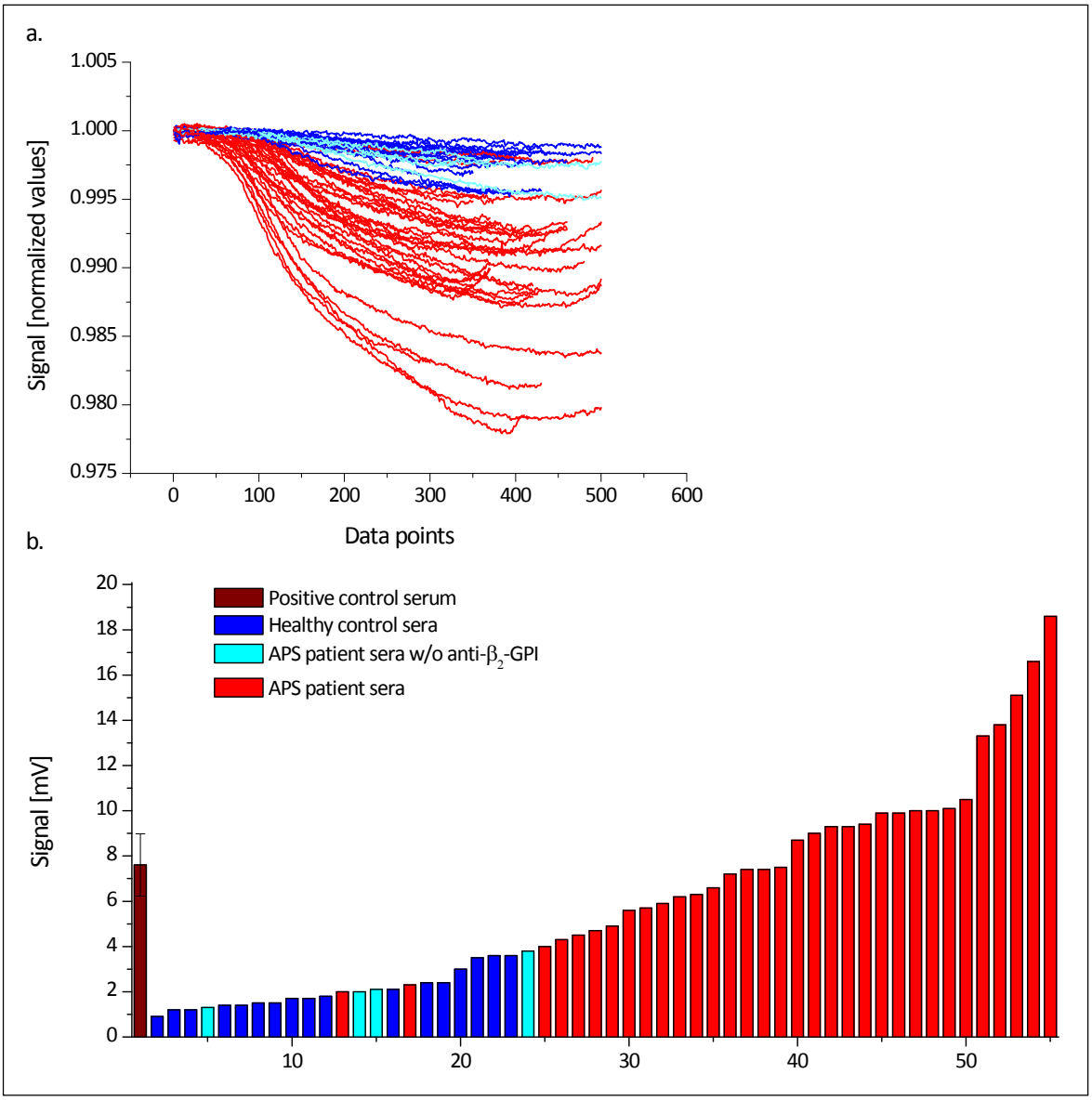

Figure 22: First patient screening on β_2-GPI modified surface with 38 APS patient sera and 17 healthy controls.

After we had shown, that stability of our biosensor was given for about 20 measurements and results obtained from different biosensor chips are comparable, a larger cohort of APS patients was investigated. 38 positiv and 17 negative samples were measured over four days, using one chip per day. As a control, repeated injections of one positive sample were performed.

In Figure 22a all binding curves are depicted with the healthy control samples in blue, APS patient sera in red and APS patient samples without β_2-GPI antibodies represented in tourquise. Latter were tested positive for lupus anticoagulant and therefore classified as positive for having APS. Blue and red curves are separated although there is a smooth transition. This is more obvious in Figure 22b where a bar plot is shown of the same results. The color scheme is identical, red bars for APS positive sera, blue for healthy controls and tourquise for APS patient sera without anti-β_2-GPI. The positive control (dark red) was injected about every 9th measurement to monitor biosensor stability.

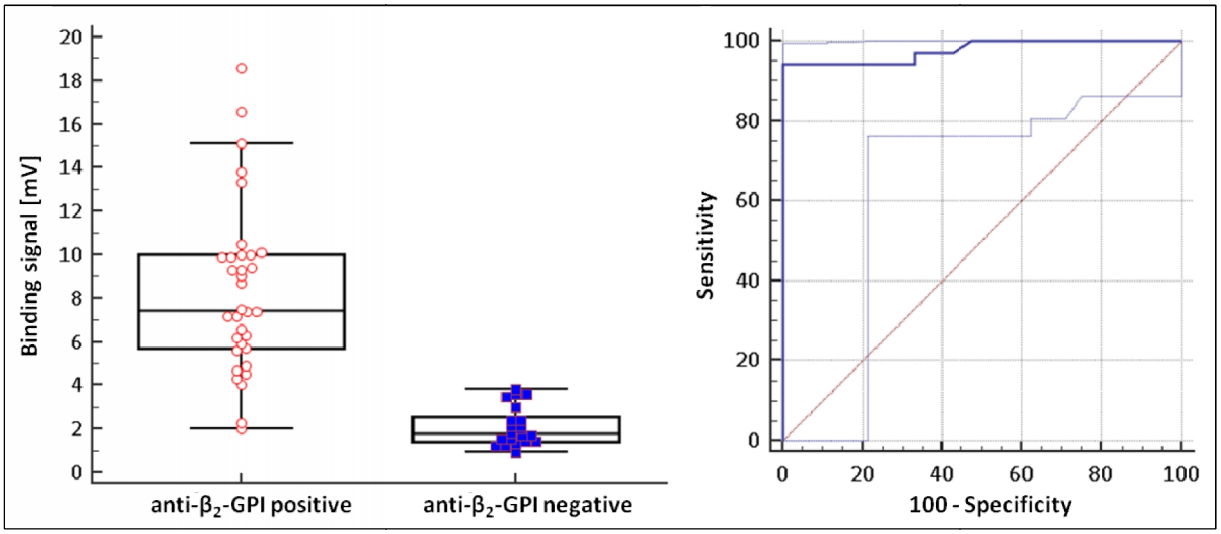

Figure 23: Box plot and ROC of the first patient screening with 1-λ-reflectometry. Except two APS patient samples that are within the group of healthy control sera, positive and negative samples are clearly separated (left). ROC curve depicted in dark blue (right) and CI (light blue) show good sensitivity and specificity for the evaluated test system.

Within the group of positive binding curves, no negative control is found. Contrarily, within the bulk of blue curves, there are two positive sera. This is reflected in specificity as well as sensitivity which were calculated to be 100 % and 94 %, respectively (Table 5). Positive and negative group size vary from the previous mentioned 34 APS patient samples and 21 healthy controls because 4 APS patients collective had no anti-β_2-GPI but other antibodies associated with APS, which are not detected with this biosensor. These individuals were added to the group of healthy controls. Area under the ROC curve (AUC) was determined as 0.977 with a confidence interval (CI) of 0.895 to 0.999 (2.5^{th} - 97.5^{th} percentile). Former is indicated by the dark blue line in the receiver operating characteristic (ROC) curve (Figure 23b), latter by the two light blue lines. The upper limit of the CI is

close to 1.000. If the calculated confidence interval of a given method includes "1", the evaluated test can discriminate between healthy and APS patient samples as good as the gold standard to which it was compared to. When calculating the Youden index the associated cut-off can be determined for the respective system. For the β_2-GPI biosensor this was 3.8 mV. This means every measured signal intensity above 3.8 mV would refer to "APS positive".

Table 5: Summary of test characteristics for anti-β_2-GPI detection. [a]DeLong et al., 1988; [b]Binomial exact.

Sample size	55
Positive group	34 (61.82 %)
Negative group	21 (38.18 %)
AUC	0.977
SE[a]	0.0173
CI (95 %)[b]	0.895 - 0.999
p-value	< 0.0001
Youden index	0.9412
Associated criterion (cut-off)	> 3.8
Sensitivity	94.12
Specificity	100.00

4.3. Prothrombin chips

Besides β_2-GPI, prothrombin plays an important role for a differential APS diagnosis. Therefore, it should be included into the microarray. The key challenge was to assimilate the immobilization technique for both proteins and to adapt the conditions for the detection of anti-prothrombin to the conditions of the anti-β_2-GPI assay. Both were indispensable prerequisites. Chips for the parallelized system were prepared off-line with a laminar coating of the polymer film, followed by antigen spotting. Chips were placed in the system and parallelized detection of different antibodies was then conducted in a single flow channel.

After the successfull immobilization of β_2-GPI and a sensitive detection of anti-β_2-GPI in patients' sera, prothrombin was coupled to a transducer, using the same surface chemistry. This was amine coupling of the protein to the 11-AUTMS modified surface. The efficient immobilization was affirmed with a monoclonal anti-prothrombin. A titration experiment is shown in Figure 24. Binding of 6.25 µg/mL of anti-prothrombin (light blue curves) was the same as with the anti-β_2-GPI (black curve). Measurements with 12.5 µg/mL of anti-prothrombin led to binding signals that are marginal stronger but a clear differentiation was achieved with 25 µg/mL of anti-prothrombin. Therefore, a concentration of 6.25 µg/mL of anti-prothrombin is below the limit of detection and 12.5 µg/mL is slightly positive (red curves). 50 µg/mL anti-prothrombin resulted in a proportional increase of

binding intensity compared to 25 µg/mL (dark blue). This correlation indicates that the detected signal arises from specific antigen-antibody interaction.

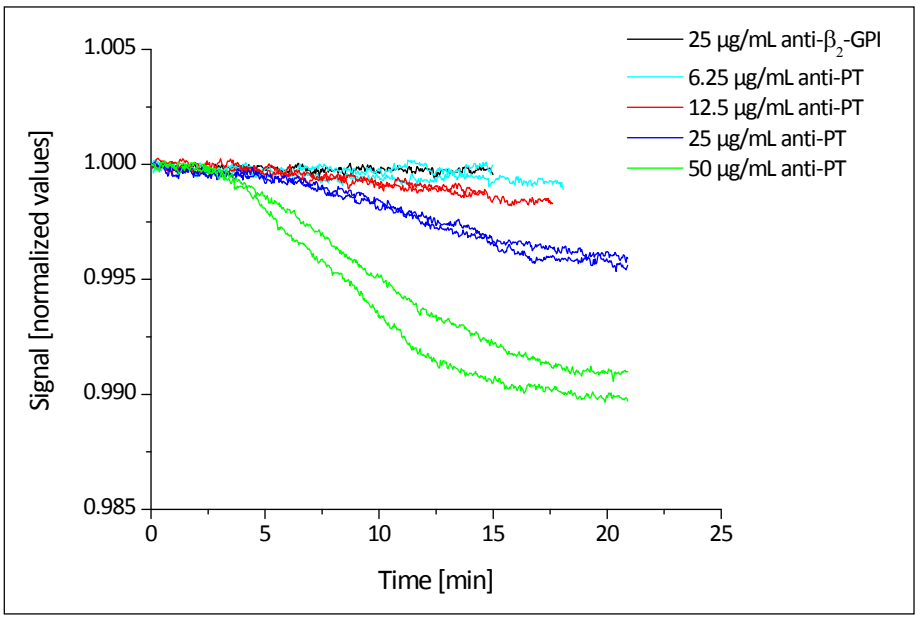

Figure 24: Titration experiment with a monoclonal anti-prothrombin (anti-PT). Injection of anti-β_2-GPI did not give a positive binding signal.

Compared to the titration series with anti-β_2-GPI, sensitivity is less for the anti-prothrombin biosensor. A possible explanations could be a minor immobilization of the antigenic protein, but in this case, one would expect a saturation of the biosensor surface with lower antibody concentrations than applied in this experiment. Another reason could be the specific antigen-antibody interaction itself. It might be hindered due to the covalent or non-directed attachment of the antigen. A non-directed immobilization might result in an orientation of the antigen, in which the epitope is hidden and not facing the analyte containing buffer solution. Furthermore, in contrast to the anti-β_2-GPI the anti-prothrombin is a monoclonal antibody. This gives less signal, because it recognized just one epitop. If this is blocked due to immobilization, binding capacity is lowered.

Following on that, five serum samples of APS patients with high anti-prothrombin titer were investigated together with five negativ control sera. Immobilization and assay conditions were the same as for the β_2-GPI biosensor. Both, patients as well as healthy control sera resulted in strong binding with about the same intensity (Figure 25). As can be seen in the bar plot, a differentiation between the two groups was not possible and measurements of monoclonal antibody spiked in negative control serum neither gave an increase in binding level. This suggests that the signals are completely due to unspecific interactions that might hamper any specific antigen-antibody recognition.

Prothrombin plays the central role in the coagulation cascade. Thus a series of coagulation factors and phospholipids bind to it. Serum specimen is obtained after clotting and centrifugation but

this process mainly eliminates fibrinogen from the sample. Clotting factors are proteases that act as enzymes and are cleaved and therefore consumed during the process of coagulation. Still, the subunits are not directly part of the blood clot and remain in the serum to some extent. The subunits of different clotting factors might interact with the immobilized prothrombin and lead to a strong background signal when injecting diluted human serum samples.

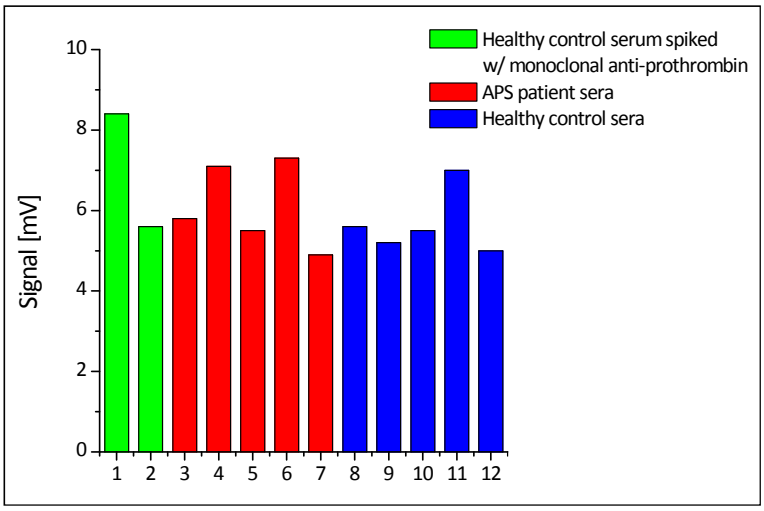

Figure 25: First measurements of five APS patient and five healthy control sera on a prothrombin sensor chip. Assay conditions were chosen as for anti-β_2-GPI detection, but were not appropriate for the anti-prothrombin biosensor.

Optimization of the anti-prothrombin assay was indispensable, but limited to few alternatives, since assay conditions had to be suitable for the detection of anti-β_2-GPI as well. Possibilities include the immobilization strategy, surface modification with a different polymer and buffer conditions. Covalent immobilization worked well for the β_2-GPI, streptavidin-biotin interaction was not applicable and, although β_2-GPI as well as prothrombin bind to phospholipids, hydrophobic interactions were excluded due to missing reproducibility. Another option would be immobilization via capture antibody, but varying the immobilization strategy is not a nearby solution and thus adjourned. Different surface polymers tested for the β_2-GPI biosensor included AMD and PEG. As AMD had turned out to be completely inappropriate, it was not considered. With PEG, serum measurements were not optimal but promising (Figure 19). Since a specific detection of a monoclonal anti-prothrombin was already achieved on the 11-AUTMS surface, the first modification considered, was a change of the buffer system.

Different buffer systems and additives were evaluated, thereunder were proteinogic additives and small surfactant molecules, that were already tested for anti-β_2-GPI detection, as well as commercially available buffer solutions. Purchased buffer systems included LowCross-Buffer® MILD and LowCross-Buffer® from CANDOR, developed for sample dilution. According to the manufactures instructions, they are able to minimise non-specific interaction as well as cross-reactivities and matrix effects in immunological assays like ELISA, Western blotting or protein arrays (CANDOR Bioscience

GmbH 2015). Furthermore, albumin was added to the HBS sample dilution buffer in different concentrations and from different sources (HSA, BSA, and FCS), as well as polysorbat 20 (Tween 20). Some of the results are depicted in Figure 26.

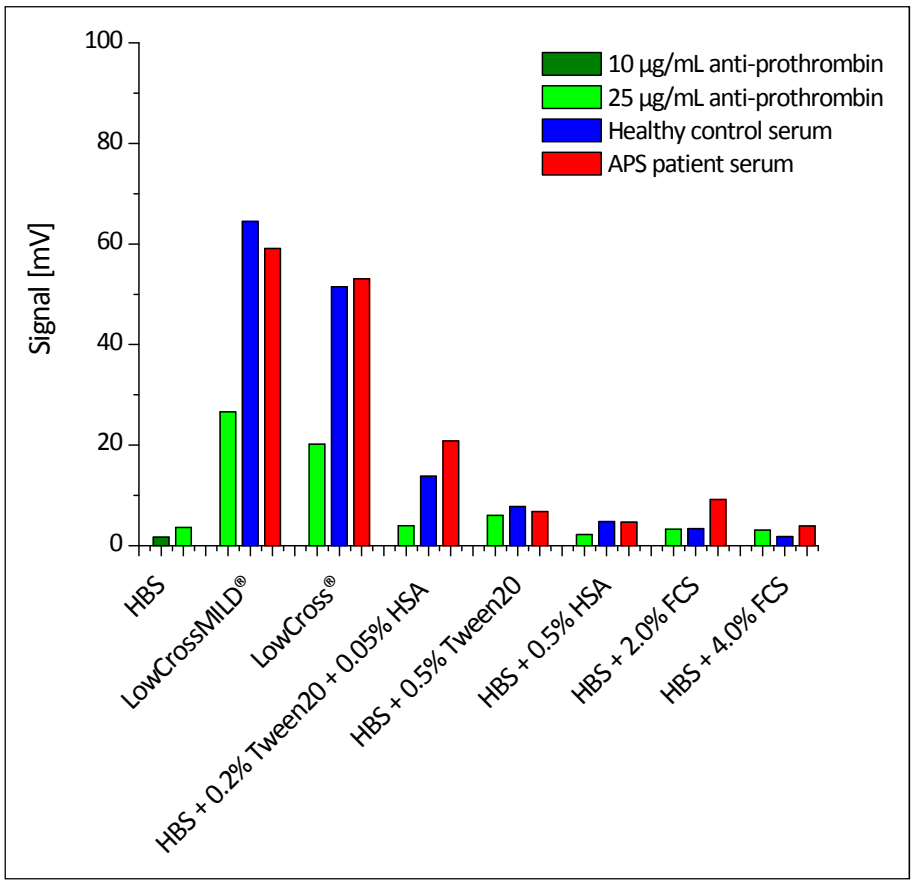

Figure 26: Different buffer additives were evaluated for anti-prothrombin detection in diluted human samples. None of the tested additives was capable to significantly reduce unspecific binding.

With the LowCross-Buffer® systems the strongest signals were obtained, but also the strongest unspecific interactions. The healthy control serum bound with the same intensity as the antibody containing APS patient sample. Application of HBS either containing FCS or Tween 20 as well as HSA, seem to be the most promising options (Figure 26, fourth and seventh set of measurements). Signal intensity for the positive sample is slightly stronger than for the negative control, but injection of an anti-human IgG subsequently after the patient sample revealed that no antibodies had bound to the biosensor surface (data not shown). Overall, none of the evaluated buffer conditions was capable to reduce the high background binding of the serum matrix to an acceptable minimum.

Next, antibodies of the serum samples were isolated using recombinant protein A/G coated sepharose spin columns. The resulting sample contains most of the antibody spectrum except IgA, IgD and IgE, but their detection is not relevant for APS diagnostics. For details of the exprimental procedure see materials and methods, chapter 5.8. With this preparative step and using the buffer

system that was optimized for anti-β_2-GPI detection, it was possible to achieve a discrimination of APS patients and healthy controls. This is illustrated in Figure 27.

Both diagrams show the binding of APS patient sera (red), APS patient sera without prothrombin antibodies (turquoise) and healty control sera (blue) purified with protein A/G. On the left, samples were diluted in plain HBS buffer without any additives. On the right, HBS containing 0.05 % HSA and 0.2 % Tween 20 was used. Blocking agents, as in this case HSA and Tween 20, not only lower the amount of background signal, but also the intensity of specific interactions. Their use is beneficial if the extent to which they lower the unspecific binding exceeds the decrease in specific signal detection. Comparing both sets of curves, the amount of backround is greatly decreased with the addition of blocking agents. Signal intensities for the APS patient samples were also reduced, but they are still significantly higher than the negative controls, which leads to a clear discrimination between the two groups.

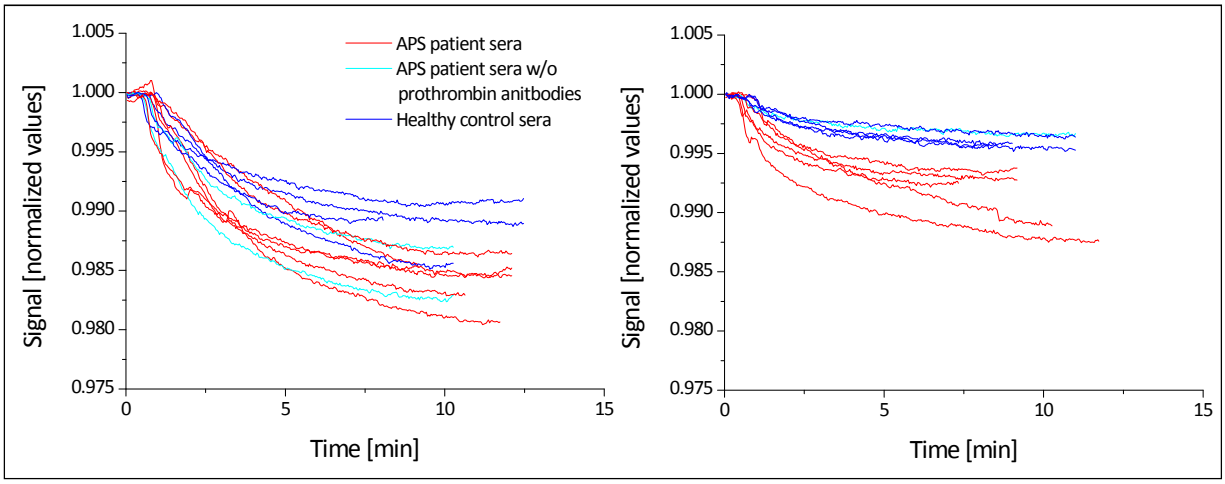

Figure 27: Measurement with purified samples from healthy donors and APS patients in HBS buffer without any additive (left) and with 0.2 % Tween 20 and 0.05 % HSA (right).

The additional step of antibody purification is a crucial modification in the assay procedure and requires an evaluation. Extraction columns were analysed in terms of variability between columns and stability of purified human antibodies was tested. Former was accomplished by purification of one positive and one negative sample as well as a solution of the monoclonal anti-prothrombin with three different columns. Mean signals and variation coefficients are given in Table 6.

Table 6: Summary of mean signals and variation coefficients detected for interaction of anti-prothrombin with the prothrombin biosensor after immunglobulin extraction using different protein A/G sepharose columns.

	25 µg/mL anti-prothrombin	**APS positive serum**	**Healthy control serum**
Mean signal (SD)	4.1 (±0.35)	5.9 (±0.14)	2.3 (±0.42)
CV	8.7 %	2.4 %	18.4 %

Variation coefficient for APS positive serum purification was the lowest with 2.4 %, followed by the monoclonal antibody (8.7 %). The healthy control sample gave a relatively high variation coefficient after column extraction (18.4 %). As can be seen from the detected binding signal for the negative control, the sample still contains protein that causes some background. Most of it is IgG and IgM, but a few other serum components probably remain in the sample, because purification is not complete. The content to which serum components that cause unspecific binding remain in the purified fraction and the low absolute value measured for the negative control are possible reasons for the high variation coefficient. The difference to the positive serum is still significant. For the antibody solution as well as the APS positiv serum, different purification columns gave a better consistency. The detected signals are mainly due to specific recognition of the prothrombin by the antibodies that were isolated from the samples.

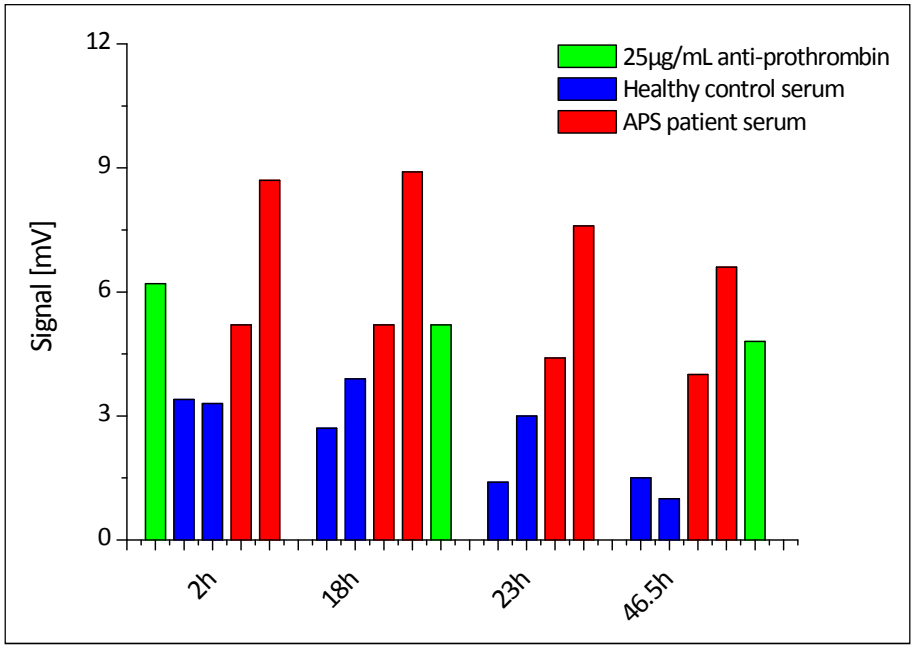

Figure 28: Stability of purified serum samples, stored in buffer at -80°C. From the detected signal intensities it can be deduced, that storage of 18 h under these conditions is not harmful for the extracted antibodies.

Stability of the purified antibodies was controlled by keeping them at -80°C after extraction for 2, 18, 23, and 46.5 hours. Samples were measured on the same chip with injections of 25 µg/mL of monoclonal antibody in between to verify antigen stability (Figure 28). Over the whole experiment (19 measurements) the decrease in signal intensity for the anti-prothrombin was 22.6 %. This is more than for the β_2-GPI biosensor. Keeping in mind, that the chip was left in the flow cell for over 46 hours, a signal intensity loss of 22.6 % over 19 measurement and regeneration cycles is acceptable. Still, for the microarray measurements with the pi-RIfS system, stability of every applied antigen should be controlled carefully. The injected human samples showed a nearly identical binding behaviour after 2 and 18 hours. 23 hours after antibody purification, signal intensity for the APS

patient sera was reduced to 84.6 % and 87.4 %, and for the healthy control samples to 41.2 % and 90.9 %, respectively. After 46.5 hours, binding signal is diminished to 76.9 % and 75.9 % for the positive and to 44.1 % and 30.3 % for the negative samples. The decrease for the human samples during storage time is greater than the decrease caused by the loss of antigen stability detected with monoclonal anti-prothrombin. Therefore, the reduction of signal intensity for the former is caused by storage of purified antibodies. Thereby, not only the extraction procedure itself is harmful for the immunoglobulins, but also the buffer system in which they are kept. Serum (or plasma) containig a whole spectrum of proteins and other component is the optimal solution for antibodies.

Taken together, specific detection of a monoclonal anti-prothrombin on the 11-AUTMS-prothrombin surface was successful, but measurements of diluted serum samples revealed strong background signal. Buffer optimization did not lead to a discrimination between positive and negative samples. This was achieved with the purification of the IgG and IgM spectrum using protein A/G. Stability of purified antibodies was evaluated as well as inter-column variability. With optimized assay conditions specific anti-prothrombin detection from human samples was accomplished and a differentiation of APS patients and healthy controls was possible. Furthermore, immobilization technique as well as buffer and regeneration conditions were the same as for the anti-β_2-GPI detection allowing for a parallelization of both systems.

4.4. Cardiolipin chips

Being part of the Sydney classification criteria, cardiolipin is the most important antigen besides β_2-GPI for the diagnosis of APS. Due to its chemical structure it is not quite simple to immobilize this phospholipid via peptide chemistry. From the group of Prof. A. B. Holmes we received an amino-functionalized cardiolipin (for a detailed structure see introduction, Figure 8). The amino group is coupled to one of the four carbohydrate chains which led to an immobilization with the head group, the recognition element, facing the running buffer.

In Figure 29, a titration series with an anti-cardiolipin positive serum is depicted. The antibody is purified from human serum and concentration is not provided by the supplier. Therefore, amounts are given in µL instead of concentrations. As negative controls, an anti-transferrin and an anti-β_2-GPI were injected. Both gave negative binding curves (black and red curve). The cardiolipin-modified sensor surface was recognized by the injected anti-cardiolipin. A limit of detection cannot be determined due to missing concentration, but this experiment prooved specific binding of the antibody and reproducibility of the single measurements. Doubling the amount of injected antibody doubled the detected signal intensity. This correlation indicates a specific antigen-antibody interaction. Recognition of the immobilized cardiolipin by the cofactor β_2-GPI was also positive and subsequent injection of an anti-β_2-GPI gave a strong binding signal (data not shown).

Following on that, human samples were investigated (Figure 29, right). Absolute binding intensity is lower for the cardiolipin biosensor and therefore, APS positive (n=3) and healthy control sera (n=3) are not as clearly separated as with the β_2-GPI- or the prothrombin-biosensor. In principle, a differentiation of the first 6 sera was possible, but for a reliable predication number of samples needs to be enlarged. Further measurements were performed with the pi-RIfS system.

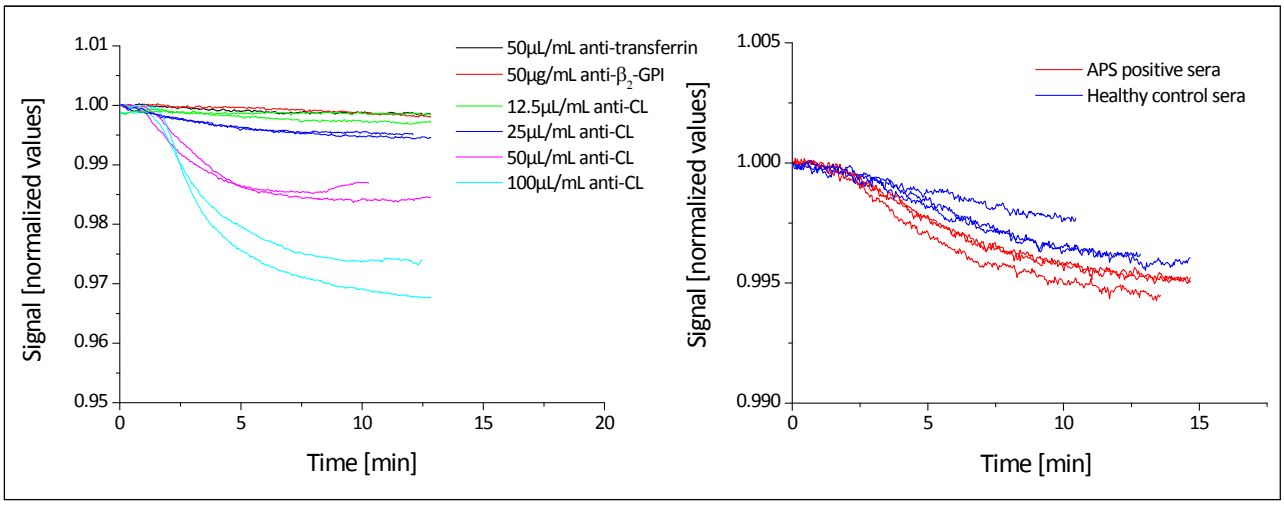

Figure 29: Titration series with anti-cardiolipin positive serum from human donor (left) and first measurement of APS positive and healthy control sera (right).

4.5. Parallelized detection with the pi-RIfS system

Characterization of a patients' antibody status is of high interest for APS diagnostics. Not only the verification of the presence of destinct antibodies but also the incidence of different antibodies can provide a better diagnostic value. After serveral APS relevant antigens had been immobilized and evaluated in terms of specific antibody recognition and discrimination between APS patients and healthy controls, the aim was to transfer the assays established on the 1-λ-reflectometry system onto the multiplexed format. As surface chemistry and immobilization techniques are the same in both set-ups the test characteristics itself should remain unaffected while transferring the assays from the simpler 1-λ-reflectometry to the parallelized system. Complications can arise from cross reactions and unspecific binding between the diverse antigen-antibody partners, but also from different fluidics caused by different sizes of the flow cells. Another problem might be the fact, that chips for the 1-λ-reflectometry are laminary coated with antigen while pi-RIfS chips contain spots. Their morphology can have a strong impact on the binding signal. Transducer chips for the pi-RIfS system are about the size of a standard microscope slide (75 × 25 mm). The PDMS flow cell has the same size with a flow channel of 30 × 8 mm and a depth of 100 µm. This is comparatively large and might cause an unequal flow over the sensor surface. The overall performance of the detection and microfluidic system was assessed with measurements of 50 µg/mL anti-BSA on a chip with 5 × 5 spots of BSA. Spot morphology can be considered as homogeneous and well defined, without spreading or

so-called “donut” effects. Latter is characterized by intense binding to the rim of the spot and almost none in the middle, which gives a ring-shaped picture. It results from inappropriate spotting conditions. After the first seconds of the injection phase, the distribution of the analyte solution is even througout the whole flow cell. Directly at the beginning of the injection, spots at the bottom first show binding, because they are first covered with analyte solution. In principle, this is not a problem, but was the reason to arrange spots of the microarray in rows rather than columns (Figure 30). In this case no time delay between spots of the same antigen occurs. More problematic would be a thinning of analyte from the part of the chip, that is reached first by sample solution (bottom) to the part that is covered last (top).

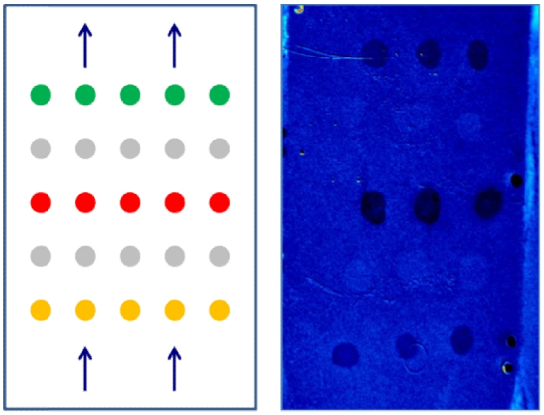

Figure 30: Schematic picture (left) of a microarray with three APS relevant antigens (depicted in yellow, red, and green) and BSA (grey) as negative control. Flow direction of the buffer is indicated with arrows. Camera picture (right) of a microarray spotted by hand. Binding of antibody causes darkening of the respective antigen spots. If no interaction takes place, spots remain bright.

The APS relevant antigens β_2-GPI, prothrombin and the ω-amine cardiolipin were immobilized using the BioOdyssey Calligrapher MiniArrayer. BSA spots served as negative control. Functionality of the coupled antigens was affirmed with polyclonal anti-β_2-GPI, anti-cardiolipin and anti-prothrombin antibodies (Figure 31).

The anti-prothrombin gives the best signal, followed by the anti-β_2-GPI. The anti-cardiolipin shows just small binding, which might have several reasons. Affinity of anti-cardiolipin could be reduced for cardiolipin that is not in complex with its cofactor β_2-GPI. Furthermore, the real concentration of the antibody is not provided by the supplier. A weaker binding compared to anti-prothrombin and anti-β_2-GPI might be due to differences in the absolute concentration of active antibody species in the sample. Yet, absolute binding signal intensities should not be overvalued, as the observed interactions are completely different. Measurements with each antibody alone further substantiate a selective recognition of each antigen-antibody system without any cross-reactivity between the respective antibody and the other antigens (data not shown).

Overall the biosensor can discriminate between different antigens displayed on one surface and gives reproducible binding curves. Differences in signal behaviour between the 1-λ-system, that

was used for assay optimization, and the parallelized set-up can be mainly explained by the differences in the microfluidic control which is more sophisticated in case of the pi-RIfS system.

After we had shown that our biosensor is capable of detecting different antibodies in parallel with a good sensitivity and specificity, the system was evaluated with antibodies purified from human samples. We obtained promising results, but after the first set of investigated APS patients and healthy controls, antigens spotted with the MiniArrayer were not recognized by any of the antibodies injected. Neither the polyclonal anti-prothrombin, anti-β_2-GPI, and anti-cardiolipin, nor the antibodies of the human samples did bind to the immobilized antigens. Immunoglobulin isolation was tested again and the same samples were measured on both systems, the 1-λ-reflectometry as well as the pi-RIfS system. With the former we recorded binding curves similar to all previous measurements, indicating that antibody purification still was functional. The same samples injected in the pi-RIfS gave no binding signals at all. Different chips were tested and the spotting buffer in which antigens were solubilized for spotting procedure was varied. β_2-GPI from two different sources was immobilized and several running and sample dilution buffers were used. The problem could not be solved by these approaches. Finally, antigens were spotted by hand. This resulted in larger spots with a diameter of about 1 mm. Spots produced by the MiniArrayer had a diameter of about 170 µm. As a consequence only three instead of seven replicate spots of one antigen could be placed in one row, but we achieved a specific detection of the antibodies.

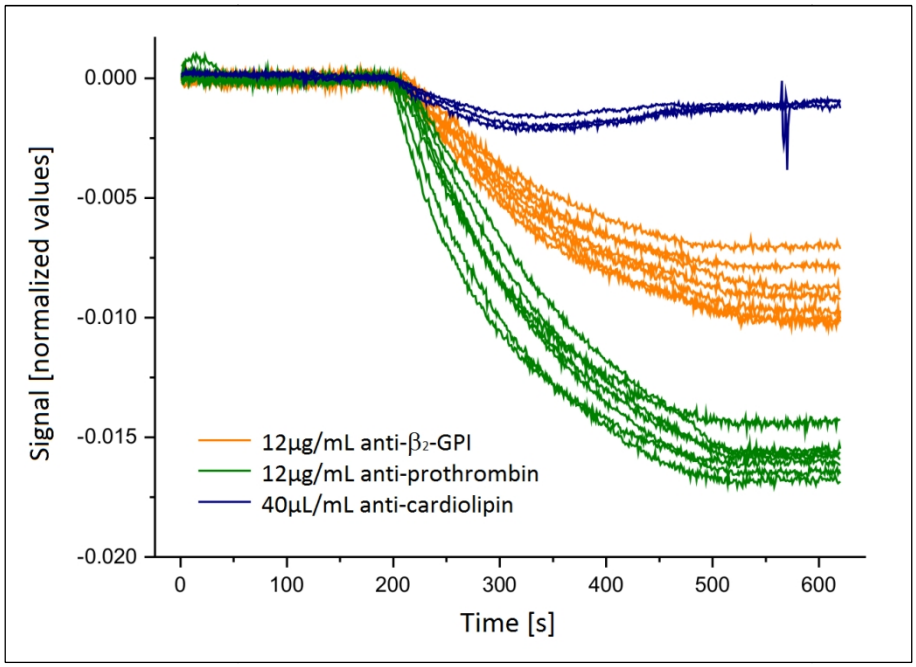

Figure 31: Parallel detection of a polyclonal anti-β_2-GPI, anti-cardiolipin and anti-prothrombin with the pi-RIfS.

With the microarrays spotted by hand, 35 APS patient sera, 6 individuals suffering from systemic lupus erythematosus (SLE), and 24 healthy control sera were investigated (ELISA results for the determination of anti-β_2-GPI, anti-cardiolipin and anti-prothrombin are listed in Table 10 of the

appendix). The SLE patients were chosen to determine possible unspecific interactions caused by other, non APS associated autoantibodies. In Figure 32 four sets of curves are depicted exemplarily. The top two (a. and b.) are obtained with two APS patient samples, the bottom two (c. and d.) with two healthy control sera. Injection starts at around data point 200. In diagram d. small drift effects were monitored within the first 100 recorded data points. Small amounts of air in the microfluidic system produce arteficial signals at second 550 (Figure 32a.) and 400 (Figure 32b.). Black curves indicate anti-β_2-GPI binding, red curves refer to anti-prothrombin, green to cardiolipin an blue curves depict interaction of patient antibodies with a complex of cardiolipin and β_2-GPI.

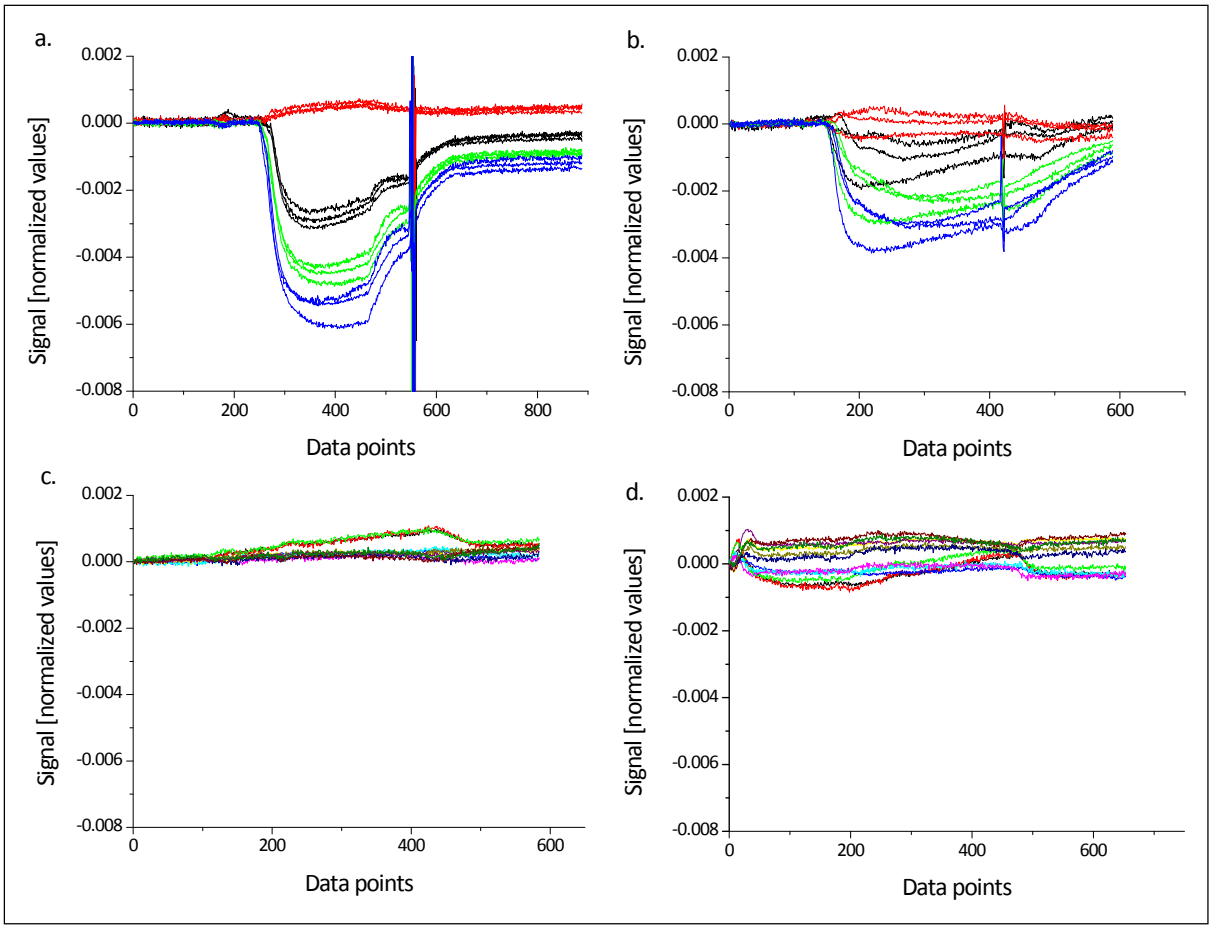

Figure 32: Two APS patient sera (a. and b.) and two healthy control samples (c. and d.) measured with the pi-RIfS microarray. Spotted antigens included β_2-GPI (black curves), prothrombin (red curves), cardiolipin (green curves), and a complex of β_2-GPI and cardiolipin (blue curves).

First, response for β_2-GPI and cardiolipin is much more intense in the case of the APS patients compared to the negative controls. There is also an observable difference between the two positiv samples. Referring to the routinely determined APS antibody titers, the left sample exhibits lower titers. Therefore, the binding curves correlate with GPL units. The differences in absolute signal intensity for the threefold determination of APS patient antibodies (Figure 32a. and b.) are due to spot inhomogeneities. Binding to cardiolipin and cardiolipin complexed with β_2-GPI is similar for the two positive samples, because those two antigenic structures probably detect the same antibody

fraction. Anti-prothrombin was negative for the sample corresponding to Figure 32a. and slightly positive for Figure 32b., but is hardly detected. There is just a slight decreas in binding signal compared to the right diagramm and the negative controls.

Evaluation of the four antigens is performed separately and binding signals are depicted as box plot (Figure 33). Thereby, APS patients without the respective antibodies were added to the group of healthy controls. A list of all results is provided in Table 10 of the appendix.

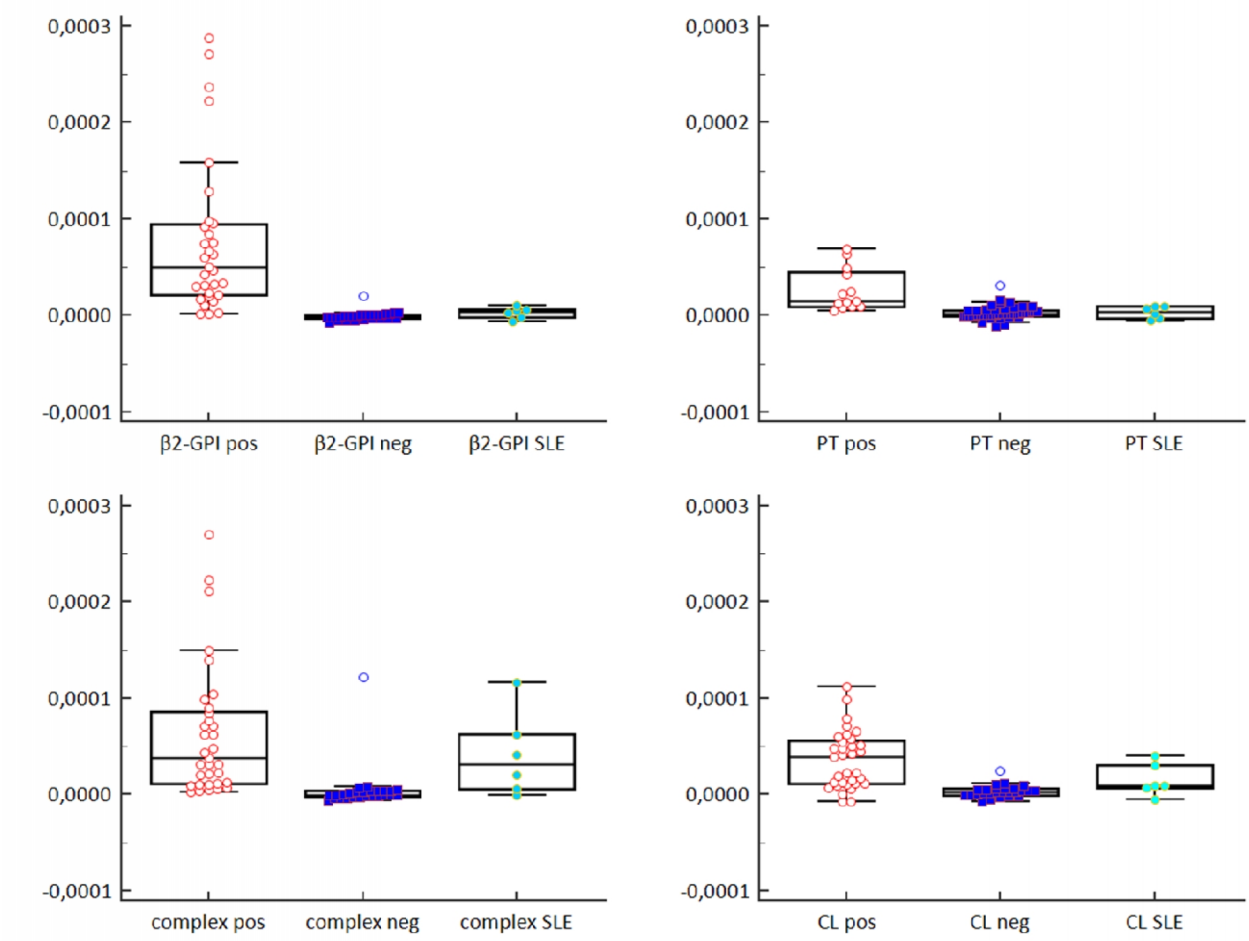

Figure 33: Box plot for every investigated antigen, namely β_2-GPI, prothrombin (termed PT), a cardiolipin/β_2-GPI complex (complex) and a cardiolipin alone (CL). APS patient samples containing the respective antibody are named "positive" (pos), APS patient sample without the respective antibody and healthy control sera are termed "negative" (neg). SLE patient are summarized in an own group (SLE).

Variation coefficients (CV) of the three indipendant curves were determined for every human sample. In over 95 % of the measurements CV was calculated to be less than 5 %. A CV of more than 20 % was only observed in about 1 % and restricted to negative controls. This can be explained by the extremely low binding intensities monitored for these samples (10^{-6} to 10^{-7} [normalized value]/sec, for details on data evaluation see materials & methods, chapter 5.11.2). Statistical parameters of all pi-RIfS measurements are summarized in Table 11 of the appendix.

The box plot depicted in Figure 33 provides a good overview of the performance of the four different antigen-antibody interactions combined on the microarray. For the detection of anti-β_2-GPI the biosensor gives the best results. Negative control as well as SLE positive sera just gave small binding signals. The APS patient samples can be clearly differentiated from the rest. This is not surprisingly, since assay development was optimized for this biosensor and all the following antibody detection assays were adapted to that. As for the β_2-GPI surface, unspecific interactions with the immobilized prothrombin was reduced to a minimum, as well. Binding intensities for the positive samples was generally lower, which can be explained by total number of available samples with a positive anti-prothrombin titer. Just few APS patients develop prothrombin antibodies and for the 14 individuals investigated, antibody titers were rather low.

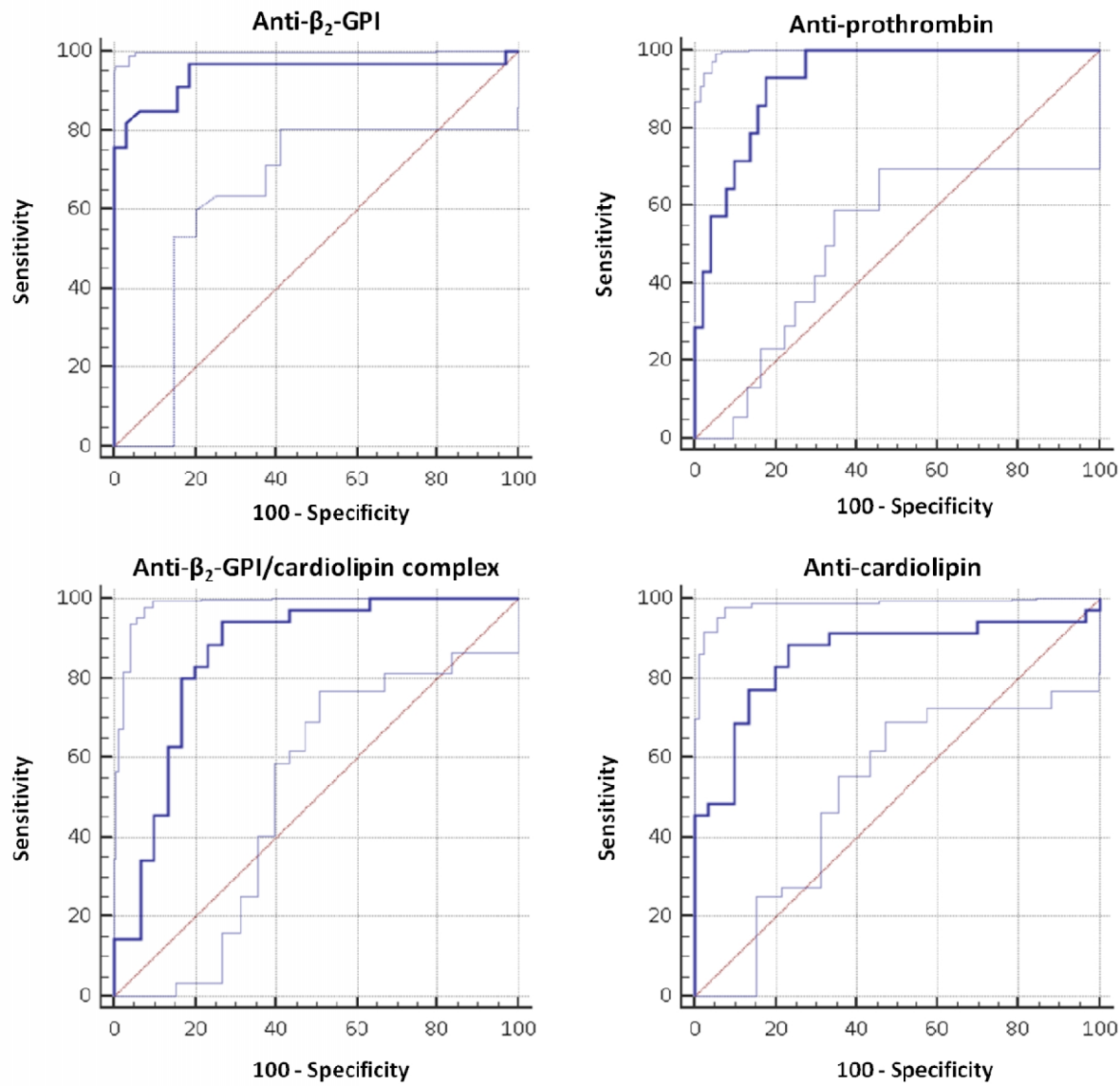

Figure 34: ROC for every investigated antigen, namely β_2-GPI, prothrombin, a cardiolipin/β_2-GPI complex and cardiolipin alone.

In contrast to the solely proteinogenic antigens, the cardiolipin as well as the cardiolipin/β_2-GPI surface lead to more background, especially for the SLE patients. Particularly, binding to the complex was enhanced and as strong as the binding of the positive samples. A receiver operating characteristic (ROC) was performed for a detailed evaluation of the test performance. ROC curves are depicted in Figure 34 and statistical characteristics are summarized inTable 7. Thereby, APS patients without the respective antibodies are classified as "negative" and included into the group of negative samples.

Table 7: Summary of statistical characterization of the four antigen-antibody interactions. [a]DeLong et al., 1988; [b]Binomial exact.

Immobilized antigen	**β_2-GPI**	**prothrombin**	**cardiolipin/ β_2-GPI**	**cardiolipin**
Sample size	65	65	65	65
Positive group	33 (50.77 %)	14 (21.54 %)	35 (53.85 %)	35 (53.85 %)
Negative group	32 (49.23 %)	51 (78.46 %)	30 (46.15 %)	30 (46.15 %)
AUC	0.946	0.926	0.857	0.859
SE[a]	0.0319	0.0319	0.0497	0.0506
CI (2.5 - 97.5 %)[b]	0.860 - 0.987	0.833 - 0.976	0.748 - 0.932	0.750 - 0.933
p-value	< 0.0001	< 0.0001	< 0.0001	< 0.0001
Youden index	0.7865	0.7521	0.6524	0.6762
Associated criterion (cut-off)	$> 11.70\times10^{-6}$	$> 8.84\times10^{-6}$	$> 10.70\times10^{-6}$	$> 4.06\times10^{-6}$
Sensitivity	81.82	92.86	88.57	94.29
Specificity	96.87	82.35	76.67	73.33

4.6. Second screening with the 1-λ-reflectometry

The collective investigated with the pi-RIfS microarray was afterward examined with the 1-λ-reflectometry but antibodies were not purified. Samples were diluted in running buffer as previously described and measured in triplicate. A box plot and a ROC curve are shown in Figure 35. An AUC of 0.955 (CI 0.872 - 0.991), a sensitivity of 93.94 % and a specificity of 96.87 % was calculated (Table 8). The statistical analysis of the β_2-GPI spots on the pi-RIfS microarray gave an AUC of 0.946 (CI 0.860 - 0.987), a sensitivity of 81.82 % at a specificity of 96.87 %. The lower sensitivity might be due to the conditions that were chosen for the microarray, the parallel detection of several biomolecular interactions as well as the sample preparation prior to the measurements. Specificity is exactly the same for both data sets, indicating that the abiliy to discriminate between healthy and APS patient

sample is the same for the β_2-GPI spots on the microarray as for the β_2-GPI biosensor chip in the 1-λ-reflectometry set-up.

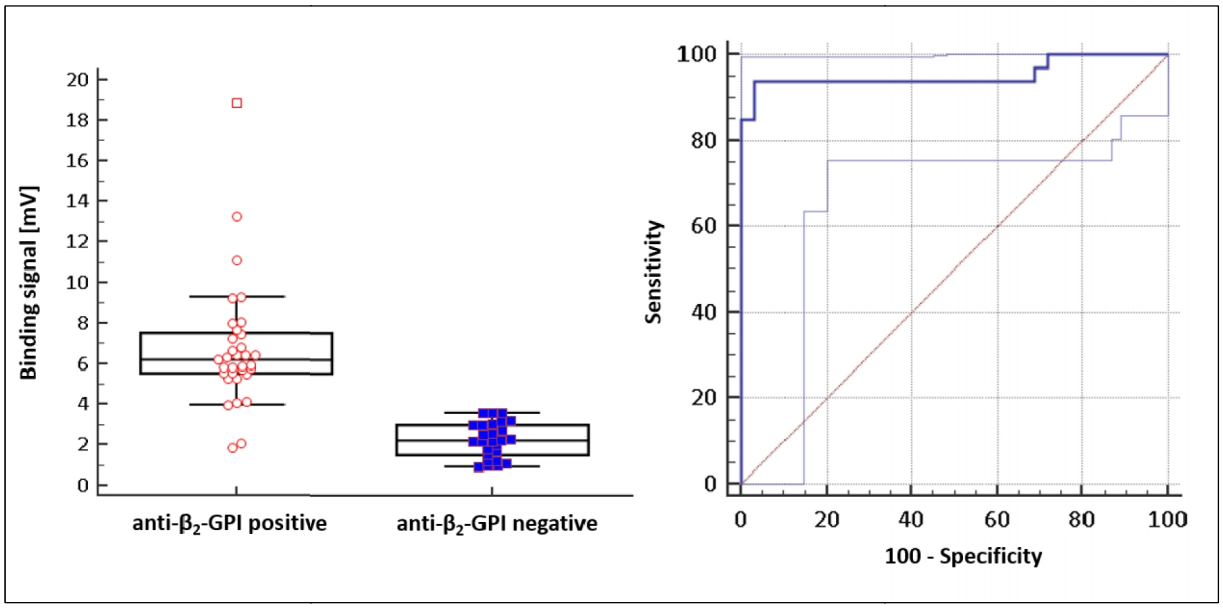

Figure 35: Box plot (left) and ROC curve (right) for 1-λ-reflectometry evaluation of the same collective investigated on the microarray with a β_2-GPI biosensor.

Table 8: : Summary of test characteristics for the second anti-β_2-GPI screening, measuring the same samples as on the pi-RIfS system. [a]DeLong et al., 1988; [b]Binomial exact.

Sample size	65
Positive group	33 (50.77 %)
Negative group	32 (49.23 %)
AUC	0.955
SE[a]	0.0302
CI (95 %)[b]	0.872 - 0.991
p-value	< 0.0001
Youden index	0.9081
Associated criterion (cut-off)	> 3.7333
Sensitivity	93.94
Specificity	96.87

5 materials & methods

5.1. Chemicals

Name	Supplier
Acetic acid, 100 %	Merck KGaA (Darmstadt, Germany)
Acetone, ≥ 99.5 %	Sigma-Aldrich (Steinheim, Germany)
Amino dextran, 40,000 Da	Invitrogen (Eugene, OR, USA)
11-Aminoundecyltrimethoxysilane, ≥ 95 %	Sikemia (Clapiers, France)
O-(Benzotriazol-1-yl)-N,N,N',N'-tetramethyluronium tetrafluoroborate	Sigma-Aldrich (Steinheim, Germany)
D-Biotin, approx 99 %	Sigma-Aldrich (Steinheim, Germany)
Diaminopoly(ethylene)glycol, 1,983 Da	Iris Biotech GmbH (Marktredwitz, Germany)
Dichloromethane, ≥ 99.5 %	Fluka Chemie GmbH (Buchs, Switzerland)
N,N'-Diisopropylcarbodiimide, 99 %	Sigma-Aldrich (Steinheim, Germany)
N,N-Diisopropylethylamine, ≥ 99 %	Sigma-Aldrich (Steinheim, Germany)
N,N-Dimethylformamide, ≥ 99.5 %	Sigma-Aldrich (Steinheim, Germany)
n-Dodecyltrimethoxysilane, 95 %	ABCR GmbH & Co. KG (Karlsruhe, Germany)
Ethanol, gradient grade	Merck KGaA (Darmstadt, Germany)
Ethanolamine hydrochloride, 1 M	GE Healthcare Bio-Sciences AB (Uppsala, Sweden)
1-Ethyl-3-(3-dimethylaminopropyl)-carbodiimide hydrochloride	GE Healthcare Bio-Sciences AB (Uppsala, Sweden)
Glutaric anhydride, 95 %	Sigma-Aldrich (Steinheim, Germany)
Glutaric anhydride, for synthesis	Merck Schuchardt OHG (Hohenbrunn, Germany)
(3-Glycidyloxypropyl)trimethoxysilane, ≥ 98 %	Sigma-Aldrich (Steinheim, Germany)
Glycine, ≥ 99.5 %	Merck KGaA (Darmstadt, Germany)
Guanidine hydrochloride, ≥ 99 %	Sigma-Aldrich (Steinheim, Germany)
Hydrochloric acid fuming 37 %, for analysis	Merck KGaA (Darmstadt, Germany)
Hydrogen peroxide 30 %	Merck KGaA (Darmstadt, Germany)
4-(2-Hydroxyethyl)piperazine-1-ethanesulfonic acid, ≥ 99.5 %	Sigma-Aldrich (Steinheim, Germany)
LowCross-Buffer®	CANDOR Bioscience GmbH (Wangen, Germany)
LowCross-Buffer® MILD	CANDOR Bioscience GmbH (Wangen, Germany)
N-Hydroxysuccinimide	Sigma-Aldrich (Steinheim, Germany)
1,1'-Oleoyl-2,2'-(12-biotinyl (aminododecanoyl))cardiolipin (ammonium salt)	Avanti Polar Lipids (Alabaster, AL, USA)

Polyethylene glycol sorbitan monolaurate (Tween®20)	Sigma-Aldrich (Steinheim, Germany)
Potassium chloride, ≥ 99.5 %	Carl Roth GmbH & Co. KG (Karlsruhe, Germany)
Potassium dihydrogen phosphate, ≥ 99 %	Fluka Chemie AG (Buchs, Switzerland)
Quick Start™ Bradford 1x dye reagent	Bio-Rad (Hercules, CA, USA)
Sodium chloride, 100 %	Merck KGaA (Darmstadt, Germany)
di-Sodium hydrogen phosphate, ≥ 99 %	Fluka Chemie GmbH (Buchs, Switzerland)
Sodium hydroxide, pellets min. 99 %	Merck KGaA (Darmstadt, Germany)
Sulfo-NHS-Biotin	Thermo Fischer Scientific (Rockford, IL, USA)
Sulfuric acid 95-97 %, for analysis	Merck KGaA (Darmstadt, Germany)
[Benzotriazol-1-yloxy(dimethylamino)methylidene]-dimethylazaniumtetrafluoroborate	Sigma Aldrich (Steinheim, Germany)
3,3',5,5'-Tetramethylbenzidine, liquid substrate system	Sigma Aldrich (Steinheim, Germany)
Tris(hydroxymethyl)aminomethane hydrochloride	Merck KGaA (Darmstadt, Germany)
VY-B-49 (ω-amine cardiolipin)	synthesized by group of Andrew B. Holmes (Melbourne, Australia) (Johns et al. 2009)

Unless otherwise indicated, chemicals had 95 % purity. Nitrogen gas for chip preparations was taken from an *in-house* pipeline.

5.2. Proteins

Name	**Supplier**
Albumin, from bovine serum, ~ 99 %	Sigma-Aldrich (Steinheim, Germany)
Albumin, from human serum, ≥ 96 %	Sigma-Aldrich (Steinheim, Germany)
Cardiolipin antibody from human serum, polyclonal	LifeSpan Biosciences Inc. (Seattle, WA, USA)
Fetal calf serum	Biochrom AG (Berlin, Germany)
Goat IgG antibody, horseradish peroxidase (HRP)-conjugated from mouse, monoclonal	Sigma Aldrich (Steinheim, Germany)
Human apolipoprotein H (β_2-GPI) antibody from goat, polyclonal	USBiological (Swampscott, MA, USA)
Human apolipoprotein H	Scipac (Sittingbourne, UK)

Human IgG antibody, HRP-conjugated from rabbit, polyclonal	Dako (Glostrup, Denmark)
Human IgG (F_{ab} specific) antibody from goat, polyclonal	Sigma-Aldrich (Taufkirchen, Germany)
Human IgG (F_c specific) antibody from goat, polyclonal	Sigma-Aldrich (Taufkirchen, Germany)
Human IgM antibody, HRP-conjugated from rabbit, polyclonal	Dako (Glostrup, Denmark)
Human prothrombin antibody from mouse, monoclonal	Haematologic Technologies Inc. (Essex Junction, VT, USA)
Human prothrombin	Haematologic Technologies Inc. (Essex Junction, VT, USA)
Mouse IgG antibody, HRP-conjugated from rabbit, polyclonal	Sigma-Aldrich (Taufkirchen, Germany)
Protein A/G	Thermo Fisher Scientific (Rockford, IL, USA)
Rabbit IgG antibody, HRP-conjugated from donkey, whole antibody	Biosciences Amersham/GE Healthcare Bio-Sciences AB (Amersham,UK)
Streptavidin	Sigma-Aldrich (Taufkirchen, Germany)
Transferrin, min. 98 %	Sigma-Aldrich (Taufkirchen, Germany)

5.3. Patients

Name	Provided by
APS positive serum according to Sydney classification	Klinikum rechts der Isar (Munich), University Hospital Wuerzburg
Systemic lupus erythematosus (SLE) patient serum	Klinikum rechts der Isar (Munich)
Healthy control serum	Klinikum rechts der Isar (Munich)

All positive patients were diagnosed with a definite APS according to the Sydney classification criteria (for details see chapter 3.1.1) (Miyakis et al. 2006). Disease controls were diagnosed with an SLE. The serological parameters of the APS- and SLE-patients as well as the negative controls were determined as follows: anti-cardiolipin and anti-β_2-GPI are routinely measured by technical assistants of the Klinikum rechts der Isar with the Alegria system from ORGENTEC (Mainz, Germany). Lupus anticoagulant is determined by using the BCS XP from Siemens Healthcare Diagnostics (Eschborn, Germany). Anti-prothrombin was detected (in own experiments) with an ELISA system from

ORGENTEC as described in this section, chapter 5.10 (results are listed in the appendix, Table 10). Patient screening was performed with 35 APS patient sera (10 female (28.6%), 25 male, average age was 45.9), 6 SLE patients (all male, average age of 42.5) and 24 healthy control samples (4 female (16.7%), 19 male, average age was 42.5). Serum aliquots (10 µL) are stored at −80 °C. The study is approved by the institutional ethics committee of the Klinikum rechts der Isar, Technische Universität München. All participants gave written informed consent. No financial compensation was paid.

5.4. Materials

Name	Supplier
Anti-annexin V IgG/IgM ELISA kit	ORGENTEC Diagnostika GmbH (Mainz, Germany)
Anti-prothrombin IgG/IgM ELISA kit	ORGENTEC Diagnostika GmbH (Mainz, Germany)
Filter, 0.2 µm	Whatman (Freiburg, Germany)
1-λ-reflectometry chips (9 x 9 mm)	Berliner Glas (Berlin, Germany)
Microcon spin columns 30 kDa	Millipore (Darmstadt, Germany)
Microtiter plate 96 well for Bradford	
N-Hydroxysuccinimide activated columns	Thermo Fisher Scientific (Waltham, MA, USA)
Nunc-Immuno™ Maxisorp™ 96 well plate	Sigma-Aldrich (Taufkirchen, Germany)
pi-RIfS chips (75 x 25 mm)	MICROS Präzisionsoptik GmbH & Co. KG (Schmiedefeld, Germany)
Protein A/G column kit	Thermo Fisher Scientific (Waltham, MA, USA)
Weighing bottle with tympan, 30*50 mm	Neubert Glas (Ilmenau, Germany)
Weighing bottle with tympan, 30*80 mm	Neubert Glas (Ilmenau, Germany)

5.5. Instruments

Name	Supplier
Absorbance Microplate Reader (ELx808)	BioTek Instruments Inc. (Winooski, VT, USA)
Analytical balance (Analytic AC 1203)	Sartorius AG (Göttingen, Germany)
Analytical balance (XS205 Dual Range)	Mettler-Toledo International Inc. (Greifensee, Switzerland)
BiacoreX	GE Healthcare Bio-Sciences AB (Freiburg, Germany)
BioOdyssey Calligrapher MiniArrayer	Bio-Rad Laboratories GmbH (Munich, Germany)
14bit CCD camera “pco.1600”	PCO AG (Kehlheim, Germany)

ESE-LOG USB detection module with LED (470 nm) and integrated photodiode	Qiagen Lake Constance GmbH (Stockach, Germany)
Magnetic mixer with heating	IKA (Staufen, Germany)
Millipore (Milli-Q plus 185)	Millipore (Schwalbach, Germany)
Orbital shaker for microtiter plates	IKA (Staufen, Germany)
PDMS flow cell	Biametrics GmbH (Tübingen, Germany)
Tecan XLP6000 syringe pump	NMI (Reutlingen, Germany)
Tecan 9-way valves	NMI (Reutlingen, Germany)
Telecentric objective "S5LPJ2060"	Sill Optics (Wendelstein, Germany)
Telecentric objective "S5LPL2060" with coaxial LED (high power, 470 nm)	Sill Optics (Wendelstein, Germany)
Tubing pump	ISMATEC, IDEX Health & Science (Wertheim, Germany)
Ultrasonic bath (Sonorex RK510S)	Bandelin electronic GmbH & Co. KG (Berlin, Germany)
Vortex-Genie 2	Scientific Industries (Bohemia, New York, USA)
Zentrifuge 5415 R	Eppendorf (Hamburg, Germany)

5.6. Software

Name	Supplier
BioOdyssey Calligrapher software	Bio-Rad Laboratories GmbH (Munich, Germany)
DSService	Qiagen Lake Constance GmbH (Stockach, Germany)
Fluidik software	Using internal software
ImageJ (version 1.46e)	Public domain, JAVA-based (developed by Wayne Rasband at the National Institutes of Health)
MedCalc (version 14.12.0)	MedCalc Software (Ostend, Belgium)
Microsoft Office (2003 and 2007)	Microsoft (Redmond, WA, USA)
OriginPro 8.1	OriginLab Corporation (Northampton, MA, USA)
Pymol	Schrödinger (Portland, OR, USA)
PCO "Camware" software version 3.03	PCO (Kehlheim, Germany)
SPSS	IBM Corp. (Armonk, NY, USA)

5.7. Surface chemistry

5.7.1. Transducer preparation and polymer coating

Cleansing of transducers

Cleaning solution	H_2SO_4, 40 mL
	H_2O_2, 20 mL

The transducers are made of a 1 mm BK7-glass substrate with a layer of 45 nm Ta_2O_5 covered by a 20 nm layer of SiO_2. The surface of the glass chips is cleaned and activated with cleaning solution for 15 min in an ultrasonic bath. With a strong acid and oxidizing solution silanol groups are formed on the SiO_2 surface. These silanol groups can then be chemically modified in the next steps. Immediately, the cleaning solution is thoroughly rinsed off with Millipore water and the transducers are dried in a nitrogen stream.

During all the following preparative steps the chips are placed on plastic caps in weighing bottles. Some of those contain small amounts of water or dimethylformamide (DMF) on the bottom to create a water or DMF atmosphere, respectively. Unless otherwise indicated, for the smaller 1-λ-reflectometry chips, 10 µL of every solution is pipetted on one chip that is subsequently covered with a second chip, forming a sandwich. For the larger pi-RIfS chips 100 µL of every solution was used and two chips were always put together to a sandwich as well.

Preparation of amino dextran (AMD) chips

Coating solution	Amino dextran, 100 mg/mL
	H_2O

First, glycidyloxypropyl trimethoxysilane is pipetted undiluted onto the activated transducers, which are left in a dry weighing bottle for 1 h at room temperature (RT). The exclusion of water is essential to prevent the silanes from condensation with each other. The chips are rinsed with acetone and dried in a nitrogen stream. Afterwards, chips are incubated with AMD solution in an H_2O atmosphere for at least 6 h at RT, rinsed with Millipore water and dried again in a nitrogen stream.

Preparation of polyethylene glycol (PEG) chips

Coating solution	Diaminopoly(ethylene)glycol, 4 mg/mL
	Dichloromethane

For immobilization of polyethylene glycol, chips are coated with glycidyloxypropyl trimethoxysilane as described above. Subsequently 20 µL of coating solution is pipetted onto the surface, without forming a sandwich. For incubation, the chips are placed in an oven for at least 6 h at 70 °C. Modified PEG transducers are rinsed with Millipore water and dried in a nitrogen stream.

Preparation of 11-aminoundecyltrimethoxysilane (AUTMS) chips

For the silanization with 11-AUTMS, 1-λ-reflectometry chips are incubated with 100 % 11-AUTMS, pi-RIfS chips with 11-AUTMS diluted 1:10 with DMF, due to the larger volume of silane solution applied. The dilution had no effect on binding signal intensities (evaluated with 1-λ-reflectometry and several dilutions of 11-AUTMS solution). Transducer sandwiches are kept in a DMF atmosphere at RT for 1 h, rinsed with acetone, and dried in a nitrogen stream.

Changing the amino-group into a carboxy-function

Reaction solution	Glutaric anhydride, 2 mg/mL DMF

The terminal amino groups of AMD-, PEG- and 11-AUTMS-modified transducers are changed into carboxyl functions by incubation with reaction solution at RT over night. Again two chips are put together as sandwich and kept under DMF atmosphere. Cleaned and dried chips can be stored at 4-6 °C for several weeks.

5.7.2. Direct immobilization of antigen

Activation solution	N-Hydroxysuccinimide (NHS), 1 M N,N'-Diisopropylcarbodiimide (DIC), 1.5 M DMF
HEPES buffered saline (HBS)	4-(2-Hydroxyethyl)piperazine-1-ethanesulfonic acid (HEPES), 20 mM NaCl, 150 mM pH 7.4
Antigen solution	Human β_2-GPI, 1 mg/mL HBS
	Human prothrombin, 1 mg/mL HBS
	ω-Amine cardiolipin HBS
	Human β_2-GPI, 1 mg/mL ω-Amine cardiolipin HBS
	Bovine serum albumin (BSA), 1 mg/mL HBS

For covalent immobilization of proteinogenic antigens as well as the ω-amine cardiolipin, transducers are activated with activation solution for 2-4 h. Then, they are rinsed with acetone, dried and immediately the antigen solution is pipetted onto the formed active esters. All chips used in the 1-λ-reflectometry are incubated with the respective antigen solution over night at RT in water atmosphere. In case of the pi-RIfS system, several antigens are spotted onto the chip surface using a pipette. Therefore, three replicate spots using 0.5 µL of the desired antigen solution are placed on the activated transducers. The diameter of each spot is about 1 mm, gaps in between the spots vary due to the manual spotting procedure. A few transducers measured in the pi-RIfS system were produced using a contact printer. This procedure is explained in chapter 5.7.4. Chips were blocked with ethanolamine.

5.7.3. Immobilization via biotin-streptavidin

Biotin solution	D-Biotin, 1 mg/50 µL O-(Benzotriazol-1-yl)-N,N,N',N'-tetramethyluronium tetrafluoroborate (TBTU), 1.4 mg/50 µL N,N-Diisopropylethylamine (DIPEA), 4 µL/50 µL DMF
HBS buffer	HEPES, 20 mM NaCl, 150 mM pH 7.4
Streptavidin solution for covalent immobilization	Streptavidin, 5 mg/mL HBS
Streptavidin solution for non-covalent immobilization	Streptavidin, 35 µg/mL HBS
Antigen solution	Biotin-cardiolipin HBS
	Human β_2-GPI, 1 mg/mL Biotin-cardiolipin HBS

Streptavidin was immobilized either directly (covalent) onto AMD-, PEG- or 11-AUTMS-modified transducers or via non-covalent interactions with a biotinylated surface. For a covalent attachment of streptavidin, terminal carboxy functions are activated as described in chapter 5.7.2.

and the streptavidin solution was applied to the surface over night at RT in water atmosphere. A non-covalent immobilization of streptavidin was achieved by incubation of the chip surface with biotin solution over night at RT. Afterwards transducers are rinsed with DMF as well as water and dried with a nitrogen stream. Biotinylated chips are placed in the flow cell and 1 mL of streptavidin solution is injected with a flow rate of 20 µL/min.

5.7.4. Antigen spotting with BioOdyssey Calligrapher MiniArrayer

PBS buffer	KCl, 2.6 mM NaCl, 138 mM HNa_2PO_4 x $2H_2O$, 10 mM H_2KPO_4, 1.8 mM pH 7.4
Washing solution	Tween®20, 0.01 % (v/v) Phosphate buffered saline (PBS)
Antigen solution	Human β_2-GPI, 1 mg/mL Tween®20, 0.01 % (v/v) PBS
	Human prothrombin, 1 mg/mL Tween®20, 0.01 % (v/v) PBS
	ω-Amine cardiolipin PBS
	Human β_2-GPI, 1 mg/mL ω-Amine cardiolipin PBS
	BSA, 1 mg/mL Tween®20, 0.01 % (v/v) PBS

Multiplexed biosensor chips produced via contact printing are activated as described in chapter 5.7.2. Each antigen solution is placed in a single cavity of a 96-well microtiter plate. Washing solution and Millipore water are used for cleaning of the pin within the spotting run. With the Bio-Rad software program antigen spots of about 170 µm in diameter were placed on the chip surface with gaps of 800 µm in between. The microarrays consist of seven replicate spots for each antigen aligned in rows with BSA spotted between every two antigens. Buffer measurements have been

performed with microarrays produced with the BioOdyssey Calligrapher, serum measurements with microarrays spotted by hand. After completion of the spotting procedure the glass transducers are incubated under water atmosphere at RT over night and rinsed thoroughly with Millipore water. Chips are always used the next day and not stored at all. This should guarantee for reproducible sensor surface conditions.

5.8. Antibody purification

PBS buffer (Thermo Fischer)	Phosphate, 100 mM NaCl, 150 mM pH 7.4
Elution buffer	Glycine, 100 mM pH 2.8
Neutralization buffer	Tris, 1 M pH 8.5

Antibody purification is carried out as described in the product information of the supplier using a recombinant A/G fusion protein covalently immobilized onto sepharose beads. Protein A is a surface protein of about 42 kDa that is found in the cell wall of *Staphylococcus aureus* (Graille et al. 2000). It comprises five homologous domains that can bind mammalian immunoglobulins, most notably human IgG_1 and IgG_2, but also IgM, IgA and IgE, but with less affinity. Protein A interacts with the heavy chain constant region of IgG immunoglobulins for example ($F_c\gamma$). This characteristic can be used not only for antibody isolation, but also for their exposition on a surface. In a following reaction step, specific antigen is "captured" by the available F_{ab} domains, thereby being isolated as well. Besides the F_c domain, protein A also binds the human F_{ab} domain of the heavy chain of the V_H3 (variable, heavy chain) family. This constitutes a possibility to select certain B cells dependent on their B cell receptor. To expand the binding properties to human IgG_3, protein A is fused to protein G from *Streptococcus* that has a binding capacity for this antibody subclass.

The protein A/G coated sepharose® beads are equilibrated three times by washing with 400 µL of PBS buffer and centrifugation at 1,000 x g for 1 min at RT. Afterwards they are incubated with 50 µL of serum for 10 min. Subsequently the columns are washed thoroughly with PBS buffer. Bound protein is eluted with 400 µL of elution buffer three times and collected in a 2 mL cup containing 40 µL of neutralization buffer. The columns are restored by washing several times with 400 µL of PBS buffer and kept at 4 °C. They can be reused for up to ten purification cycles. All eluted fractions of one patient sample are pooled in centrifugal filter devices with a cut off of 30 kDa from Millipore and buffer is exchanged into HEPES running buffer by spinning at least 4 times at 13,000 x g for 5 min at

RT. Final volume of each sample is adjusted to 250 µL. The protein content is verified with Bradford (Bradford 1976) solution from Bio-Rad (Hercules, CA, USA). Purified antibody samples were either measured the same day or stored over night at 4 °C.

5.9. Quantification of protein content using Bradford assay

The Bradford assay is a fast and sensitive spectroscopic method for the quantitation of protein (Bradford 1976). The colorimetric test is based on the absorbance shift of the dye Coomassie Brilliant Blue G-250 that binds to cationic and non-polar amino acid residues in acidic solutions. The unbound, cationic form of the dye has an absorption maximum at 470 nm in the red spectral range. Under acidic conditions it is converted into its anionic blue form that is stabilized by the formation of dye-protein-complexes and has an absorption maximum of 595 nm. Thus, the increase in absorbance at 595 nm is a direct measure of the protein concentration. Since the amount of dye-protein-complex is dependent on the type of protein, the calibration should be performed with a dilution series of the respective protein. If this is not possible or the concentration of a protein mixture shall be determined, a standard protein solution like chymotrypsin, lysozyme or BSA can be used, but it should be kept in mind that this might cause slight inaccuracies.

The ready to use Bradford solution as well as a BSA standard with concentrations of 0.15 mg/mL – 2.0 mg/mL was obtained from Bio-Rad. 5 µL of each protein sample and BSA standard was pipetted into the wells of a 96 well plate. As negative control, 5 µL of the respective buffer system was used. After adding 250 µL of Bradford reagent to every well and incubating the plate in the dark for 10 min at RT, the absorbance at 595 nm was determined with an ELx808 Absorbance Microplate Reader.

5.10. Enzyme-Linked Immunosorbent Assay (ELISA)

The enzyme-linked immunosorbent assay is an antibody based test format to identify a substance in a wet or liquid sample (Engvall & Perlmann 1971). This can be a protein or a virus, but also small molecules, like hormones or toxins. The antigen is attached to a polystyrene microtiter plate either directly through absorption to the surface or via capture with an immobilized antibody (sandwich ELISA). The capture method can be chosen if the antigenic protein is denatured upon binding to the plastic well. After a blocking step, a specific antibody is added that binds to the exposed antigen. This antibody can be conjugated to an enzyme or is recognized by a secondary antibody conjugated to an enzyme. The advantage of a secondary antibody is a signal enhancement due to the fact that a polyclonal secondary antibody can bind to multiple sites of the primary antibody's F_c part. Furthermore, not all primary antibodies, which are just specific for one reaction, have to be conjugated with an enzyme, whereas a secondary antibody can be used in several

different assays. In the last step the substrate of the enzyme is added which produces the detectable signal, usually a colour change. An alkaline phosphatase or a horseradish peroxidase (HRP) are often used as enzymes. The former converts *para*-nitrophenylphosphate (pNPP) into the yellow substance *para*-nitrophenol, which can then be measured at 405 nM. The peroxidase catalyzes the reaction of several chromogenic compounds like 3,3',5,5'-tetramethylbenzidine (TMB) or 3,3'-diaminobenzidine (DAB) as well as of enhanced chemiluminescent substrates (ECL). The limit of detection varies between 10 ng/well in the case of pNPP to 2 pg/well for ultra TMB (Thermo Fisher Sientific Inc 2015).

ELISAs obtained from ORGENTEC

Microplate (ORGENTEC)	Ready to use, coated with respective antigen
Diluent (5x) (ORGENTEC)	PBS BSA Detergent NaN_3 0.09 %
Calibrator and control (ORGENTEC)	0 – 100 U/mL antibody PBS BSA Detergent NaN_3 0.09 %
Conjugate IgG/IgM (ORGENTEC)	Human IgG/IgM antibody, peroxidase (POD)-labeled PBS BSA Detergent PROCLIN 0.05 %
Human samples	APS patient or healthy control serum, diluted 1:100 with diluent
Wash (50x) (ORGENTEC)	Tris Detergent NaN_3 0.09 %
TMB (ORGENTEC)	Ready to use TMB substrate
Stop (ORGENTEC)	Ready to use acidic solution

All concentrates were diluted with Millipore water as requested by the supplier. 100 µL of each calibrator solution, the controls and the human samples was pipetted into the cavities of the provided microtiter plate and incubated for 30 min at RT. After three times washing with 300 µL

wash solution, 100 µL of either IgG or IgM conjugate was added to the wells for 15 min at RT. Again, the plate was washed three times and then 100 µL of TMB substrate was applied to the cavities. The plate was kept in the dark for 15 min at RT and finally 100 µL of stop solution was used to terminate the enzymatic reaction. Absorbance was determined at 450 nm with an ELx808 Absorbance Microplate Reader.

5.11. Reflectometric Interference Spectroscopy (RIfS)

5.11.1. 1-λ-reflectometry

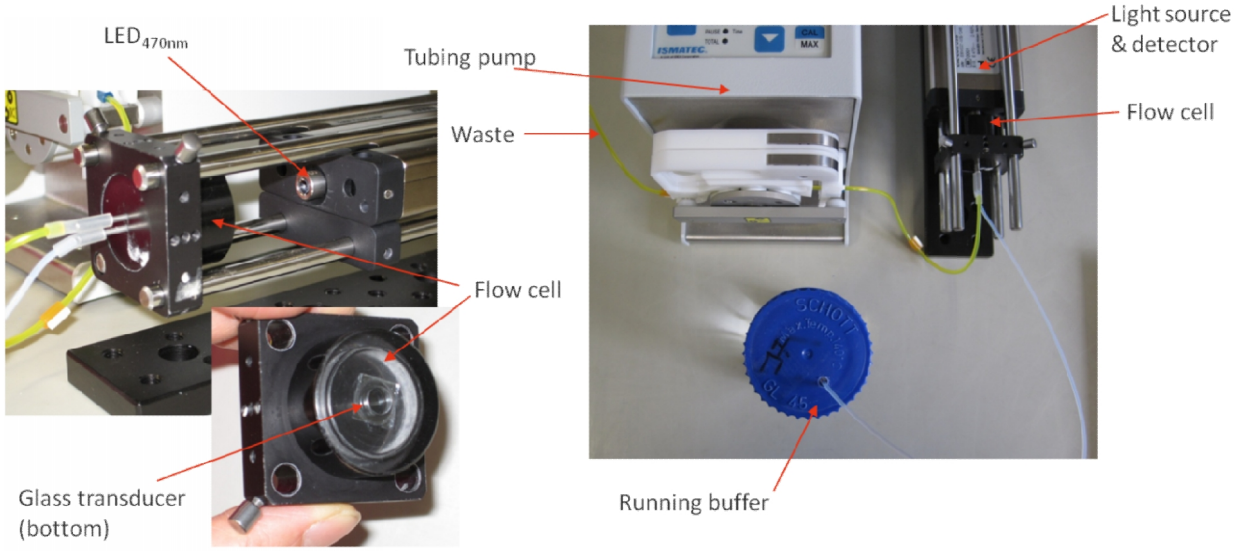

Figure 36: Picture of the 1-λ-reflectometry set-up. The transducer is in an upright position with its back side facing the LED (470 nm). The sample runs through the white tube into the flow cell and through the yellow tube into the waste. Change in reflectometric characteristics is detected by an optical fibre and communicated via USB interface to a computer.

The 1-λ-reflectometry set-up utilized in this work consists of a detection module (ESE-LOG USB) including a diode that emits light at 470 nm. The transducer is made of 1 mm BK7 glass substrate with a 45 nm layer of Ta_2O_5 and a 20 nm deposit of SiO_2 on top (Ewald et al. 2013). It is placed upright in the flow cell with its backside facing the diode (Figure 36). The flow cell is connected to a tubing pump (ISMATEC) that allows for manual control of the injection speed between 2 and 57,000 µL/min. The emitted light from the detection module hits the backside of the transducer and the light is partially reflected at every interface of the biosensors layer system. This results in a characteristic interference spectrum that changes upon binding of the analyte (for details see chapter 3.2.5) (Gauglitz 2010).The reflected light is guided through the same Y-optical fibre as the incident light and is monitored by an integrated photodiode (Fechner et al. 2011). All liquids for one measurement had to be injected by hand.

1-λ-reflectometry measurements

Running and dilution buffer	HEPES, 20 mM NaCl, 150 mM Tween®20, 0.2 % (v/v) Human serum albumin (HSA), 0.05 % (w/v) pH 7.4
Regeneration solution	Guanidine hydrochloride, 6 M pH 2
Antibody solution	Anti-β_2-GPI, polyclonal, 25 µg/mL
	Anti-prothrombin, monoclonal, 25 µg/mL
Human sample solution	APS patient or healthy control serum, diluted 1:10, final volume: 100 µL

Measurements for assay development were conducted with 500 µL of sample volume. Furthermore, different buffer systems were evaluated, that are not listed here due to complexity. They are described in the text (see chapters 4.2 and 4.2.3). Sample volume was reduced to 100 µL for detection of antibodies in patient sample as well as all measurements performed for characterization of the system. This included intra-chip stability and inter-chip variability as well as specificity of the antigenic biosensor surface. For all these experiments, buffers and solutions are listed above.

Chip validity was verified by measurements with 100 µL of antibody solution injected into the flow cell with a flow rate of 10 µL/min. Serum measurements were performed with 100 µL human sample solution. Flow rates are the same as for the antibody measurements. The dissociation phase was recorded by injection of 200 µL running buffer at a flow rate of 10 µL/min. Using 100 µL of regeneration solution (50 µL/min) the chip surface could be completely restored and was ready for injection of the next sample. Intra chip stability was tested by repeated injections of one patient sample over three days. Inter chip variability was determined by measurements of the same five APS patient samples and healthy controls on three different chips prepared in parallel.

Data processing for 1-λ-reflectometric measurements

Data from 1-λ-reflectometry is obtained from the detection module in mV with one data point every 2.2 sec. The curve progression is negative caused by the same reflectivity behaviour as for the pi-RIfS set-up (for further details see "pi-RIfS set-up", explained below). All obtained values of one binding event are divided by the first data point. This results in normalized values which are then plotted as a function of time (in seconds). Binding intensities are calculated by the difference between the maximum and the minimum signal intensity (curve progression is negative). The former

refers to the base line monitored before injection of the sample, latter is determined after the binding event is completed, before the dissociation phase has started.

5.11.2. polarized imaging (pi)-RIfS

The central parts of the pi-RIfS set-up include a polydimethylsiloxane (PDMS) flow-cell (Biametrics GmbH, Tübingen, Germany) that covers the sensor chip. Glass transducers are made of the same substrate as for the 1-λ-reflectometry. A telecentric objective (S5LPL2060, Sill Optics, Kelheim, Germany) combined with an LED (high power, 470 nm wavelength) is used as light-source. Signal detection is managed with a 14 bit CCD camera "pco.1600" (PCO AG, Kelheim, Germany, controlled by PCO "Camware" software version 3.03). Small components, optical mountings, and adjusting plates are obtained from Qioptiq (Göttingen, Germany) and Edmund Optics GmbH (Karlsruhe, Germany), respectively. The fluidic system includes two Tecan XLP 6000 syringe pumps as well as two Tecan 9-way valves (NMI, Reutlingen, Germany). The pump rates can be regulated between 6.25 µL/min and 7500 µL/min (the set-up is depicted in chapter 3.2.5). The camera as well as the telecentric objective, including the light source, were assembled on rotary plates. This allows an adjustment of the angle of incidence with an accuracy of ±1° related to the perpendicular axis of the transducer surface. Referring to Fresnel's equations, reflection coefficients are dependent on the polarization of the light that hits the surface as well as the angle of incidence. Therefore, a sigma-polarization according to the plane of incidence and an angle of 35° were chosen for this set-up. This was experimentally optimized by Oliver Bleher and part of his doctoral thesis.

pi-RIfS measurements

Running & dilution buffer	HEPES, 20 mM NaCl, 150 mM Tween®20, 0.2 % (v/v) HSA, 0.05 % (w/v) pH 7.4
Regeneration solution	Guanidine hydrochloride, 6 M pH 2
Antibody solution	Anti-β_2-GPI, polyclonal, 12 µg/mL Anti-prothrombin, monoclonal, 12 µg/mL Anti-BSA, monoclonal, 50 µg/mL Anti-cardiolipin, polyclonal, 40 µL/mL
Human sample solution	APS patient or healthy control serum, 50 µL purified with protein A/G

Measurements with anti-BSA, anti-prothrombin, anti-β_2-GPI or anti-cardiolipin are performed to test for chip performance. Concentration of the anti-cardiolipin is not provided by the supplier, therefore amounts are always given in microliters and cannot be compared with the amounts of the other antibodies used. For the detection of patients' antibodies, the whole IgG fraction of 50 µL serum is isolated as described in chapter 5.8.. All samples are diluted to a final volume of 250 µL with dilution buffer and injected automatically with a flow rate of 50 µL/min. Prior to every measurement a baseline of 200 s is recorded. The dissociation phase is carried out with a higher flow rate of 200 µL/min for a total of 200 s. Using 500 µL of regeneration solution at a flow rate of 200 µL/min, the antigenic surface is restored which allows about 20 consecutive measurements on a single biosensor chip. The instrumental set-up does not include a temperature control device; therefore all measurements were performed at RT. The resulting binding signals are of negative values, due to the properties of the transducers layer system and the resulting intensity shifts by changing the optical thickness of the sensitive layer.

Data processing for pi-RIfS measurements

The pi-RIfS data is obtained from the CCD detector as pixel values (counts) and processed as follows. Mean values of each spot are calculated using ImageJ (Version 1.46e) and referenced to mean pixel values of spots on the sensor chip, where no specific binding occurs. The calculated mean values of one measurement are normalized by subtraction of the starting value of every spot from all following values of this spot (see equation below). This eliminates possible discrepancies in the general illumination levels that can slightly vary between different spots on one sensor chip due to the fact that one chip is comparatively large with 75 x 25 mm.

$$I_j = \frac{1}{n}\sum_{j=1}^{n} s_j \Big/ \frac{1}{n}\sum_{i=1}^{n} r_i - Z_j$$

In Equation 1, I_j refers to the referenced and normalized signal intensity of each spot *j*. s_j stands for the count value of each pixel within the spot *j* and r_i for the count value of each pixel within the reference spot *i*. *Z* is the referenced intensity of the zero point where the sample injection starts and *n* the number of pixel values added. The resulting signals are plotted as a function of time (in seconds) giving a real-time binding curve. Each curve is further evaluated by applying a linear fit to the onset of the binding event directly after injection of the sample. To this end always a set of 20 data points (equates to 20 s of measurement time) was selected. In general, this region of a binding curve is characterized by the diffusion controlled linear behaviour that is a common for every binding event at that point. Therefore this should provide for data which is reasonable to compare with each other. Further discussions of the results are based on the slope of this linear fit.

6 conclusion

Parallelized screenings like microarrays are of growing importance because they provide a unique tool to evaluate different interactions simultaneously. Thereby, the combination of a short analysis time and low sample consumption are important advantages. We developed a biosensor platform to monitor several antigen-antibody interactions relevant in the autoimmune disorder antiphospholipid syndrome (APS). APS diagnostic is still a challenging field due to the heterogeneous group of antibodies developed by the patients.

Prerequisite for a microarray is a similar surface bioconjugation of the antigenic structures as well as identical assay conditions. Different surface modifications were compared in terms of immobilization efficiency, unspecific binding and recognition by the antibodies. These included the coating of the glass transducers with PEG, AMD, and 11-AUTMS. Antigens were coupled either directly or via biotin-streptavidin interaction. Immobilization of different proteins as well as a ω-amine cardiolipin via 11-AUTMS allowed for a sensitive and selective discrimination of APS patients and healthy controls. 11-AUTMS forms a two dimensional surface on the glass transducer, which only provides for a low density coating of the antigenic structures, but presents a platform with low unspecific binding of the serum matrix. Buffer and regeneration solution were optimized and stability of the antigenic surface tested with repeated measurements. Latter is given for about 20 consecutive measurements and inter-chip variability was determined to be about 13 % (mean).

Detection of anti-β_2-GPI alone could be performed in diluted serum with a sensitivity of 94.12 % and a specificity of 100 %. To monitor the specific interaction of prothrombin and a prothrombin antibody, a purification of the whole IgG fraction from serum was necessary. With this preparative step APS patients and healthy controls could be clearly differentiated. Finally, several antigenic structure, namely β_2-GPI, prothrombin, cardiolipin and a β_2-GPI/cardioliopin complex were combined on one glass transducer and investigated with the pi-RIfS system. The reason to immobilize these four antigens is their relevance in APS. After anti-β_2-GPI and anti-CL, which are laboratory criteria for the diagnosis of APS, anti-prothrombin are the most present antibodies, APS patients develop.

For the detection of anti-β_2-GPI and anti-,prothrombin the pi-RIfS microarray gave excellent results. Sensitivity was calculated to be 81.82 and 92.86 %, respectively and specificity was 96.87 and 82.35 %. The test for anti-cardiolipin and anti-β_2-GPI/cardiolipin-complex shows lower sensitivity (88.57 and 94.29 %) as well as specificity (76.67 and 73.33 %). Reason might be the hydrophobicity of the cardiolipin which causes stronger background signals than a solely proteinogenic surface coating. Furthermore, the assay conditions were initially optimized for the detection of anti-β_2-GPI and adapted to all other antigens.

Comparing the pi-RIfS data with the respective ELISA assays, it can be concluded that both systems are in good agreement. Especially the detection of anti-β_2-GPI seems to be as valid as the ELISA with a confidence interval (CI) of 0.860-0.987.

The single spot biosensor has the advantage of easy handling and no necessity of any purification steps prior to the measurement. In contrast, the microarray requires more preparation, but allows a multiplexed detection of several serological parameters. The parallel detection of multiple parameters is becoming more and more important, not only in the field of clinical diagnostics. Thereby, real-time assays play a central role among a great variety of readout systems, as they may provide kinetic data for analyte binding. By introducing further antigens, this system could provide a broader characterization of the patients' antibody spectrum. Both aspects, kinetic data as well as APS-antibody complexity, might provide helpful information about the state of the disease in every investigated indiviual. The broad spectrum of possible clinical symptoms might be dependant on the kind of antibody developed. Thereby not only the specificity could be important (whether anti-prothrombin or anti-β_2-GPI) but also its affinity. As a consequence, a more personalized treatment of this autoimmune disorder could be achieved.

7 appendix

Table 9: Differential diagnosis for APS and CAPS.

Venous thrombosis:

1. Inherited and acquired coagulation and anticoagulation factor disorders
2. Defective clot lysis
3. Cancer and myeloproliferative disorders
4. Nephrotic syndrome

Arterial thrombosis:

1. Atherosclerosis
2. Embolic disease (such as endocarditis, cholesterol emboli, atrial fibrillation or atrial myxoma, paradoxical embolism or marked left ventricular dysfunction)
3. Decompression sickness
4. Thrombotic thrombocytopenic purpura/haemolytic-uremic syndrome
5. Polyarteritis nodosa and other forms of systemic vasculitis

Both, venous and arterial thrombosis:

1. HIT (heparin-induced thrombocytopenia)
2. Defective clot lysis due to dysfibrinogenemia or plasminogen activator deficiency
3. Homocysteinemia
4. Myeloproliferative disorders, polycythemia vera (P vera), or paroxysmal nocturnal hemoglobinuria
5. Hyperviscosity due to P vera, Waldenstrom's macroglobulinemia, sickle cell disease
6. Systemic vasculititis
7. Paradoxical embolism

All above named disorders can be excluded by a second positive test for aPL after 12 weeks.

Thrombotic microangiopathies:

1. Thrombotic thrombocytopenic purpura/Hemolytic uremic syndrome (TTP/HUS)
2. HELLP syndrome (Haemolysis, Elevated Liver enzyme levels, Low Platelet count)
3. Sepsis with multiorgan failure and disseminated intravascular coagulation

These are difficult to distinguish from CAPS, because thrombotic microangiopathies occur in multiple organs simultaneously.

Table 10: Summary of all samples investigated with ELISA, pi-RIfS system, and 1-λ-reflectometry (from left to right). CL refers to cardiolipin, PT to prothrombin. Patients are identified by their identification number (ID). Positive and negative are listed separately. SLE indicates disease controls suffering from systemic lupus erythematosus.

ID	ELISA			pi-RIfS			1-λ-RIfS	
positive	Anti-CL-IgG	Anti-β_2GPI-IgG	Anti-PT-IgG	Anti-β_2GPI	Anti-PT	Anti-β_2GPI/CL	Anti-CL-IgG	Anti-β_2GPI
15	>120	>100	0.8	2.92E-06	3.14E-07	4.60E-06	7.32E-07	10.0
40	>120	83.0	6.4	3.23E-05	5.34E-06	2.04E-05	1.22E-05	7.3
113	64.0	68.5	3.7	2.11E-05	3.83E-06	1.20E-05	1.24E-05	4.7
262	81.5	80.0	4.6	9.55E-05	-9.34E-06	1.02E-05	4.44E-05	7.2
270	24.5	27.0	6.4	4.65E-05	1.33E-05	7.66E-05	7.91E-05	7.4
272	28.5	23.3	7.2	8.43E-05	3.15E-05	1.04E-04	5.79E-05	4.9
273	>120	>100	4.0	2.71E-04	-1.17E-05	2.23E-04	7.12E-05	18.6
274	113.0	73.0	4.8	7.50E-05	6.29E-06	6.20E-05	-7.15E-06	11.1
276	77.0	75.0	3.2	1.59E-04	4.80E-06	9.90E-05	5.89E-06	9.9
296	16.0	7.0	72.4	-2.99E-06	1.44E-05	2.99E-06	6.78E-06	5.4
302	85.4	>100	17.4	1.93E-06	1.39E-05	2.18E-05	-6.63E-06	7.6
304	63.0	69.0	10.6	7.60E-05	9.85E-06	6.21E-05	4.20E-05	5.2
307	>120	>100	>105	9.79E-05	4.95E-05	7.08E-05	5.14E-05	7.4
308	>120	>100	2.5	4.99E-05	3.57E-06	3.77E-05	4.19E-05	5.6
310	24.8	10.6	1.8	2.34E-05	1.46E-06	3.19E-05	6.23E-05	4.0
313	68.0	72.0	3.7	1.49E-05	2.62E-06	1.29E-05	1.66E-05	5.7
318	>120	>100	4.8	4.30E-05	9.55E-06	4.39E-05	5.06E-05	9.9
325	>120	28.5	14.5	6.40E-05	4.83E-06	8.43E-05	6.54E-05	10.0
327	34.7	28.5	4.3	6.65E-05	9.59E-06	9.04E-05	4.85E-05	2.2
328	>120	>100	11.2	2.23E-04	2.25E-05	2.12E-04	1.12E-04	5.7
330	>120	>100	29.4	2.88E-04	4.28E-05	2.70E-04	9.91E-05	6.3
333	106.8	>100	20.1	1.70E-05	9.51E-06	4.79E-05	9.37E-06	7.2
340	117.0	>100	2.0	3.16E-05	5.89E-06	1.09E-05	1.97E-05	6.2
341	61.0	67.0	22.4	3.38E-05	1.27E-05	7.45E-06	1.12E-05	9.0
350	20.3	11.8	86.5	6.03E-05	6.32E-05	7.10E-05	4.82E-05	6.8

357	4.9	7.8	11.3	2.02E-05	6.89E-05	1.22E-04	1.06E-05	4.6
358	37.4	20.8	1.6	1.09E-05	1.66E-06	8.95E-06	1.08E-05	4.5
365	70.3	2.5	3.3	-2.45E-06	3.39E-06	6.43E-06	1.47E-05	7.9
370	91.0	81.0	4.1	1.29E-04	7.57E-06	1.50E-04	5.48E-05	10.6
371	>120	43.8	60.7	2.37E-04	8.18E-06	1.40E-04	6.02E-05	6.7
372	10.7	9.6	9.2	1.92E-06	1.07E-05	4.14E-06	1.18E-05	4.5
374	>120	>100	6.9	9.24E-05	8.53E-06	3.12E-05	3.95E-05	6.6
377	62.0	66.9	2.0	2.10E-05	5.70E-07	2.21E-05	2.30E-05	5.8
378	76.0	72.0	23.9	3.06E-05	2.48E-05	3.16E-05	2.28E-05	5.2
386	8.0	6.7	4.0	-1.58E-06	1.65E-05	5.02E-06	3.48E-06	11.5
negative								
278	2.6	2.7	4.6	-9.49E-08	1.84E-06	-2.92E-06	5.47E-06	1.4
281	2.1	2.4	1.4	4.23E-07	1.80E-07	-1.85E-06	-4.62E-07	0.8
282	3.0	3.1	1.9	-1.30E-06	-8.65E-07	-1.44E-06	6.03E-06	3.6
283	3.0	2.9	3.6	-1.28E-06	2.18E-06	-3.56E-06	-1.79E-06	2.1
284	4.6	2.9	2.9	-2.83E-06	7.32E-07	3.46E-06	8.91E-06	3.1
286	2.5	2.6	2.3	-4.66E-06	-1.85E-06	-3.41E-06	-2.04E-06	1.7
288	2.5	2.2	2.1	-1.43E-06	1.24E-06	-1.24E-06	-1.88E-07	2.4
289	2.2	2.5	2.3	9.36E-07	8.64E-07	3.59E-06	2.75E-06	2.6
290	2.5	2.4	2.7	-9.28E-07	-1.08E-06	3.85E-06	4.16E-06	3.5
291	3.8	2.7	7.3	1.36E-06	5.95E-07	-1.06E-06	2.80E-06	3.6
292	3.1	2.8	1.9	-4.51E-07	-2.49E-07	1.18E-06	1.40E-06	3.3
294	2.4	2.5	1.2	-7.70E-06	-2.94E-06	-3.58E-06	-5.48E-06	4.2
319	2.2	2.3	2.0	9.51E-07	-4.16E-07	-3.22E-06	2.26E-06	2.1
320	2.4	2.4	2.4	9.78E-07	-2.44E-06	-8.47E-08	6.54E-06	1.5
321	2.5	2.3	2.5	2.10E-07	1.29E-05	6.57E-07	3.18E-06	2.8
322	3.5	2.3	2.2	-5.25E-06	2.79E-06	-1.96E-07	-2.46E-06	1.5
323	2.5	2.3	1.6	1.36E-06	1.01E-06	8.58E-06	6.30E-06	1.8
334	2.8	2.4	2.1	-2.89E-06	-2.01E-06	-9.39E-07	4.24E-06	1.2

336	2.7	2.7	1.1	-7.33E-07	2.06E-06	-5.88E-07	4.97E-06	0.7
337	2.5	2.4	2.0	2.36E-06	2.33E-06	2.48E-06	1.50E-06	6.5
338	2.5	3.0	1.4	-3.41E-06	1.58E-06	3.08E-06	1.19E-05	0.9
363	2.6	2.7	3.2	3.04E-06	-1.07E-06	7.30E-06	2.49E-05	3.7
389	2.3	2.0	1.2	6.57E-07	1.61E-06	3.48E-06	6.02E-07	2.3
392	2.2	1.9	1.5	-4.45E-06	-6.66E-06	-5.76E-06	-6.84E-06	4.1
SLE19	2.3	2.8	3.8	5.46E-06	9.39E-06	6.22E-05	3.99E-05	2.7
SLE57	3.8	3.8	10.1	-1.55E-06	1.23E-06	2.08E-05	9.50E-06	2.9
SLE93	11.0	9.0	4.2	2.75E-06	7.20E-06	6.28E-06	7.33E-06	6.2
SLE106	23.0	8.0	7.2	-6.32E-06	-4.55E-06	-7.00E-07	9.19E-06	2.5
SLE112	2.6	3.4	2.2	1.09E-05	-2.73E-06	1.17E-04	3.03E-05	2.3
SLE161	2.3	2.7	24.1	5.87E-06	9.14E-06	4.12E-05	-4.64E-06	2.2

Table 11: Summary of statistical parameters calculated for pi-RIfS measurements. Listed are mean values, standard deviation (SD) and variation coefficient (CV) for the four detected antibodies directed against β_2-GPI, prothrombin (PT), a complex of β_2-GPI and cardiolipin (CL), and cardiolipin alone (from left to right).

	Anti-β_2-GPI			**Anti-PT**			**Anti-β_2GPI/CL**			**Anti-CL**		
ID	**Mean**	**SD**	**CV[%]**	**Mean**	**SD**	**CV[%]**	**Mean**	**SD**	**CV[%]**	**Mean**	**SD**	**CV[%]**
pos.												
15	2.92E-06	4.90E-06	1.7	3.14E-07	1.98E-06	6.3	4.60E-06	4.52E-06	1.0	7.32E-07	1.11E-06	1.5
40	3.23E-05	2.57E-05	0.8	5.34E-06	4.39E-07	0.1	2.04E-05	4.84E-06	0.2	1.22E-05	6.80E-06	0.6
113	2.11E-05	5.72E-06	0.3	3.83E-06	3.49E-06	0.9	1.20E-05	3.97E-06	0.3	1.24E-05	4.47E-06	0.4
262	9.55E-05	1.65E-05	0.2	-9.34E-06	9.22E-06	1.0	1.02E-05	1.03E-05	1.0	4.44E-05	1.13E-05	0.3
270	4.65E-05	1.40E-05	0.3	1.33E-05	8.98E-06	0.7	7.66E-05	2.75E-05	0.4	7.91E-05	2.20E-05	0.3
272	8.43E-05	1.87E-05	0.2	3.15E-05	5.08E-06	0.2	1.04E-04	3.51E-05	0.3	5.79E-05	5.65E-06	0.1
273	2.71E-04	7.33E-05	0.3	-1.17E-05	2.29E-05	2.0	2.23E-04	4.94E-05	0.2	7.12E-05	2.15E-05	0.3
274	7.50E-05	1.27E-05	0.2	6.29E-06	2.98E-06	0.5	6.20E-05	1.64E-05	0.3	-7.15E-06	7.24E-06	1.0
276	1.59E-04	3.45E-05	0.2	4.80E-06	5.82E-06	1.2	9.90E-05	1.13E-05	0.1	5.89E-06	7.84E-06	1.3
296	-2.99E-06	3.95E-06	1.3	1.44E-05	4.30E-06	0.3	2.99E-06	2.90E-06	1.0	6.78E-06	2.35E-06	0.3

302	1.93E-06	2.19E-06	1.1	1.39E-05	4.12E-06	0.3	2.18E-05	5.97E-06	0.3	-6.63E-06	4.67E-06	0.7
304	7.60E-05	3.34E-05	0.4	9.85E-06	5.09E-06	0.5	6.21E-05	2.20E-05	0.4	4.20E-05	1.41E-05	0.3
307	9.79E-05	1.58E-05	0.2	4.95E-05	8.02E-06	0.2	7.08E-05	1.12E-05	0.2	5.14E-05	8.90E-06	0.2
308	4.99E-05	1.48E-05	0.3	3.57E-06	9.99E-07	0.3	3.77E-05	5.98E-06	0.2	4.19E-05	9.72E-06	0.2
310	2.34E-05	5.65E-06	0.2	1.46E-06	5.94E-06	4.1	3.19E-05	4.88E-06	0.2	6.23E-05	9.69E-06	0.2
313	1.49E-05	4.48E-06	0.3	2.62E-06	1.56E-06	0.6	1.29E-05	3.23E-06	0.3	1.66E-05	3.11E-06	0.2
318	4.30E-05	8.23E-06	0.2	9.55E-06	2.75E-06	0.3	4.39E-05	1.18E-05	0.3	5.06E-05	1.36E-05	0.3
325	6.40E-05	5.40E-06	0.1	4.83E-06	9.01E-07	0.2	8.43E-05	1.63E-06	0.0	6.54E-05	8.25E-07	0.0
327	6.65E-05	2.82E-06	0.0	9.59E-06	3.25E-06	0.3	9.04E-05	8.12E-06	0.1	4.85E-05	5.86E-06	0.1
328	2.23E-04	2.15E-05	0.1	2.25E-05	5.78E-06	0.3	2.12E-04	1.84E-05	0.1	1.12E-04	8.72E-06	0.1
330	2.88E-04	7.32E-05	0.3	4.28E-05	3.55E-05	0.8	2.70E-04	4.79E-05	0.2	9.91E-05	1.96E-05	0.2
333	1.70E-05	5.59E-06	0.3	9.51E-06	4.13E-06	0.4	4.79E-05	1.14E-05	0.2	9.37E-06	4.76E-06	0.5
340	3.16E-05	8.54E-06	0.3	5.89E-06	1.71E-06	0.3	1.09E-05	1.24E-06	0.1	1.97E-05	2.93E-07	0.0
341	3.38E-05	8.95E-06	0.3	1.27E-05	8.91E-06	0.7	7.45E-06	5.46E-06	0.7	1.12E-05	5.58E-06	0.5
350	6.03E-05	2.22E-05	0.4	6.32E-05	1.84E-05	0.3	7.10E-05	2.47E-05	0.3	4.82E-05	1.98E-05	0.4
357	2.02E-05	7.10E-06	0.4	6.89E-05	1.46E-05	0.2	1.22E-04	1.64E-05	0.1	1.06E-05	9.97E-06	0.9
358	1.09E-05	4.10E-06	0.4	1.66E-06	9.75E-07	0.6	8.95E-06	9.56E-07	0.1	1.08E-05	1.77E-06	0.2
365	-2.45E-06	3.43E-06	1.4	3.39E-06	7.71E-06	2.3	6.43E-06	7.23E-06	1.1	1.47E-05	1.33E-05	0.9
370	1.29E-04	6.18E-05	0.5	7.57E-06	3.57E-06	0.5	1.50E-04	2.07E-05	0.1	5.48E-05	4.22E-06	0.1
371	2.37E-04	7.00E-05	0.3	8.18E-06	1.11E-05	1.4	1.40E-04	8.85E-05	0.6	6.02E-05	5.44E-05	0.9
372	1.92E-06	2.43E-06	1.3	1.07E-05	5.25E-06	0.5	4.14E-06	3.07E-06	0.7	1.18E-05	4.35E-06	0.4
374	9.24E-05	2.46E-05	0.3	8.53E-06	2.49E-06	0.3	3.12E-05	5.34E-06	0.2	3.95E-05	7.19E-06	0.2
377	2.10E-05	5.73E-06	0.3	5.70E-07	2.84E-06	5.0	2.21E-05	1.08E-05	0.5	2.30E-05	6.46E-06	0.3
378	3.06E-05	1.38E-05	0.5	2.48E-05	1.38E-05	0.6	3.16E-05	1.81E-05	0.6	2.28E-05	1.60E-05	0.7
386	-1.58E-06	2.87E-06	1.8	1.65E-05	3.68E-06	0.2	5.02E-06	3.53E-06	0.7	3.48E-06	3.14E-06	0.9
neg.												
278	-9.49E-08	1.48E-06	15.5	1.84E-06	2.40E-06	1.3	-2.92E-06	2.34E-06	0.8	5.47E-06	3.81E-06	0.7
281	4.23E-07	6.56E-07	1.5	1.80E-07	7.48E-07	4.1	-1.85E-06	5.63E-07	0.3	-4.62E-07	1.30E-06	2.8
282	-1.30E-06	3.69E-06	2.8	-8.65E-07	5.53E-06	6.4	-1.44E-06	1.81E-06	1.3	6.03E-06	6.82E-06	1.1

283	-1.28E-06	2.20E-06	1.7	2.18E-06	3.53E-06	1.6	-3.56E-06	2.60E-06	0.7	-1.79E-06	3.58E-06	2.0
284	-2.83E-06	4.69E-06	1.7	7.32E-07	5.75E-06	7.9	3.46E-06	2.19E-06	0.6	8.91E-06	3.51E-06	0.4
286	-4.66E-06	3.95E-06	0.8	-1.85E-06	2.30E-06	1.2	-3.41E-06	2.85E-06	0.8	-2.04E-06	4.82E-06	2.4
288	-1.43E-06	3.37E-06	2.4	1.24E-06	1.41E-06	1.1	-1.24E-06	3.21E-06	2.6	-1.88E-07	5.09E-06	27.1
289	9.36E-07	2.19E-06	2.3	8.64E-07	5.07E-07	0.6	3.59E-06	3.11E-06	0.9	2.75E-06	1.29E-06	0.5
290	-9.28E-07	2.27E-06	2.5	-1.08E-06	3.88E-06	3.6	3.85E-06	5.16E-06	1.3	4.16E-06	5.52E-06	1.3
291	1.36E-06	3.13E-06	2.3	5.95E-07	3.01E-06	5.1	-1.06E-06	3.09E-06	2.9	2.80E-06	1.13E-06	0.4
292	-4.51E-07	5.10E-06	11.3	-2.49E-07	3.26E-06	13.1	1.18E-06	2.82E-06	2.4	1.40E-06	2.95E-06	2.1
294	-7.70E-06	4.58E-06	0.6	-2.94E-06	4.60E-06	1.6	-3.58E-06	3.52E-06	1.0	-5.48E-06	4.74E-06	0.9
319	9.51E-07	2.65E-06	2.8	-4.16E-07	4.14E-06	9.9	-3.22E-06	2.44E-06	0.8	2.26E-06	3.60E-06	1.6
320	9.78E-07	3.96E-06	4.0	-2.44E-06	2.82E-06	1.2	-8.47E-08	2.75E-06	32.5	6.54E-06	1.50E-06	0.2
321	2.10E-07	5.12E-06	24.4	1.29E-05	5.77E-06	0.4	6.57E-07	4.17E-06	6.3	3.18E-06	2.21E-06	0.7
322	-5.25E-06	2.95E-06	0.6	2.79E-06	3.30E-06	1.2	-1.96E-07	3.42E-06	17.5	-2.46E-06	4.03E-06	1.6
323	1.36E-06	3.85E-06	2.8	1.01E-06	6.02E-06	6.0	8.58E-06	3.97E-06	0.5	6.30E-06	2.18E-06	0.3
334	-2.89E-06	2.88E-06	1.0	-2.01E-06	5.25E-06	2.6	-9.39E-07	3.02E-06	3.2	4.24E-06	3.46E-06	0.8
336	-7.33E-07	2.70E-06	3.7	2.06E-06	2.62E-06	1.3	-5.88E-07	5.32E-06	9.0	4.97E-06	3.01E-06	0.6
337	2.36E-06	1.59E-06	0.7	2.33E-06	9.31E-07	0.4	2.48E-06	1.67E-06	0.7	1.50E-06	2.90E-07	0.2
338	-3.41E-06	1.61E-06	0.5	1.58E-06	3.54E-06	2.2	3.08E-06	3.02E-06	1.0	1.19E-05	7.08E-06	0.6
363	3.04E-06	1.32E-06	0.4	-1.07E-06	2.33E-06	2.2	7.30E-06	2.46E-06	0.3	2.49E-05	7.73E-07	0.0
389	6.57E-07	3.24E-06	4.9	1.61E-06	2.48E-06	1.5	3.48E-06	4.86E-06	1.4	6.02E-07	1.75E-06	2.9
392	-4.45E-06	1.89E-06	0.4	-6.66E-06	2.11E-06	0.3	-5.76E-06	2.37E-06	0.4	-6.84E-06	2.19E-06	0.3
SLE19	5.46E-06	4.45E-06	0.8	9.39E-06	5.28E-06	0.6	6.22E-05	2.03E-05	0.3	3.99E-05	3.77E-06	0.1
SLE57	-1.55E-06	2.51E-06	1.6	1.23E-06	3.66E-06	3.0	2.08E-05	6.08E-06	0.3	9.50E-06	3.14E-06	0.3
SLE93	2.75E-06	5.64E-06	2.1	7.20E-06	1.27E-05	1.8	6.28E-06	1.08E-05	1.7	7.33E-06	9.48E-06	1.3
SLE106	-6.32E-06	2.49E-06	0.4	-4.55E-06	9.18E-06	2.0	-7.00E-07	4.76E-06	6.8	9.19E-06	3.57E-06	0.4
SLE112	1.09E-05	1.02E-05	0.9	-2.73E-06	4.05E-06	1.5	1.17E-04	3.63E-05	0.3	3.03E-05	5.23E-06	0.2
SLE161	5.87E-06	2.82E-06	0.5	9.14E-06	4.80E-06	0.5	4.12E-05	4.63E-06	0.1	-4.64E-06	6.24E-06	1.3

8 abbreviations

AMD	Aminodextrane
apoER2	Apolipoprotein E receptor 2
ApoH/β_2-GPI	ApolipoproteinH/β_2-Glycoprotein I
aPL	Antiphospholipid antibody
APS	Antiphospholipid syndrome
aPTT	Activated partial thromboplastin time
AUC	Area under curve
11-AUTMS	11-Aminoundecyltrimethoxysilane
BFP-STS	Biologic false positive serological tests for syphilis
BSA	Bovine serum albumin
CAPS	Catastrophic APS
CCD	Charge-coupled device
CI	Confidence interval
CL	Cardiolipin
CV	Variation coefficient
DMF	N,N-Dimehtylformadide
dRVVT	Dilute Russell's viper venom time
ELISA	Enzyme-linked immunosorbent assay
Fab	Fragment, antigen-binding
Fc	Fragment, crystallisable
FCS	Fetal calf serum
GPL	IgG with specificity for phospholipid antigens (arbitrary units)
HBS	HEPES buffered saline
HRP	Horseradish peroxidise
HSA	Human serum albumin
ICAM-1	Intercellular cell adhesion molecule-1
Ig	Immunoglobulin
IL	Interleukin
INR	International normalized ratio
kDa	Kilo Dalton
LA	Lupus anticoagulant
LED	Light-emitting diode
LMWH	Low-molecular-weight heparin
MAC	Membrane attack complex
MAPK	Mitogen activated protein kinase
MPL	IgM with specificity for phospholipid antigens (arbitrary units)
NF-κB	Nuclear factor κB
PAI-1	Plasminogen activator inhibitor 1
PBS	Phosphate buffered saline
PEG	Polyethylene glycol
pi-RIfS	Polarized imaging reflectometric interference spectroscopy
PT	Prothrombin
RIfS	Reflectometric interference spectroscopy
ROC	Receiver operating characteristic
RT	Room temperature
SA	Streptavidine

SAM	Self assembled monolayer
SD	Standard deviation
SE	Standard error
SLE	Systemic lupus erythematosus
SPR	Surface plasmon resonance
TF	Tissue factor
TLR	Toll-like receptor
TNF-α	Tumor necrosis factor α
tPA	Tissue plasminogen activator
UFH	Unfractionated heparin
VCAM-1	Vascular cell adhesion molecule-1
VDRL	Veneral Disease Research Laboratory

9 literature

Agar, C. et al., 2010. β2-Glycoprotein I can exist in 2 conformations: implications for our understanding of the antiphospholipid syndrome. *Blood*, 116(8), pp.1336–1343.

Agostinis, C. et al., 2014. A non-complement-fixing antibody to β2 glycoprotein I as a novel therapy for antiphospholipid syndrome. *Blood*, 123(22), pp.3478–3487.

Ames, P.R. et al., 1996. Coagulation activation and fibrinolytic imbalance in subjects with idiopathic antiphospholipid antibodies-a crucial role for acquired free protein S deficiency. *Thromb Haemostasis*, 76(2), pp.190–194.

Andreoli, L. et al., 2008. Antinucleosome antibodies in primary antiphospholipid syndrome: A hint at systemic autoimmunity? *J Autoimmun*, 30(1-2), pp.51–57.

Balboni, I. et al., 2006. Multiplexed Protein Array Platforms for Analysis of Autoimmune Diseases. *Annu Rev Immunol*, 24(1), pp.391–418.

Bermas, B.L., Erkan, D. & Schur, P.H., 2014. Diagnosis of the antiphospholipid syndrome. Available at: http://www.uptodate.com/contents/diagnosis-of-the-antiphospholipid-syndrome.

Bermas, B.L. & Schur, P.H., 2014. Pathogenesis of the antiphospholipid syndrome. Available at: http://www.uptodate.com/contents/pathogenesis-of-the-antiphospholipid-syndrome.

Bevers, E.M. et al., 1991. Lupus anticoagulant IgG's (LA) are not directed to phospholipids only, but to a complex of lipid-bound human prothrombin. *Thromb Haemostasis*, 66(6), pp.905–912.

Bleher, O. et al., 2014. Development of a new parallelized , optical biosensor platform for label-free detection of autoimmunity-related antibodies. *Anal Bioanal Chem*, 406(14), pp.3305–3314.

BMJ, 2014. Antiphospholipid syndrome. *BMJ Best Practice*. Available at: http://bestpractice.bmj.com/best-practice/monograph/469/basics/epidemiology.html.

Borisov, S.M. & Wolfbeis, O.S., 2008. Optical Biosensors. *Chem Rev*, 108(2), pp.423–461.

Božič, B. et al., 2005. Avidity of anti-beta-2-glycoprotein I antibodies. *Autoimmun Rev*, 4(5), pp.303–308.

Bradford, M.M., 1976. A rapid and sensitive method for the quantitation of microgram quantities of protein utilizing the principle of protein-dye binding. *Anal Biochem*, 72, pp.248–254.

Bucciarelli, S., Espinosa, G. & Cervera, R., 2009. The CAPS Registry: morbidity and mortality of the catastrophic antiphospholipid syndrome. *Lupus*, 18(10), pp.905–912.

Burry, R.W., 2009. *Immunocytochemistry: A Practical Guide for Biomedical Research*, Springer Science & Business Media.

CANDOR Bioscience GmbH, 2015. LowCross-Buffer® MILD and LowCross-Buffer® STRONG. Available at: http://www.candor-bioscience.de/en.

Cervera, R. et al., 2015. Morbidity and mortality in the antiphospholipid syndrome during a 10-year period: a multicentre prospective study of 1000 patients. *Annals of the rheumatic diseases*, 74, pp.1011–1018.

Cervera, R., Rodríguez-Pintó, I. & Espinosa, G., 2014. Catastrophic antiphospholipid syndrome: task force report summary. *Lupus*, 23, pp.1283–1285.

Comarmond, C. & Cacoub, P., 2013. Antiphospholipid syndrome: from pathogenesis to novel immunomodulatory therapies. *Autoimmun Rev*, 12(7), pp.752–757.

Donohoe, S. et al., 2001. Anti-prothrombin antibodies: assay conditions and clinical associations in the anti-phospholipid syndrome. *Brit J Haematol*, 113(2), pp.544–549.

Ekins, R.P., 1998. Ligand assays : from electrophoresis to miniaturized microarrays. *Clin Chem*, 44(9), pp.2015–2030.

Engvall, E. & Perlmann, P., 1971. Enzyme-linked immunosorbent assay (ELISA): Quantitative assay of immunoglobulin G. *Immunochemistry*, 8(9), pp.871–874.

Ericsson, E., 2013. *Biosensor surface chemistry for oriented protein immobilization and biochip patterning*. Linköping University.

Erkan, D. et al., 2014. 14th International Congress on Antiphospholipid Antibodies: task force report on antiphospholipid syndrome treatment trends. *Autoimmun Rev*, 13(6), pp.685–696.

Espinola, R.G. et al., 2003. E-Selectin mediates pathogenic effects of antiphospholipid antibodies. *J Thromb Haemost*, 1, pp.843–848.

Espinola, R.G. et al., 2002. Hydroxychloroquine Reverses Platelet Activation Induced by Human IgG Antiphospholipid Antibodies. *Thromb Haemostasis*, 87, pp.518–522.

Espinosa, G. & Cervera, R., 2010. Antiphospholipid syndrome: frequency, main causes and risk factors of mortality. *Nat Rev Rheumatol*, 6(5), pp.296–300.

Ewald, M. et al., 2013. A robust sensor platform for label-free detection of anti-Salmonella antibodies using undiluted animal sera. *Anal Bioanal Chem*, 405(20), pp.6461–6469.

Fan, X. et al., 2008. Sensitive optical biosensors for unlabeled targets: A review. *Anal Chim Acta*, 620(1-2), pp.8–26.

Fawcett, T., 2003. ROC Graphs : Notes and Practical Considerations for Data Mining Researchers.

Fechner, P. et al., 2011. Kinetic analysis of the estrogen receptor alpha using RIfS. *Anal Bioanal Chem*, 400(3), pp.729–735.

Fischetti, F. et al., 2005. Thrombus formation induced by antibodies to beta2-glycoprotein I is complement dependent and requires a priming factor. *Blood*, 106(7), pp.2340–2346.

Galli, M. & Barbui, T., 1999. Antiprothrombin Antibodies: Detection and Clinical Significance in the Antiphospholipid Syndrome. *Blood*, 93(7), pp.2149–2157.

Gamsjaeger, R. et al., 2005. Membrane binding of β2-glycoprotein I can be described by a two-state reaction model: an atomic force microscopy and surface plasmon resonance study. *Biochem J*, 389(Pt 3), pp.665–673.

Gauglitz, G., 2010. Direct optical detection in bioanalysis: an update. *Anal Bioanal Chem*, 398(6), pp.2363–2372.

Gesellchen, F., Zimmermann, B. & W. Herberg, F., 2003. Direct Optical Detection of Protein–Ligand Interactions. In G. U. N. ©. H. P. Inc., ed. *Methods in Molecular Biology*. pp. 17–45.

Gezer, S., 2003. Antiphospholipid syndrome. *DM-Dis Mon*, 49(12), pp.696–741.

Giannakopoulos, B. et al., 2009. How we diagnose the antiphospholipid syndrome. *Blood*, 113(5), pp.985–994.

Girardi, G. et al., 2003. Complement C5a receptors and neutrophils mediate fetal injury in the antiphospholipid syndrome. *J Clin Invest*, 112(11), pp.1644–1654.

Girardi, G., Redecha, P. & Salmon, J.E., 2004. Heparin prevents antiphospholipid antibody – induced fetal loss by inhibiting complement activation. *Nat Med*, 10(11), pp.1222–1226.

Graille, M. et al., 2000. Crystal structure of a Staphylococcus aureus protein A domain complexed with the Fab fragment of a human IgM antibody: structural basis for recognition of B-cell receptors and superantigen activity. *P Natl Acad Sci USA*, 97(10), pp.5399–5404.

De Groot, P.G. & Meijers, J.C.M., 2011. β2-Glycoprotein I: evolution, structure and function. *J Thromb Haemost*, 9(7), pp.1275–1284.

De Groot, P.G., Meijers, J.C.M. & Urbanus, R.T., 2012. Recent developments in our understanding of the antiphospholipid syndrome. *Int J Lab Hematol*, 34(3), pp.223–231.

De Groot, P.G. & Urbanus, R.T., 2012. The significance of autoantibodies against β2-glycoprotein I. *Blood*, 120(2), pp.266–274.

Häkkinen, H., 2012. The gold-sulfur interface at the nanoscale. *Nature Chemistry*, 4(6), pp.443–455.

Hanly, J.G., 2003. Antiphospholipid syndrome: an overview. *Can Med Assoc J*, 168(13), pp.1675–1682.

Harris, E.N. & Pierangeli, S.S., 2002. Revisiting the anticardiolipin test and its standardization. *Lupus*, 11(5), pp.269–275.

Hartmann, M. et al., 2009. Protein microarrays for diagnostic assays. *Anal Bioanal Chem*, 393(5), pp.1407–1416.

Hermanson, G.T., 2008. *Bioconjugate Techniques*, Academic Press, Elsevier.

Hilbig, U. et al., 2012. A biomimetic sensor surface to detect anti-β2-glycoprotein-I antibodies as a marker for antiphospholipid syndrome. *Anal Bioanal Chem*, 403(3), pp.713–717.

Homola, J. et al., 2006. *Springer Series on Chemical Sensors and Biosensors; Volume 4: Surface Plasmon Resonance Based Sensors* 4th ed. O. S. Wolfbeis & J. Homola, eds., Springer-Verlag Berlin Heidelberg.

Horstman, L.L. et al., 2009. Antiphospholipid antibodies: Paradigm in transition. *J Neuroinflamm*, 6(3).

Huisgen, R., 1961. Proceedings of the Chemical Society. October 1961. *P Chem Soc London*, (October), p.357.

Iverson, G.M. et al., 2002. Use of Single Point Mutations in Domain I of β2 -Glycoprotein I to Determine Fine Antigenic Specificity of Antiphospholipid Autoantibodies. *J Immunol*, 169(12), pp.7097–7103.

Iverson, G.M., Victoria, E.J. & Marquis, D.M., 1998. Anti-β2 glycoprotein I (β2GPI) autoantibodies recognize an epitope on the first domain of β2GPI. *P Natl Acad Sci USA*, 95(26), pp.15542–15546.

Janeway, C.A., Travers, P. & Walport, M., 2001. The complement system and innate immunity. *Immunobiology: The Immune System in Health and Disease*. Available at: http://www.ncbi.nlm.nih.gov/books.

Jayakody Arachchillage, D. & Greaves, M., 2014. The chequered history of the antiphospholipid syndrome. *Brit J Haematol*, 165(5), pp.609–617.

Johns, M.K. et al., 2009. Synthesis and biological evaluation of a novel cardiolipin affinity matrix. *Org Biomol Chem*, 7(18), pp.3691–3697.

Johnsson, B. et al., 1995. Comparison of methods for immobilization to carboxymethyl dextran sensor surfaces by analysis of the specific activity of monoclonal antibodies. *J Mol Recognit*, 8(1-2), pp.125–131.

Johnsson, B., Löfås, S. & Lindquist, G., 1991. Immobilization of Proteins to a Carboxymethyldextran-Modified Gold Surface for Biospecific Interaction Analysis in Surface Plasmon Resonance Sensors. *Anal Biochem*, 198(2), pp.268–277.

Kattah, M.G., Utz, P.J. & Balboni, I., 2008. Protein Microarrays Address the Elephant in the Room. *Clin Chem*, 54(6), pp.937–939.

Keeling, D.M. et al., 1993. Role of β2-glycoprotein I and anti-phospholipid antibodies in activation of protein C in vitro. *J Clin Pathol*, 46(10), pp.908–911.

Kricka, L.J. et al., 2006. Current perspectives in protein array technology. *Ann Clin Biochem*, 43(6), pp.457–467.

De Laat, H.B. et al., 2004. β2-glycoprotein I-dependent lupus anticoagulant highly correlates with thrombosis in the antiphospholipid syndrome. *Blood*, 104(12), pp.3598–3602.

Lakos, G. et al., 2012. International Consensus Guidelines on Anticardiolipin and Anti–β2-Glycoprotein I Testing. *Arthritis Rheum*, 64(1), pp.1–10.

Leopold, N. et al., 2009. IR absorption and reflectometric interference spectroscopy (RIfS) combined to a new sensing approach for gas analytes absorbed into thin polymer films. *Spectrochim Acta A*, 72(5), pp.994–999.

Levine, J.S., Branch, D.W. & Rauch, J., 2002. The Antiphospholipid Syndrome. *New Engl J Med*, 346(10), pp.752–763.

Liedberg, B., Nylander, C. & Lunström, I., 1983. Surface plasmon resonance for gas detection and biosensing. *Sensor Actuator*, 4, pp.299–304.

Lockshin, M.D., Sammaritano, L.R. & Schwartzman, S., 2000. Validation of the Sapporo criteria for antiphospholipid syndrome. *Arthritis Rheum*, 43(2), pp.440–443.

Louisville APL Diagnostics, 2013. Calibrators for the Measurement of Anticardiolipin Antibodies IgG and IgM: Instructions Manual. , pp.1–10. Available at: http://www.louisvilleapl.com/pdf/GM_300_Instructions_English.pdf.

Luppa, P.B., Sokoll, L.J. & Chan, D.W., 2001. Immunosensors-principles and applications to clinical chemistry. *Clin Chim Acta*, 314(1-2), pp.1–26.

Maskos, U. & Southern, E.M., 1992. Oligonucleotide hybridizations on glass supports: a novel linker for oligonucleotide synthesis and hybridization properties of oligonucleotides synthesised in situ. *Nucleic Acids Res*, 20(7), pp.1679–1684.

McIntyre, J.A., Wagenknecht, D.R. & Faulk, W.P., 2003. Antiphospholipid antibodies: discovery, definitions, detection and disease. *Prog Lipid Res*, 42(3), pp.176–237.

Mehdi, A. a, Uthman, I. & Khamashta, M., 2010. Antiphospholipid syndrome: pathogenesis and a window of treatment opportunities in the future. *European J Clin Invest*, 40(5), pp.451–464.

Metzger, J. et al., 2007. Biosensor Analysis of β2-Glycoprotein I-Reactive Autoantibodies: Evidence for Isotype-Specific Binding and Differentiation of Pathogenic from Infection-Induced Antibodies. *Clin Chem*, 53(6), pp.1137–1143.

Miyakis, S. et al., 2006. International consensus statement on an update of the classification criteria for definite antiphospholipid syndrome (APS). *J Thromb Haemost*, 4(2), pp.295–306.

Miyakis, S., Robertson, S. a & Krilis, S. a, 2004. Beta-2 glycoprotein I and its role in antiphospholipid syndrome-lessons from knockout mice. *Clin Immunol*, 112(2), pp.136–143.

Möhrle, B. et al., 2006. Label-free characterization of cell adhesion using reflectometric interference spectroscopy (RIfS). *Anal Bioanal Chem*, 384(2), pp.407–413.

Müller, C. et al., 2010. β2-Glycoprotein I-derived peptides as antigenic structures for the detection of antiphospholipid antibodies. *J Thromb Haemost*, 8(9), pp.2073–2075.

Nagel, B., Dellweg, H. & Gierasch, L.M., 1992. Glossary for Chemists of Terms Used in Biotechnology (IUPAC Recommendations 1992). *Pure Appl Chem*, 64(1), pp.143–168.

Nayer, A. & Ortega, L.M., 2014. Catastrophic antiphospholipid syndrome: a clinical review. *J Nephropathol*, 3(1), pp.9–17.

Nimpf, J. et al., 1986. Prothrombinase activity of human platelets is inhibited by β2-glycoprotein-I. *Biochim Biophys Acta*, 884(1), pp.142–149.

Nowicki, M., Müller, F. & Frentzen, M., 2005. Cardiolipin synthase of Arabidopsis thaliana. *FEBS Lett*, 579(10), pp.2161–2165.

Oku, K. et al., 2009. Complement activation in patients with primary antiphospholipid syndrome. *Ann Rheum Dis*, 68(6), pp.1030–1035.

Ortiz, A. et al., 1999. Membrane Fusion and the Lamellar-to-Inverted-Hexagonal Phase Transition in Cardiolipin Vesicle Systems Induced by Divalent Cations. *Biophys J*, 77(4), pp.2003–2014.

Pangborn, M.C., 1941. A New Serologically Active Phospholipid from Beef Heart. *Exp Biol Med (Maywood)*, 48(2), pp.484–486.

Paradies, G. et al., 2009. Role of cardiolipin peroxidation and Ca2+ in mitochondrial dysfunction and disease. *Cell Calcium*, 45(6), pp.643–650.

Pengo, V. et al., 2009. Update of the guidelines for lupus anticoagulant detection. *J Thromb Haemost*, 7(10), pp.1737–1740.

Pierangeli, S.S. et al., 2005. Requirement of activation of complement C3 and C5 for antiphospholipid antibody-mediated thrombophilia. *Arthritis Rheum*, 52(7), pp.2120–4.

Proll, G. et al., 2007. Potential of label-free detection in high-content-screening applications. *J Chromatogr A*, 1161(1-2), pp.2–8.

Reber, G. et al., 2005. Variability of anti-ß2glycoprotein I antibodies measurement by commercial assays. *Thromb Haemostasis*, 94(3), pp.665–672.

Redecha, P. et al., 2007. Tissue factor: a link between C5a and neutrophil activation in antiphospholipid antibody induced fetal injury. *Blood*, 110(7), pp.2423–2431.

Rumbaut, R.E. & Thiagarajan, P., 2010. Platelet Recruitment and Blood Coagulation. *Platelet-Vessel Wall Interactions in Hemostasis and Thrombosis*. Available at: http://www.ncbi.nlm.nih.gov/books.

Rusmini, F., Zhong, Z. & Feijen, J., 2007. Protein Immobilization Strategies for Protein Biochips. *Biomacromolecules*, 8(6), pp.1775–1789.

Schena, M. et al., 1995. Quantitative Monitoring of Gene Expression Patterns with a Complementary DNA Microarray. *Science*, 270(5235), pp.467–470.

Schlichtiger, A. et al., 2013. Covalent attachment of functionalized cardiolipin on a biosensor gold surface allows repetitive measurements of anticardiolipin antibodies in serum. *Anal Bioanal Chem*, 405(1), pp.275–285.

Schmitt, H.-M. et al., 1997. An integrated system for optical biomolecular interaction analysis. *Biosens Bioelectron*, 12(8), pp.809–816.

Schmitt, K. et al., 2008. Evanescent field Sensors Based on Tantalum Pentoxide Waveguides – A Review. *Sensors*, 8(2), pp.711–738.

Schousboe, I. & Rasmussen, M.S., 1995. Synchronized inhibition of the phospholipid mediated autoactivation of factor XII in plasma by beta 2-glycoprotein I and anti-beta 2-glycoprotein I. *Thromb Haemostasis*, 73(5), pp.798–804.

Schwarzenbacher, R. et al., 1999. Crystal structure of human β2-glycoprotein I: implications for phospholipid binding and the antiphospholipid syndrome. *EMBO J*, 18(22), pp.6228–6239.

Sciascia, S., Khamashta, M. & Bertolaccini, M., 2014. New Tests to Detect Antiphospholipid Antibodies: Antiprothrombin (aPT) and Anti-Phosphatidylserine/Prothrombin (aPS/PT) Antibodies. *Curr Rheumatol Rep*, 16(5), pp.1–6.

Seidel, M. & Niessner, R., 2008. Automated analytical microarrays: a critical review. *Anal Bioanal Chem*, 391(5), pp.1521–1544.

Senaratne, W., Andruzzi, L. & Ober, C.K., 2005. Self-Assembled Monolayers and Polymer Brushes in Biotechnology: Current Applications and Future Perspectives. *Biomacromolecules*, 6(5), pp.2427–2448.

Sheng, Y., Kandiah, D.A. & Krilis, S.A., 1998. Anti-β2-Glycoprotein I Autoantibodies from Patients with the "Antiphospholipid" Syndrome Bind to β2-Glycoprotein I with Low Affinity: Dimerization of β2-Glycoprotein I Induces a Significant Increase in Anti-β2-Glycoprotein I Antibody Affinity. *J Immunol*, 161, pp.2038–2043.

Sherer, Y. et al., 2004. Autoantibody Explosion in Systemic Lupus Erythematosus: More than 100 Different Antibodies Found in SLE Patients. *Semin Arthritis Rheu*, 34(2), pp.501–537.

Tan, Y.H. et al., 2011. Bioconjugation reactions for covalent coupling of proteins to gold surfaces. *Glob J Biochem*, 3(6), pp.1–21.

Thermo Fisher Sientific Inc, 2015. ELISA Enzyme Substrate Selection Guide. Available at: http://www.piercenet.com/guide/guide-elisa-substrates.

Thévenot, D.R. et al., 2001. Electrochemical biosensors: recommended definitions and classification. *Biosens Bioelectron*, 16(1-2), pp.121–131.

Tipler, P.A. & Mosca, G., 2003a. Properties of Light. In *Physics for scientists and engineers*. W. H. Freeman, pp. 1029–1071.

Tipler, P.A. & Mosca, G., 2003b. Superposition and Standing Waves. In *Physics for scientists and engineers*. W. H. Freeman, pp. 485–514.

Ulman, A., 1996. Formation and Structure of Self-Assembled Monolayers. *Chem Rev*, 96(4), pp.1533–1554.

Vlachoyiannopoulos, P.G. et al., 2007. Antiphospholipid Antibodies: Laboratory and Pathogenetic Aspects. *Crit Rev Cl Lab Sci*, 44(3), pp.271–338.

Wang, H. & Chiang, A., 2004. Cloning and characterization of the human β2-glycoprotein I (β2-GPI) gene promoter: roles of the atypical TATA box and hepatic nuclear factor-1α in regulating β2 -GPI promoter activity. *Biochem J*, 380(2), pp.455–463.

Wilson, W.A. et al., 1999. International Consensus Statement on Preliminary Classification Criteria for Definite Antiphospholipid Syndrome. *Arthritis Rheum*, 42(7), pp.1309–1311.

Wong, R.C.W. & Favaloro, E.J., 2008. Clinical Features, Diagnosis, and Management of the Antiphospholipid Syndrome. *Semin Thromb Hemost*, 34(3), pp.295–304.

Wood, J.P. et al., 2011. Prothrombin activation on the activated platelet surface optimizes expression of procoagulant activity. *Blood2*, 117(5), pp.1710–1718.

Yasuda, S. et al., 2004. β2-glycoprotein I, anti-β2-glycoprotein I, and fibrinolysis. *Thromb Res*, 114(5-6), pp.461–465.

Yeste, A. & Quintana, F.J., 2013. Antigen microarrays for the study of autoimmune diseases. *Clin Chem*, 59(7), pp.1036–1044.

Zhu, H. & Snyder, M., 2003. Protein chip technology. *Curr Opin Chem Biol*, 7(1), pp.55–63.

Žigon, P. et al., 2011. Modified phosphatidylserine-dependent antithrombin ELISA enables identification of patients negative for other antiphospholipid antibodies and also detects low avidity antibodies. *Clin Chem Lab Med*, 49(6), pp.1011–1018.